

NATIONAL BUREAU OF STANDARDS REPORT

10 246

EFFECT OF SHEAR CONNECTOR
SPACING ON THE ULTIMATE STRENGTH
OF CONCRETE-ON-STEEL COMPOSITE BEAMS



U.S. DEPARTMENT OF COMMERCE
NATIONAL BUREAU OF STANDARDS

NATIONAL BUREAU OF STANDARDS

The National Bureau of Standards¹ was established by an act of Congress March 3, 1901. Today, in addition to serving as the Nation's central measurement laboratory, the Bureau is a principal focal point in the Federal Government for assuring maximum application of the physical and engineering sciences to the advancement of technology in industry and commerce. To this end the Bureau conducts research and provides central national services in four broad program areas. These are: (1) basic measurements and standards, (2) materials measurements and standards, (3) technological measurements and standards, and (4) transfer of technology.

The Bureau comprises the Institute for Basic Standards, the Institute for Materials Research, the Institute for Applied Technology, the Center for Radiation Research, the Center for Computer Sciences and Technology, and the Office for Information Programs.

THE INSTITUTE FOR BASIC STANDARDS provides the central basis within the United States of a complete and consistent system of physical measurement; coordinates that system with measurement systems of other nations; and furnishes essential services leading to accurate and uniform physical measurements throughout the Nation's scientific community, industry, and commerce. The Institute consists of an Office of Measurement Services and the following technical divisions:

Applied Mathematics—Electricity—Metrology—Mechanics—Heat—Atomic and Molecular Physics—Radio Physics²—Radio Engineering²—Time and Frequency²—Astrophysics²—Cryogenics.²

THE INSTITUTE FOR MATERIALS RESEARCH conducts materials research leading to improved methods of measurement standards, and data on the properties of well-characterized materials needed by industry, commerce, educational institutions, and Government; develops, produces, and distributes standard reference materials; relates the physical and chemical properties of materials to their behavior and their interaction with their environments; and provides advisory and research services to other Government agencies. The Institute consists of an Office of Standard Reference Materials and the following divisions:

Analytical Chemistry—Polymers—Metallurgy—Inorganic Materials—Physical Chemistry.

THE INSTITUTE FOR APPLIED TECHNOLOGY provides technical services to promote the use of available technology and to facilitate technological innovation in industry and Government; cooperates with public and private organizations in the development of technological standards, and test methodologies; and provides advisory and research services for Federal, state, and local government agencies. The Institute consists of the following technical divisions and offices:

Engineering Standards—Weights and Measures—Invention and Innovation—Vehicle Systems Research—Product Evaluation—Building Research—Instrument Shops—Measurement Engineering—Electronic Technology—Technical Analysis.

THE CENTER FOR RADIATION RESEARCH engages in research, measurement, and application of radiation to the solution of Bureau mission problems and the problems of other agencies and institutions. The Center consists of the following divisions:

Reactor Radiation—Linac Radiation—Nuclear Radiation—Applied Radiation.

THE CENTER FOR COMPUTER SCIENCES AND TECHNOLOGY conducts research and provides technical services designed to aid Government agencies in the selection, acquisition, and effective use of automatic data processing equipment; and serves as the principal focus for the development of Federal standards for automatic data processing equipment, techniques, and computer languages. The Center consists of the following offices and divisions:

Information Processing Standards—Computer Information—Computer Services—Systems Development—Information Processing Technology.

THE OFFICE FOR INFORMATION PROGRAMS promotes optimum dissemination and accessibility of scientific information generated within NBS and other agencies of the Federal government; promotes the development of the National Standard Reference Data System and a system of information analysis centers dealing with the broader aspects of the National Measurement System, and provides appropriate services to ensure that the NBS staff has optimum accessibility to the scientific information of the world. The Office consists of the following organizational units:

Office of Standard Reference Data—Clearinghouse for Federal Scientific and Technical Information³—Office of Technical Information and Publications—Library—Office of Public Information—Office of International Relations.

¹ Headquarters and Laboratories at Gaithersburg, Maryland, unless otherwise noted; mailing address Washington, D.C. 20234.

² Located at Boulder, Colorado 80302.

³ Located at 5285 Port Royal Road, Springfield, Virginia 22151.

NATIONAL BUREAU OF STANDARDS REPORT

NBS PROJECT

4212115

1 August 1970

NBS REPORT

10 246

EFFECT OF SHEAR CONNECTOR SPACING ON THE ULTIMATE STRENGTH OF CONCRETE-ON-STEEL COMPOSITE BEAMS

By

H. S. Lew

IMPORTANT NOTICE

NATIONAL BUREAU OF STANDARDS
for use within the Government. Before
and review. For this reason, the report
whole or in part, is not authorized
Bureau of Standards, Washington, D.C.
the Report has been specifically pre-

Approved for public release by the
director of the National Institute of
Standards and Technology (NIST)
on October 9, 2015

Accounting documents intended
subjected to additional evaluation
ting of this Report, either in
office of the Director, National
ie Government agency for which
as for its own use.



U.S. DEPARTMENT OF COMMERCE
NATIONAL BUREAU OF STANDARDS

ABSTRACT

This report presents the results of an experimental study on the ultimate strength of concrete-on-steel composite beams. The variables investigated were: (1) longitudinal spacing of shear connectors; and (2) the position of loads within the span.

A total of six beams were tested, each comprising 4 in x 48 in slab and a W12x27 steel beam with headed stud shear connectors. The test results were analyzed and compared with results predicted by the existing theories, including the results obtained from a computer analysis. It was found that while the AISC design method provides a conservative estimate of the ultimate strength of composite beams, the computer analysis gave a closer prediction.

TABLE OF CONTENTS

	<u>Page</u>
ABSTRACT.	ii
1. INTRODUCTION.	1
1.1 Object	1
1.2 Background	1
1.3 Notation	4
1.4 SI Conversion Units.	4
2. EXPERIMENTAL INVESTIGATION.	6
2.1 Scope.	6
2.2 Description of Specimens	7
2.3 Fabrication of Specimens	8
2.4 Test Setup	10
2.5 Instrumentation.	10
2.6 Test Procedure	11
3. TEST RESULTS.	13
3.1 Mode of Failure.	13
3.2 Ultimate Loads	14
3.3 Slip Measurements.	15
3.4 Load-Deflection Curves	18
3.5 Strain Measurements.	22
3.6 Pushout Tests.	25
4. DISCUSSION OF TEST RESULTS.	28
4.1 Computer Program	28
4.2 Interface Slip	30
4.3 Deflection	32
4.4 Comparison of Test Results with Theories	34
4.5 Effect of Shear Connector Distribution on Ultimate Strength	35
4.6 Distribution of the Interface Shear Force on Connectors.	36
5. SUMMARY AND CONCLUSION.	39
5.1 Summary.	39
5.2 Conclusion	40
6. ACKNOWLEDGMENT.	42

	<u>Page</u>
7. APPENDIX I REFERENCE	43
8. APPENDIX II NOTATION	45
9. TABLES AND FIGURES	47

1. INTRODUCTION

1.1 Object

The purpose of this investigation was to study the effect of shear connector spacing on the behavior and strength of composite beams subjected to heavy concentrated loads near the supports.

1.2 Background

The problem of determining the ultimate strength of concrete-steel composite beams has received much attention in recent years. A large number of laboratory experiments has been reported in the United States and abroad (4, 5, 8 through 18). Among the analytical methods proposed in predicting the ultimate strength of composite beams, that proposed by Slutter and Driscoll (18) has been adopted as the basis of the 1963 AISC specification (2). This theory is based on the results of an experimental study in which no appreciable difference in the ultimate load was observed under a nearly uniformly distributed load, whether a beam had shear connectors spaced uniformly or had the same number of shear connectors spaced according to the shear intensity. The attainment of the same ultimate strength

was explained by redistribution of the horizontal shear force from shear connectors which were heavily stressed to those stressed less heavily. Consequently, for this theory no allowance is required for loss of interaction due to slip at the concrete-steel interface. Following this investigation, the 1963 version of the AISC specification simply recommended that the required number of shear connectors may be spaced uniformly between points of zero and maximum moment.

Under most loading conditions, the above provision provides a satisfactory means of estimating the ultimate strength of composite beams with uniformly spaced shear connectors. However, for certain loading conditions the effectiveness of uniform spacing is questionable.

For example consider a simply supported beam having a uniformly distributed load plus two equal concentrated loads symmetrically placed about midspan so that the magnitude of moment at the concentrated load is only slightly less than the moment at midspan, figure 1.1. The 1963 AISC specification would allow the uniform spacing of connectors over the full span, but under this loading condition it is questionable whether the redistribution of shear force would

take place among the connectors prior to complete fracture of the connectors in the shear span.

To eliminate a possible pitfall resulting from uniform distribution of shear connectors, the British Standard, CP117: Part I (6), has a special provision on the distribution of shear connectors for a loading condition such as the one described. This provision is based primarily on the respective areas of the shear diagram between points of zero and maximum moments, and the distribution of the shear connectors according to the intensity of shear force along the span.

At the time this investigation was initiated, no such design guide was available in this country. Since then the AISC has adopted (February 1969) a new specification in which a provision similar to the one in the British Standard has been incorporated. To date, however, experimental data to substantiate either of the two methods of shear connector spacing, spacing according to the shear force or a uniform spacing, are insufficient.

1.3 Notation

The symbols used in this paper are defined where they first appear and are listed alphabetically for easy reference in Appendix II.

1.4 SI Conversion Units

In view of present accepted practice in this country in this technological area, common U.S. units of measurement have been used throughout this paper. In recognition of the position of the USA as a signatory to the General Conference on Weights and Measures, which gave official status to the metric SI system of units in 1960, the author assists readers interested in making use of the coherent system of SI units, by giving conversion factors applicable to U.S. units used in this paper.

Length 1 in = 0.0254* meter
 1 ft = 0.3048* meter

Area 1 in² = 6.4516* x 10⁻⁴ meter²
 1 ft² = 0.09290 meter²

Force 1 lb(lbf) = 4.448 newton
 1 kip = 4448 newton

*Exactly

Pressure, Stress

$$1 \text{ psi} = 6895. \text{ newton/meter}^2$$

$$1 \text{ ksi} = 6.895 \times 10^6 \text{ newton/meter}^2$$

Mass Volume

$$1 \text{ lb/ft}^3 \text{ (1bm/ft}^3\text{)} = 16.02 \text{ kilogram/meter}^3$$

Moment

$$1 \text{ kip-in.} = 113.0 \text{ newton/meter}$$

*Exactly

2. EXPERIMENTAL INVESTIGATION

2.1 Scope

Six beams were tested under two symmetrically placed concentrated loads near the support (figure 2.1). To examine the influence of the length of shear span on strength, the position of these loads was varied for each of three pairs of beams. The loads were placed at 3, 4, and 5 feet away from the end supports, thus giving shear-span ratios (the ratio of shear span to the length of the beam) of 0.15, 0.20, and 0.25, respectively, for the 20-foot-span beam. Each pair of beams consisted of one beam with shear connectors spaced according to the shear force diagram, and the other with shear connectors uniformly spaced. The former had the required number of studs as obtained from a theoretical analysis spaced within the shear span, and the latter had the same total number of studs spaced uniformly over the entire length of the beam. These beams all had headed stud shear connectors of the type most commonly used in building structures.

The six beams were designated 3G1, 3U1, 4G1, 4U1, 5G1 and 5U1 where in each case the first number represents the length of shear span in feet. The letter G or U respectively

denotes group spacing of studs in the shear span or a uniform spacing along the length of the beam. The last number is used to differentiate between these six beams and other tests which will be covered in subsequent reports.

2.2 Description of Specimens

The test specimens were designed on the basis of the provisions given in the 1963 AISC specification (2) with the following two limiting criteria: the cross section was proportioned so that the steel beam could yield before the concrete slab reached its full compressive strength; the number of shear stud connectors used for each half of the span was about 50 percent of the number that would be needed to develop complete interaction between the concrete slab and the steel beam. The first limitation was to avoid a sudden failure of the beam at ultimate load, and the second limitation was to ensure shear failure of studs instead of flexural failure of either the steel beam due to general yielding or the concrete slab due to crushing.

All test specimens had the same cross sectional dimensions and length. The salient dimensions of the specimens are shown in figure 2.2. The steel beams were cut from rolled sections of W12x27 of ASTM A36 steel. The mechanical

properties of the steel beams, determined from the standard tensile coupon test, are listed in table 2.1. Two standard tensile coupons having an 18 in gage length were cut from each of the top and bottom flanges and from the web. Static yield stresses listed in the table were those obtained beyond the yield point under a zero rate of straining. All steel beams had a pair of full-length $3 \frac{1}{8} \times \frac{1}{4}$ in plate bearing web stiffeners at the load points and end supports.

The location of the studs on each beam is shown in figure 2.3. In the G series specimens, a total of 10 headed studs, $\frac{1}{2} \times 3$ in long, was used in the shear span. To prevent the separation of the concrete slab from the steel beam, additional studs were placed between the two load points (constant moment region) at a distance not greater than 3 feet center-to-center. In the U series beams, the same total number of studs used in the G series beams was placed uniformly over the full span.

2.3 Fabrication of Specimen

Prior to welding the studs on the steel beams, the welding equipment was calibrated by welding several studs on a steel stub cut from the same rolled section as was used for the beams. The quality of the weld was verified by

inspecting visually the weld-fillet around the stud and by bending the stud through an angle of 45 degrees by striking it with a hammer. The mechanical properties of the stud were obtained by means of tensile tests using the stud itself as a test specimen, and these are given in table 2.1.

Ready-mix concrete made from silica sand and 3/4 in maximum size crushed limestone was used for the slab. The average compressive strength of three 6 x 12 in cylinders at the time of test is given for each specimen in table 2.2 together with the computed modulus of elasticity of concrete (1) and the modular ratio n . The slab was reinforced by 6 x 6 in - 4/4 gage welded wire fabric at 1 1/2 in above the bottom surface. In addition, to prevent longitudinal splitting of the slab over the beam, #5 deformed bars were placed transversely on top of the welded wire fabric at 6 in on centers; the reinforcement is shown in figure 2.4. The slab was moist-cured for three days with the exposed surface covered with wet burlap and a polyethylene sheet. The form was then removed, and the specimens were allowed to cure in the dry condition in the laboratory for at least one week prior to testing. Concrete test cylinders were cured alongside the concrete slab under the same curing conditions.

2.4 Test Setup

A schematic diagram depicting the loading system and the test setup is shown in figure 2.5. Two symmetrically-disposed line loads were applied to the top surface of the slab by means of spreader beams pulled down by two 60-kip capacity hydraulic rams anchored to the tie-down floor. These rams were supplied with oil fed through a common manifold which provided equalized hydraulic pressure in each ram at all times.

2.5 Instrumentation

Three types of measurements were taken in this test series: load, strains and displacements. The magnitude of the applied loads was measured by load cell placed in series with each ram. Strain measurements on the slab were taken by means of electrical resistance SR-4 paper-back gages of 1 in gage length and those on the steel beam by foil gages of 1/4 in gage length. The strain gages were located only at midspan.

All displacements, including vertical deflections and slip measurements along the interface between the slab and beam, were measured by means of linear variable differential

transformers (LVDT), calibrated to read increments of ± 0.0001 in. The locations of the LVDT's and strain gages are shown in figure 2.6. For midspan vertical deflections an LVDT of ± 3.0 in stroke was used, while for the remaining displacement measurements LVDT's of ± 1.0 in stroke were used. Dial gages graduated in 0.001 in division were also used to supplement the LVDT readings as a potential error check.

All data were monitored by an automatic digital data acquisition system and were processed with SPEED* using the UNIVAC 1108 electronic digital computer located in the Computer Center of the National Bureau of Standards. In addition, both vertical deflections at midspan and slip between the slab and the steel beam at the ends were recorded on X-Y plotters for visual display during the tests.

2.6 Test Procedures

The loads were applied in increments of predetermined magnitude. In the elastic range this magnitude was controlled by the amount of the load indicated by the load cell

*SPEED is a problem-oriented language for computer use written in FORTRAN IV developed at the National Bureau of Standards for general purpose data processing.

readings, whereas in the inelastic range it was controlled by the magnitude of the midspan deflection. Readings of all instruments were taken at each load level. This procedure was followed throughout a test until the midspan load-deflection curve plotted during the test by the X-Y recorder indicated a decrease in load level with a substantial increase in the deflection. At this point the specimen was unloaded to zero load.

Upon completion of each test, the specimen was removed from the test bed and the concrete slab was air-hammered from the steel beam for visual inspection of stud failure. In order to assess the soundness of studs remaining on the steel beam, these were bent at least 45 degrees with a sledge hammer. The studs were assumed to be undamaged if no evidence of cracks was observed in the weld or in the stem of the stud.

3. TEST RESULTS

3.1 Mode of Failure

Visual observations during tests and post-failure examinations of the beams, the latter made by removing the concrete slab, indicated that all test beams failed due to fracture of shear connectors, either in the stem of the stud or in the base metal. This is in agreement with the original design criterion that shear failure of studs would precede flexural failure of either the concrete or the steel beam. Those studs which were sheared from the steel beam and those remaining on the beam after the "bend test" are shown in figure 3.1. It is seen in this figure that the final failure of the beams was brought about by stud failure primarily in one end of the beam. The actual number of studs that sheared from the beam at ultimate load is not known since fracture of studs undoubtedly took place mostly in the post ultimate load range. However, it is worthy of note here that the shear failure of studs was not confined to the shear span alone but also extended into the constant moment region. This suggests the transfer of shear force from studs in the shear span to studs in the constant moment region. Since no direct measurements were taken of the force distribution on individual studs in this series of

tests, no conclusive assessment can be made as to the validity of such a postulation. It will be shown later, however, that such a force transfer is possible as indicated by computer analysis.

3.2 Ultimate Loads

The numerical values of the failure loads, P_u^{ex} , are listed in table 3.1, together with several reference loads for comparison. These include the working load, P_w , computed with the connectors in the shear span according to the 1969 AISC specification*, the load corresponding to the plastic moment of the steel beam alone, P_p , the load corresponding to initial yielding of the tension flange computed using transformed section, P_y , the theoretical ultimate load based on the birectangular stress block, P_u^{th} , assuming complete composite action, and the ultimate load obtained from computer analysis P_u^C . It is apparent from this table that while none of the beams reached the respective ultimate load of complete composite action, the number of studs used in the beams was sufficient for all beams to exceeded P_y .

*No provision was given in the 1963 AISC specification to compute the load capacity of composite beams having partial shear connection.

3.3 Slip Measurements

The progressive increase in interface slip between the concrete slab and the steel beam along the length of the beam is plotted in figures 3.2 through 3.7. At several load levels up to the ultimate load slip readings are plotted on the vertical axis at specific points along the beam (see Section 2.3). These points are connected by straight lines with an assumption that the slip at midspan is zero due to symmetry of the geometry of the beam and of the position of the loads. The load positions are indicated by arrows.

The following points are worth noting in these figures. First, in all beams the amount of slip developed along the beam was nearly negligible up to about 20 kips. Subsequently slip increased at greater rates, and in several beams, slip increased more than tenfold for a load increment of about 20 percent of the previous load level. In beam 5G1 slip increased substantially while the load dropped about 10 percent. The above observations seem to suggest that both frictional and bond resistances were active up to this load level. Secondly, contrary to a common supposition that the maximum slip would take place at the ends of composite beams, in several beams a maximum slip was observed at some distance away from the end, although this maximum value was not

significantly greater than that of the end slip. An examination of the slip plots indicates that this phenomena is not related to either the location of loads or the arrangement of shear connectors.

Since the degree of composite action, in general, is dependent upon the amount of slip at the interface, the end slip, although not the maximal value, does indicate the overall slip behavior, and the loss of composite action may be seen from plots of end slip. For each pair of beams of the same shear span, the progressive growth of end slip at the end which had the most slip is plotted in figures 3.8, 3.9, and 3.10. In these figures, it is apparent that as noted in the previous figures, the slip at the end of the beams was almost negligible up to the load level of about 20 kips for both the G and U series beams, indicating a negligible loss of interaction between the concrete slab and steel beam at this load level. Thus, it can be said that, with the working load near or below the 20-kip load for all the beams, complete interaction may be expected within the working load range.

The magnitude of the end slip, except in the 3-ft shear span beams, remained negligible up to about 85 percent of the ultimate load. Only when near, or after reaching, the

ultimate load did the end slip increase rapidly. This result indicates that a high degree of composite action could be expected if the load level is maintained below about 85 percent of ultimate load.

From this discussion it becomes apparent that discernible differences in beam behavior due to different arrangements of connectors should not be expected until after bond and friction have been overcome, which would be in the post working load range. A comparative examination of the test results of the two types of beams having the same shear span - figures 3.2 through 3.7 - reveals that in the post working load range, the overall magnitude of slip along the beam was indeed greater in the U series beams than in the G series beams. When end slips are compared - figures 3.8, 3.9, and 3.10 -, a pronounced difference can only be seen in the beams having 3-ft shear span. As the shear span increased to 4 and 5 feet, the difference in the end slip in the post working load range became negligible. For example, in beam 3U1 the end slip was about 0.09 inch at 47.4 kip, while in beam 3G1 it was about 0.035 inch at the same load, or less than half the slip in beam 3U1. On the other hand, in beams 4U1 and 5U1 the end slip was either less than or equal to that of beams 4G1 and 5G1, respectively. The difference in the slip behavior in the 3-foot-shear-span

beams should be expected because the total number of shear connectors in the shear span of beam 3U1 was only 40 percent of those in beam 3G1.

In summary, slip was negligible up to the working load level due to the restraint offered by bond and friction at the concrete-steel interface. Slip would increase rapidly beyond the working load level with the U series beams having a greater slip than the G series beams, particularly when the number of shear connectors in the shear span of the former beams are less than 50 percent of that of the latter beams. Thus, it follows that in order to resist slip, shear connectors placed in the shear span are more effective than the same number of shear connectors spaced over the entire beam.

3.4 Load-Deflection Curves

Midspan deflection, Δ_{ϕ} , plotted against the applied load, P, is shown for all six beams in figures 3.11, 3.12 and 3.13. In each figure the test points of a pair of beams of the same shear span are plotted for direct comparison of the difference in load-deflection behavior between the G series beam and the U series beam. For ease of reference, the elastic load-deflection curves of full composite section and of steel

beam alone and the levels of the reference loads P_w , P_y , P_p , and P_u^{th} are also indicated.

The curves of elastic deflection due of bending and shear were calculated using transformed sections. In calculating shear deflection, the vertical shear carried by the slab and by the steel beam are proportioned accordingly to the respective area of the shear flow diagram, and only the steel beam with its proportion of the vertical shear (about 75 percent) was used with an assumption that the web carries all the shear. It was found that the shear deflection so computed was sufficiently accurate when compared with the one calculated by the strain energy method using the entire cross section. For the beams reported herein, the shear deflection ranged from 6 to 7 percent of the bending deflection.

These predicted deflections are close to the test results for all six beams within the working load range. The deflection plots thus indicate that, since no allowance was made for interface slip in computing the elastic curves of the composite sections, all the beams essentially behaved as a beam having full composite action. This agrees with the observation of negligible end slip in all beams below the working load level. However, as pointed out earlier the

delay in the development of slip probably results from the resistances offered by bond and friction.

Beyond the working load range, the experimental deflection curves of the G and U series beams deviated from the linear elastic curve with a rate of deviation greater in the U series beam than in the G series. Since the diminution of the flexural stiffness (EI) is directly related to the loss of interaction, this behavior can be related to the difference in the magnitude of slip distribution discussed in the previous section, where slip was, in general, greater in the U series beams than in the G series. With greater deflections in the U series beams than in the G series beams, it follows that the loss of the flexural stiffness would be greater in the former beams than in the latter.

The difference between the load-deflection behavior of the G series beams and the U series beams was also evidenced by the ascending and descending branches of the load-deflection curve near the ultimate load. For example, if at ultimate load, the deflection curves of beams 4G1 and 5G1 are compared with those of beams 4U1 and 5U1 (figures 3.12 and 3.13), it is seen that while beams 4U1 and 5U1 attained the ultimate load gradually and thereafter unloaded in the same manner, beams 4G1 and 5G1 reached the ultimate load shortly after

the deflection deviated from linearity and subsequently unloaded at a steeper rate than beams 4U1 and 5U1.

A similar difference in the deflection behavior, as was observed between the G and U series beams of the 4- and 5-ft shear spans, however, was not noted in the beams of 3-ft shear span. The deflection curves of beams 3G1 and 3U1 in figure 3.11 shows that both beams behaved the same where the ultimate load was attained gradually and unloaded in the same manner. This deflection behavior of beam 3G1 was certainly contrary to what might have been expected if the difference in deflection behavior is related to how shear connectors are distributed. Having the extreme disparity in stud arrangements between beam 3G1 and 3U1, it is expected that such a difference to be more pronounced in the 3-ft shear span beams than in the beams of 4- and 5-ft shear span. One of reasons for absence of this behavior may be related to the considerably lower concrete strength which beam 3G1 had (2900 psi) compared with the others (4200-5200 psi). The effect of concrete strength on the shear connector behavior investigated by others (19, 20) showed that shear connectors behave in a more ductile manner in low strength concrete than in high strength concrete. By extending this result to the behavior of the studs in beam 3G1, the ductile behavior observed in beam 3G1 can be accounted for.

In summary, below the working load level, all test beams essentially behaved as beams having complete interaction irrespective of the types of shear connector arrangement, resulting in essentially elastic deflection behavior. However, above the working load level, a greater inelastic deflection was observed in the U series beams than in the G series.

3.5 Strain Measurements

Strain distributions over the cross section of each beam at the midspan are shown in figures 3.14 through 3.19. It can be seen in these figures that the discontinuity of the strain at the concrete-steel interface developed from the early stage of loading, indicating some small losses in interaction between the concrete slab and the steel beam. This discontinuity of strain became greater as the load increased and, with the exception of beam 4G1, the top flange strain of steel beams changed its sign from tension to compression at ultimate load, thereby losing considerable amount of composite action.

The degree of loss of interaction can be estimated qualitatively from the discontinuity of strains at the interface. In the case of no composite action, the slab and the steel

beam act independently of each other resulting in a complete discontinuity of strain at the interface with the magnitude of strains equal but in opposite signs both at the top and bottom of the concrete slab and at the top and bottom of the steel beam. On the other hand, in the case of full composite action, both the concrete slab and the steel beam act as a single member resulting in no discontinuity of strain at the interface. Thus, the magnitude of strain at the bottom of the concrete slab and the top of the steel beam are equal and also in the same sign. By considering these two extreme conditions, it is seen from the strain distribution plots that all beams retained a high degree of interaction up to the load level of about 85 percent of the failure load. The magnitude of the strain discontinuity was less than 100 micro in/in at this load level. In addition, the top flange strain of all steel beams remained in tension, indicating the compressive force was acting only on the slab in developing the cross-sectional moment. Only near or at the failure load, the strain in the top flange, except in beam 4G1, changed from tension to compression as a consequence of a large slip at the interface.

Aside from the development of the discontinuity at the interface, slip also had an influence on the curvature of the slab and the steel beam since it reduced the

effectiveness of composite action. When the slab or the steel beam act either together or separately, they have the same curvature. Any other intermediate interaction conditions resulting from partial-composite action leads to a condition where the slab and the steel beam take different curvatures. Change in curvature as indicated by the slope of strain gradient across the slab and the beam can be seen in figures 3.14 through 3.19. At low loads the slope was about the same in the slab and the beam. It was not until the bottom flange of the steel beam began to yield (refer to figures 3.20 through 3.25), that the slope began to differ appreciably. Subsequently, except in beam 4G1, the steel beam assumed its own neutral axis, which resulted in the slab and the steel beam assuming different curvature.

The magnitude and the way in which the stress was distributed over the cross section of the beams tested can be derived from the cross-sectional strain plots (figures 3.14 through 3.19). For reference, the extent to which yielding had penetrated into the steel beam is indicated by the limiting line of the yield strain of the flange, ϵ_{yf} , in each figure. From these figures it is seen that the bottom flanges of all the beams had yielded prior to failure. In beams 3G1 and 5U1, yielding extended up to about the mid depth of the web. For the remaining beams, the yield penetration remained in the lower part of the web.

The concrete strain, on the other hand, remained elastic throughout the entire loading range. The magnitude of the strain at the top of the slab was only about 10 to 20 percent of the ACI Code crushing strain of 0.003. The maximum stresses that correspond to the observed strains at failure were about 1800 psi. Hence, an approximate stress distribution in the slab may be obtained directly from strain distributions by multiplying strain by the modulus of elasticity.

3.6 Pushout Tests

In order to obtain the load-slip relationship of the studs used in the beams, three pushout tests were performed. The pushout specimens comprised a short steel column of W12x27 and a 6 in rectangular normal weight concrete slab cast on each flange. The slabs were attached to the steel column by means of two 1/2 x 3 in studs welded on each flange. The flanges were greased prior to casting the slabs to prevent bond and to reduce the effect of friction during testing. The salient dimensions of the specimen and the reinforcing details are shown in figure 3.26.

The specimens were covered with wet burlap and a sheet of polyethelyne and cured for three days. After curing in the

dry condition in the laboratory for a week, the specimens were tested in a hydraulic testing machine of 600,000 lb capacity. Load was applied on the steel column through the spherical head of the testing machine and was distributed evenly to the specimen through a 1 in steel plate and a 3/4 in plywood sheet.

The slip which took place between the steel column and the slab at the level of the stud was measured with LVDTs (refer to section 2.3). The transducers were mounted on the steel flange and the plunger which travels through the core of the transducer rested on an angle piece attached to the slab.

The averages of individual slip readings taken at each stud location are plotted in figure 3.27. It is seen in this figure that the load-slip relationship is nonlinear over the entire range of the curve. It also appears from this figure that the ultimate shear strength of studs is related to the strength of concrete; however, the magnitude of slip corresponding to the maximum load was about the same for all specimens, 0.25 in.

For the theoretical analysis described in the next section, a nonlinear mathematical expression representing the load-slip relationship (Ref. 7, also refer to section 4.1) was

used. The coefficients of the expression were determined by means of the least square method based on the two curves of higher strength concrete (4210 psi). This expression is shown in figure 3.27 by a dotted curve and it was used throughout the theoretical analysis whenever the computer program was used to analyze the test results.

4. DISCUSSION OF TEST RESULTS

4.1 Computer Program

For theoretical analysis of the composite beams reported herein, a computer program developed by Baldwin, et al., (3) was used. This program assumes that the load-slip relationship of a shear connector in the beam is the same as for a shear connector in the pushout specimen. To express this relationship the authors have adopted a nonlinear equation (7), $Q = A\gamma/(1 + B\gamma)$, where Q is the load on a shear connector, γ is the slip, and A and B are constants determined from pushout tests. Since the analysis is applicable only to symmetrical beams under symmetrical loading condition, the program was developed based on a criterion that the slip at midspan is equal to zero.

To start the computational process, an arbitrary magnitude of the center-span curvature is assumed and the corresponding axial forces at midspan are evaluated. The moment and the corresponding applied load are then computed. To evaluate axial forces acting on any cross section along the beam, the beam is sliced into many segments, each segment containing an individual connector. The axial forces on the cross section of each segment is computed successively from

the center-most section to the end section over the support. The axial forces on the center-most section are computed using the axial forces computed from the assumed curvature and the load-slip relationship obtained from pushout tests. The axial forces on the next segment are computed by applying the compatibility relationship between the slip at the connector and the difference in the interface strain between two successive connectors. This process is continued for each segment of the beam toward the end of the beam. By an iterative procedure the midspan force is corrected by means of assuming different values of the midspan curvature until the force in the slab at the end of the beam becomes zero.

A typical output includes beam deflections at quarter- and midspan, slip distribution along the beam, force in shear connectors and strain distribution in the cross section of two consecutive connectors along the beam.

The computer time for each run of the program varies according to the number of shear connectors in the beam and more importantly the type of computer used. For the beams reported herein and using UNIVAC 1108, the computer time varied between 15 sec. to 1 minute. The author learned after many trials that an intelligent guess on the magnitude of the curvature increment, a part of the iterative procedure

for the correction of the midspan force, is needed in order to reduce the computer time.

In this report unless otherwise specifically stated, the theoretical solution refers to the results obtained using this computer program.

4.2 Interface Slip

It was pointed out in section 3.3 that the growth of slip is greatly affected by friction and bond resistance at the interface of the slab and the steel beam. In order to assess the actual slip which would develop in the absence of these resistances, the theoretical end-slip curves based on computer analysis, which does not take these into account, are plotted for each test beam in figures 4.1, 4.2 and 4.3. In these figures the theoretical predictions are indicated in lines and the experimental results in symbols as described in the figures. In the case where the iterative process did not converge uniquely within a specified number of iterative cycles, the computer analysis was terminated at that point and only the curve obtained to that point is shown in the figures. It is evident from the theoretical curves that if bond and friction resistance were absent, end-slip would develop immediately upon loading

and would increase gradually. This indicates that, in the absence of bond and friction, slip is a gradual process rather than the abrupt phenomenon which was seen in actual tests. In tests a sudden increase in slip is seen when the force in the concrete slab became sufficient to overcome these resistances.

In order to see whether the experimental slip distribution along the beam seen in section 3.3 could be predicted analytically, theoretical slip distributions along the beam are plotted in figures 4.4 through 4.9. For comparison, experimentally observed slip distributions are also shown in the same figures in broken lines. It is seen that, in general, the computer solution predicts remarkably well the magnitude and shape of the slip distribution up to a load level of about 85 percent of ultimate load. However, at or near ultimate load a considerable discrepancy exists between the two because a small change in load results in a large change in slip. This seems to imply that while at low loads the load-slip relationship of studs in the beam can closely be approximated by the one obtained from pushout tests, the same correlation cannot be expected at high loads.

4.3 Deflection

To examine the influence of the bond and friction resistances on the load-deflection behavior, the theoretical load-deflection curves of all six beams are plotted in figures 4.10, 4.11 and 4.12, together with the experimental points and the elastic curves. The computational procedure of the theoretical deflection curve is such that it includes the effect of slip, but it does not include the effect of the bond- and friction-resistance. Thus, any difference in the deflection characteristics resulting from these resistances could be detected from the theoretical curves.

It is seen that in the elastic range, the theoretical curves indicate greater deflection than the respective linear elastic curves based on full composite action and experimental results, except in beams 3G1 and 3U1. Thus, at any given load level the theoretical deflection is about 20 percent greater than the corresponding value on the linear elastic curve. It is also evident that at low loads the theoretical curves departed earlier from straight line than the experimental curves. Since both of these disagreements are attributable to the loss of composite action due to the interface slip, it can be said that in the elastic range

bond and friction provide a sufficient resistance to warrant a complete interaction between the concrete slab and the steel beam.

When over-all deflection curves predicted by the theory are compared with the experimental results, the theory tends to indicate more ductile behavior than observed in tests. This tendency was more pronounced in the G series beams than in the U series beams. In tests of beams 4G1 and 5G1 the load dropped sharply after attaining the ultimate load at a deflection of about one inch, whereas the theoretical curves show a gradual unloading after attaining the ultimate load at a deflection of more than three inches.

Since the characteristics of a composite beam predicted by computer analysis are dependent mainly upon the input of the load-slip relationship of studs, any difference in the deflection characteristics between the ones predicted by computer analysis and experimental results can be attributed to the behavior of studs in the beam which is known to differ from that in the push out. It appears from a comparison of the theoretical deflection curves to the experimental results that studs behave stiffer in beams than in push outs.

4.4 Comparison of Test Results with Theories

Table 4.1 lists the ultimate test moments, M_u^{ex} , and four reference moments. The reference moments include the ultimate moment obtained using the computer program, M_u^C , the ultimate moment based on incomplete composite action by Slutter and Driscoll (18), M_u' , the ultimate moment computed in accordance with the 1969 AISC specification with a load factor of 2.0, M_u^W , and the moment computed based on the simple birectangular stress block, M_u . For comparison the ratios of the experimental moments to the reference moments are tabulated in columns (7), (8), (9) and (10) in the same table.

The ratios of the moments reveal that the Slutter-Driscoll theory gives an upper bound estimate (col. 9) and the AISC method gives a lower bound (col. 10). The spread of the ratios is about 7 to 9 percent on either side of the perfect correlation, 1.0. It is worth noting that all ratios in column 9 are less than 1.0 (the Slutter-Driscoll theory), whereas all ratios in column 10 are more than 1.0. This suggests that, on average, the AISC method would estimate conservatively the ultimate strength of composite beams such as the ones reported herein.

When the three solutions are compared, the computer analysis gives a closer estimate than both the Slutter-Driscoll theory and the AISC method. An average deviation is only 2 percent from the perfect correlation. To obtain such a reasonably accurate estimate, several runs were necessary using the present computer program. Even for a user who is proficient with the program, the author feels that a minimum of two runs is needed to obtain a solution within 5 percent of ultimate load. However, it should be realized that the computer output yields not only the ultimate strength but also provides such useful information as slip and deflection.

4.5 Effect of Shear Connector Distribution on Ultimate Strength

The difference in the ultimate strength as affected by the distribution of shear connectors can be examined by plotting the ratios of the maximum moments of two beams having the same length of shear span but having different distribution of connectors. A plot of such ratios of moments versus the shear-span ratio (a/L) is shown in figure 4.13. In this figure, because the strength of each beam was affected by concrete strength, the maximum experimental moment of each beam was divided by its own full-composite ultimate moment before taking the moment ratios. The ratios so obtained are designated as K^U/K^G in the figure.

For comparison, the ratios of moments predicted by various theories are also plotted in this figure together with the experimental results. It can be seen that theoretical moment ratios range from about 0.8 to 0.9 for shear-span ratios between 0.15 and 0.25. The test result, on the other hand, shows a greater increase in the moment ratio from a shear span ratio of 0.15 to 0.20. At 0.20 the difference in the experimental ultimate moments of the two beams, one having uniform spacing of studs and the other group spacing, is only about 3 percent. As the shear-span ratio increased to 0.25, the moment ratio remained nearly constant at about 0.98. Although a specific inference can not be drawn to such a substantial increase in the moment ratio at $a/L = 0.2$, the experimental results indicate that the loss of ultimate strength due to uniform spacing of studs, as compared with spacing of studs within the shear span, is not as great as the theories predict.

4.6 Distribution of the Interface Shear Force on Connectors

It was pointed out in section 3.1 that the removal of the slab from the steel beam after testing revealed that the failure of studs was not confined only to the shear span but also extended into the constant moment region. This experimental evidence indicates that not only those studs

in the shear span were resisting the shear force but also studs in the constant moment region participated in resisting the shear force. From this reasoning it follows that the horizontal shear force at the interface between points of maximum and zero moment had been greater than the sum of the shear force provided by the connectors in the shear span. Therefore, the excess shear force must have been transferred to the studs in the constant bending moment zone.

To gain an insight into this shear force redistribution, the analytical distribution of the force in studs along the beam at ultimate load for each beam is plotted in figure 4.14 and 4.15 together with the corresponding analytical slip distribution. These plots indicate that although shear ceases to exist beyond the load point (see figure 2.1) the studs in the constant bending moment region do participate in carrying the shear force. The amount of shear force carried by individual connectors is proportional to relative positions of connectors to the position of the applied load. The closer the position of connector to the load, the greater the force it carries.

In order for the above described redistribution of shear force to be valid, a mechanical means of transferring the

force is needed, since the concrete alone is not able to carry a large tensile force. The task of such force transfer can only be assigned to the longitudinal reinforcement in the slab.

At present, knowledge is limited to answer the question of such shear transfer. A research program specifically designed to study the effect of the longitudinal reinforcement on the carrying capacity of composite beams is being undertaken at the National Bureau of Standards.

5. SUMMARY AND CONCLUSION

5.1 Summary

This report has described an experimental study of the behavior and strength of concrete-on-steel composite beams as affected by shear connector spacing. As a primary variable, two types of shear connector arrangements were investigated: spacing of connectors according to shear diagram and spacing uniformly over the entire beam span.

A total of six simply-supported beams was tested under two symmetrically placed concentrated loads about midspan. As the second variable, the position of the loads was varied to study the effect of the shear-span ratio.

Tests were performed on composite beams comprising a 4 x 48 in concrete slab and a W12x27 steel beam of ASTM A36 steel. The slab and steel beam were interconnected by 1/2 x 3 in long headed studs. In addition to beam tests, three pushout tests were made to evaluate the load-slip relationship of the studs used in the beams.

Data procured consisted of vertical deflection measurements, slip at specific points along the beam and cross-sectional strain readings at midspan.

Test results were analyzed and compared with existing theories including the method given in the 1969 AISC Specification.

5.2 Conclusion

Based on the experimental results obtained and analytical studies presented herein, the following conclusions can be stated:

- 1) Variation in shear connector arrangement has little effect on the magnitude and distribution of slip below working load level. However, in the post-working-load range, the test results show that placing shear connectors according to the shear diagram is more effective in resisting slip than having the same number of shear connectors spaced uniformly over the entire beam span.
- 2) Within the working load range, all beams behaved as if there were complete interaction. Thus, the predicted deflections by elastic theory using a transformed section were very close to the experimental results. Deflections observed in the post-working-load range, however, indicate that a greater deflection will occur in a beam with studs spaced uniformly over the beam span than in a beam with studs spaced according to the shear diagram.
- 3) The design procedure given in the 1969 AISC specification gives a lower bound ultimate strength and the incomplete-interaction theory by Slutter and Driscoll gives an upper bound. For the test results reported herein, the computer analysis predicted the ultimate strength better than the above two solutions.
- 4) Test results show that the provision given in the 1963 AISC specification on the spacing of

shear connector is acceptable without impairing the ultimate strength for most loading conditions including the one reported herein, provide the ratio of the length of the concentrated shear span to the length of beam is greater than 0.2. Reduction of the ultimate strength due to uniform spacing of shear connectors appears to be less than 5 percent for the shear-span ratio of 0.2 or greater.

6. ACKNOWLEDGMENT

The investigation reported herein was carried out at the Structures Laboratory of the National Bureau of Standards. The tests were conducted under the direction of Robert G. Mathey, formerly Assistant Chief of the Structures Section.

The author wishes to acknowledge Dr. Edward O. Pfrang, Chief of the Structures Section, and Dr. E. V. Leyendecker, Research Structural Engineer, for their constructive criticisms and suggestions during the courses of this investigation. The author also wishes to express his appreciation to Professor John E. Breen of the University of Texas at Austin and to Dr. Norman F. Some, Assistant Chief of the Structures Section, for reviewing the report and many comments which were incorporated in this report.

Acknowledgment is extended to the laboratory and electronic technicians, particularly Messrs. J. Raines, J. Seiler and F. Rankin of the Structures Laboratory, Building Research Division, who assisted in several phases throughout this research program.

7. APPENDIX I REFERENCE

1. American Concrete Institute, "Building Code Requirements for Reinforced Concrete (ACI-318)," Detroit, Michigan, June 1963.
2. American Institute of Steel Construction, "Specification for the Design, Fabrication and Erection of Structural Steel for Buildings," New York.
3. Baldwin, Jr. J. W., Henry, J. R. and Sweeney, G. M., "Study of Composite Bridge Stringers - Phase II," University of Missouri at Columbia, May 1965.
4. Barnard, P. R. and Johnson, R. P., "Ultimate Strength of Composite Beams," Proc. Inst. Civ. Eng., Vol. 32, October 1965.
5. Barnard, P. R. and Johnson, R. P., "Plastic Behavior of Continuous Composite Beams," Proc. Inst. Civ. Eng., Vol. 32, October 1965.
6. British Standards Institution, "CP 117, Composite Construction in Structural Steel and Concrete, Part 1: Simply-Supported Beams in Building," London, 1965.
7. Buttry, K. E., "Behavior of Stud Shear Connectors in Light-weight and Normal-Weight Concrete," M.Sc. Thesis, University of Missouri, August 1965.
8. Chapman, J. C., "Composite Construction in Steel and Concrete - The Behavior of Composite Beams," Structural Engineer, Vol. 42, April 1964.
9. Chapman, J. C. and Balakrishnan, S., "Experiments on Composite Beams," Structural Engineer, Vol. 42, November 1964.
10. Chapman, J. C. and Teraszkiewicz, J. S., "Research on Composite Construction at Imperial College," Proceedings, Conference on Steel Bridges, London, June 1968.
11. Culver, C. and Coston, R., "Tests of Composite Beams with Stud Shear Connectors," Jour. of St. Div., ASCE, ST2, Proc. Paper 2742, February 1961.

12. Culver, C., Zarzeczny, P. J. and Driscoll, Jr., G. C., "Composite Design for Buildings - Progress Report 12," Fritz Eng. Lab. Report No. 179.2, Lehigh University, June 1960 and January 1961.
13. Daniels, J. H. and Fisher, J. W., "Static Behavior of Continuous Composite Beams" and "Static Behavior of Composite Beams with Variable Load Position," Reports No. 324.2 and 324.3, Dept. of Civ. Eng., Lehigh University, March 1967.
14. Davies, C., "Tests on Half-scale Steel-Concrete Composite Beams with Welded Stud Connectors," Structural Engineer, Vol. 47, January 1969.
15. Johnson, R. P., "Ultimate Strength Design of Sagging Moment Regions of Composite Beams," Cambridge University Eng. Lab. Technical Report S/11, August 1967.
16. Johnson, R. P., Finlinson, J. C. H., and Heyman, J., "A Plastic Composite Design," Proc. Inst. Civ. Eng., Vol. 32, October 1965.
17. Roderick, J. W. et al., "Behavior of Composite Steel and Lightweight Concrete Beams," University of Sydney Civ. Eng. Res. Report R 74, November 1966.
18. Slutter, R. G. and Driscoll, Jr., G. C., "Flexural Strength of Steel - Concrete Beams," Jour. of St. Div., ASCE, ST2, Proc. Paper 4294, April 1965.
19. Viest, I. M. et al., "Studies of Slab and Beam Highway Bridges, Part IV - Full-Scale Tests of Channel Shear Connectors and Composite T-Beams," Univ. of Illinois Eng. Exp. Station, Bull. Series No. 405.
20. Viest, I. M., "Investigation of Stud Shear Connectors for Composite Concrete and Steel T-Beams," Jour. of ACI, Proc. Vol. 52, April 1956.

8. APPENDIX II NOTATION

The following symbols are used in this paper:

- a = length of shear span;
- f'_c = average compressive strength of 6 in. x 12 in. concrete cylinder;
- L = length of beam (support to support);
- M'_u = ultimate moment based on incomplete interaction theory;
- M_u^c = ultimate moment by computer analysis;
- M_u^{ex} = experimental ultimate moment;
- M_u^G = ultimate moment of a beam with studs spaced according to shear diagram;
- M_u^{th} = ultimate moment based on birectangular stress block (complete interaction);
- M_u^u = ultimate moment of a beam with studs spaced uniformly over the beam span;
- M_u^w = ultimate moment corresponding to the working load;
- P = applied load;
- P_p = load corresponding to plastic moment;
- P_u^c = load corresponding to M_u^c ;
- P_u^{ex} = experimental ultimate load;
- P_u^{th} = ultimate load corresponding to M_u^{th} ;
- P_w = working load based on the 1969 AISC Specification;
- P_y = theoretical first yield load of tension flange;
- Q = load on shear connector;
- γ = slip;

ϵ_{yf} = flange yield strain of steel beam;

$\Delta \xi$ = midspan deflection,

σ_y = yield strength of steel beam; and

μ = micro (0.000001).

9. TABLES AND FIGURES

Type of Specimen	No. of Tests	Yield* Strength (ksi)	Static Yield Stress (ksi)	Tensile Strength (ksi)
Flange	4	-	31.71	59.24
Web	4	-	38.51	64.47
1/2 in. Stud	3	54.57	-	68.00

*Based on 0.2 percent offset strain

TABLE 2.1 Material Properties of Steel

Beam	No. of* Tests	Age (Days)	Compressive Strength f'_c (psi)	Splitting Tensile Strength f'_{sp} (psi)	Computed** Modulus of Elasticity E_c (psi)	n***
3G1	3/3	7	2900	360	3,103,000	9.54
4G1	3/3	7	5280	475	4,187,000	7.07
5G1	3/3	9	4370	420	3,809,000	7.77
3U1	3/3	6	4490	430	3,861,000	7.67
4U1	3/3	8	5000	400	4,070,000	7.27
5U1	3/3	6	4260	400	3,760,000	7.87

* 3 tests for f'_c and 3 tests for f'_{sp}
 ** $W = 145$ lb per cubic ft. was assumed
 *** Based on $E_{steel} = 29,600,000$ psi

TABLE 2.2 Properties of Concrete

Specimen	P_u^{ex}	P_w	P_p	P_y	P_u^{th}	P_u^c
3G1	53.3*	23.4	34.4	44.8	65.6	54.6
4G1	39.4	18.8	25.8	34.4	52.1	41.9
5G1	29.7	14.7	20.6	27.3	41.0	33.4
3U1	47.9	21.7	34.4	45.6	68.6	46.5
4U1	38.8	16.8	25.8	34.3	51.9	36.4
5U1	29.3	13.6	20.6	27.3	41.0	30.1

*All loads are in kip

P_u^{ex} = Experimental ultimate load.

P_w = Working load according to the 1969 AISC specification.

P_p = Load corresponding to the plastic moment of the steel beam alone.

P_y = Load corresponding to initial yielding of the tension flange for the composite beam.

P_u^{th} = Theoretical ultimate load based on birectangular stress block assuming full composite action.

P_u^c = Theoretical ultimate load based on computer program solution.

TABLE 3.1 Experimental and Reference Loads

(1) Specimen	(2)	(3)	(4)	(5)	(6)	(7)	(8)	(9)	(10)
	Moments in kip-ft					$\frac{M_u^{ex}}{M_u}$	$\frac{M_u^{ex}}{M_u^C}$	$\frac{M_u^{ex}}{M_u^{M'}}$	$\frac{M_u^{ex}}{M_u^{W}}$
M_u^{ex}	M_u^C	$M_u^{M'}$	M_u^W	M_u					
3G1	159.9	163.7	170.8	140.7	196.9	0.81	0.98	0.94	1.14
4G1	157.7	167.5	178.8	150.5	208.2	0.76	0.94	0.88	1.05
5G1	148.9	166.9	177.9	146.9	205.2	0.73	0.89	0.84	1.01
3U1	143.8	139.6	145.1	130.3	205.8	0.70	1.03	0.99	1.10
4U1	153.1	145.7	152.6	134.1	207.5	0.74	1.05	1.00	1.14
5U1	146.5	150.5	155.9	135.3	205.0	0.71	0.97	0.94	1.08
					AVG.	0.74	0.98	0.93	1.09

Column (2) - Experimental ultimate moment

Column (3) - Ultimate moment computed by theory (computer solution)

Column (4) - Ultimate moment computed using Eq. (15) of Ref. 18

Column (5) - Ultimate moment computed using the 1969 AISC specification with a load factor of 2.0.

Column (6) - Ultimate moments of composite beam with sufficient shear connectors to develop full composite action (Based on birectangular stress block)

TABLE 4.1 Comparison of Experimental Moments to Theoretical Moments

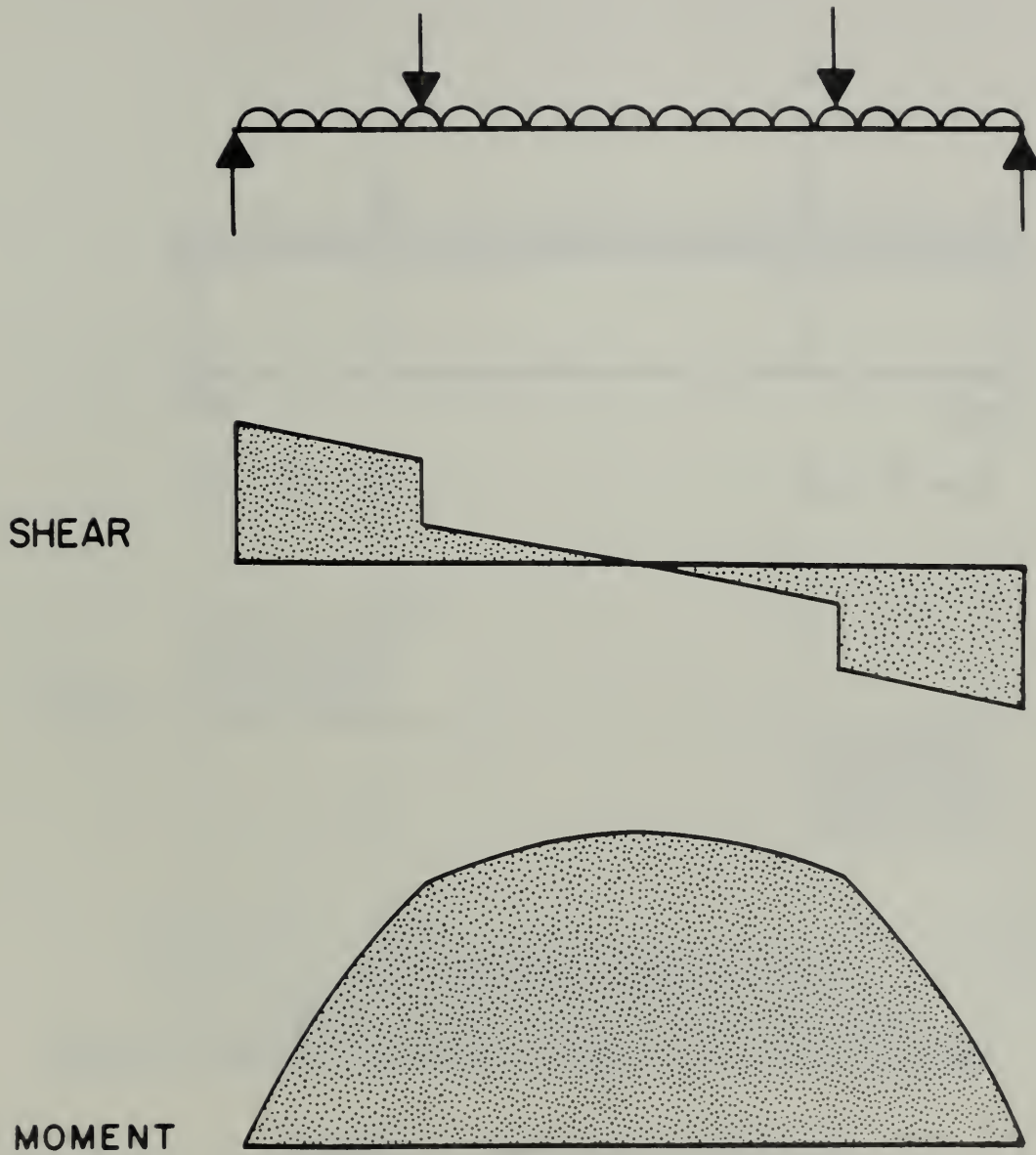


FIGURE 1.1 Shear and Moment Diagrams for a Beam with Distributed and Heavy Concentrated Loads

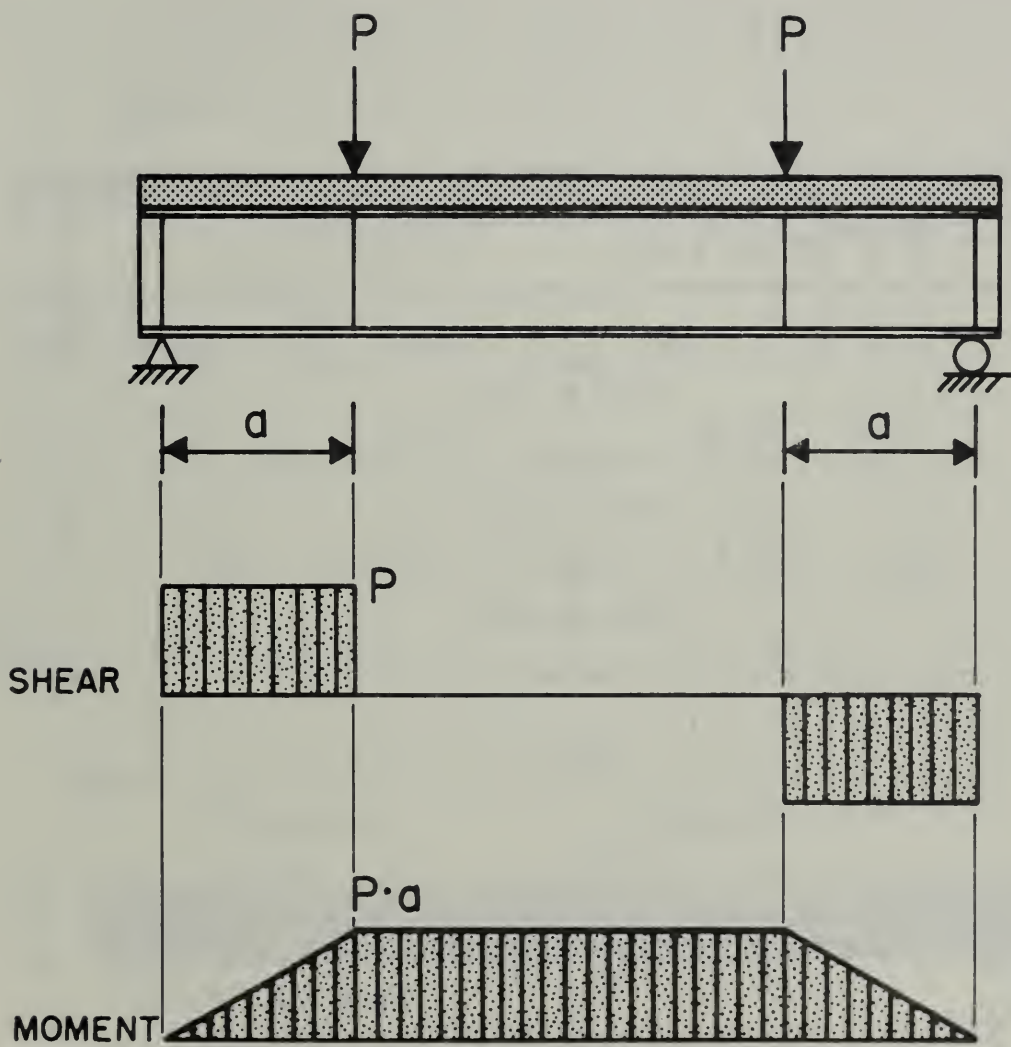


FIGURE 2.1 Test Loading Condition

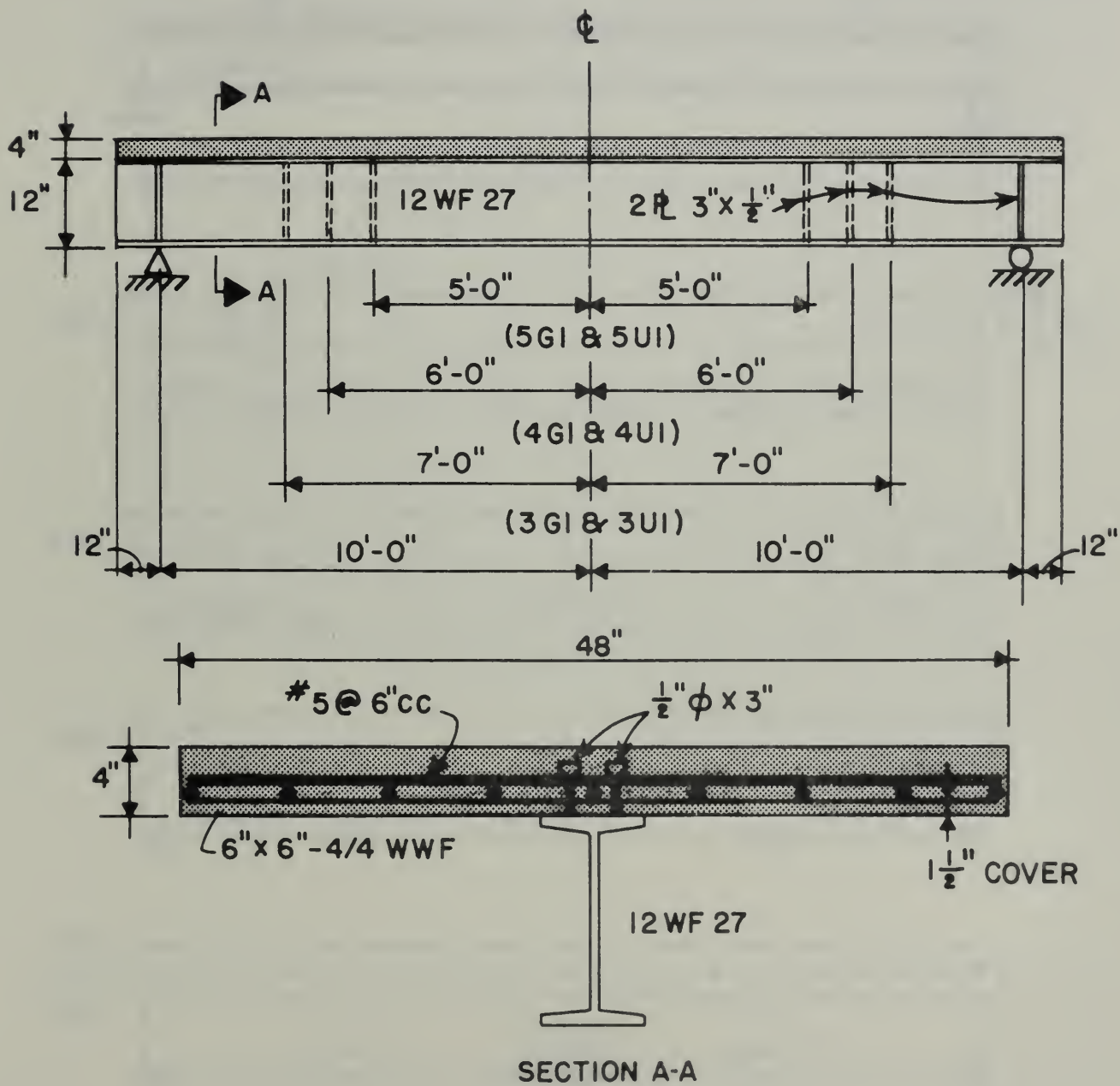


FIGURE 2.2 Dimensions and Details of Test Specimens



[Illegible text block]

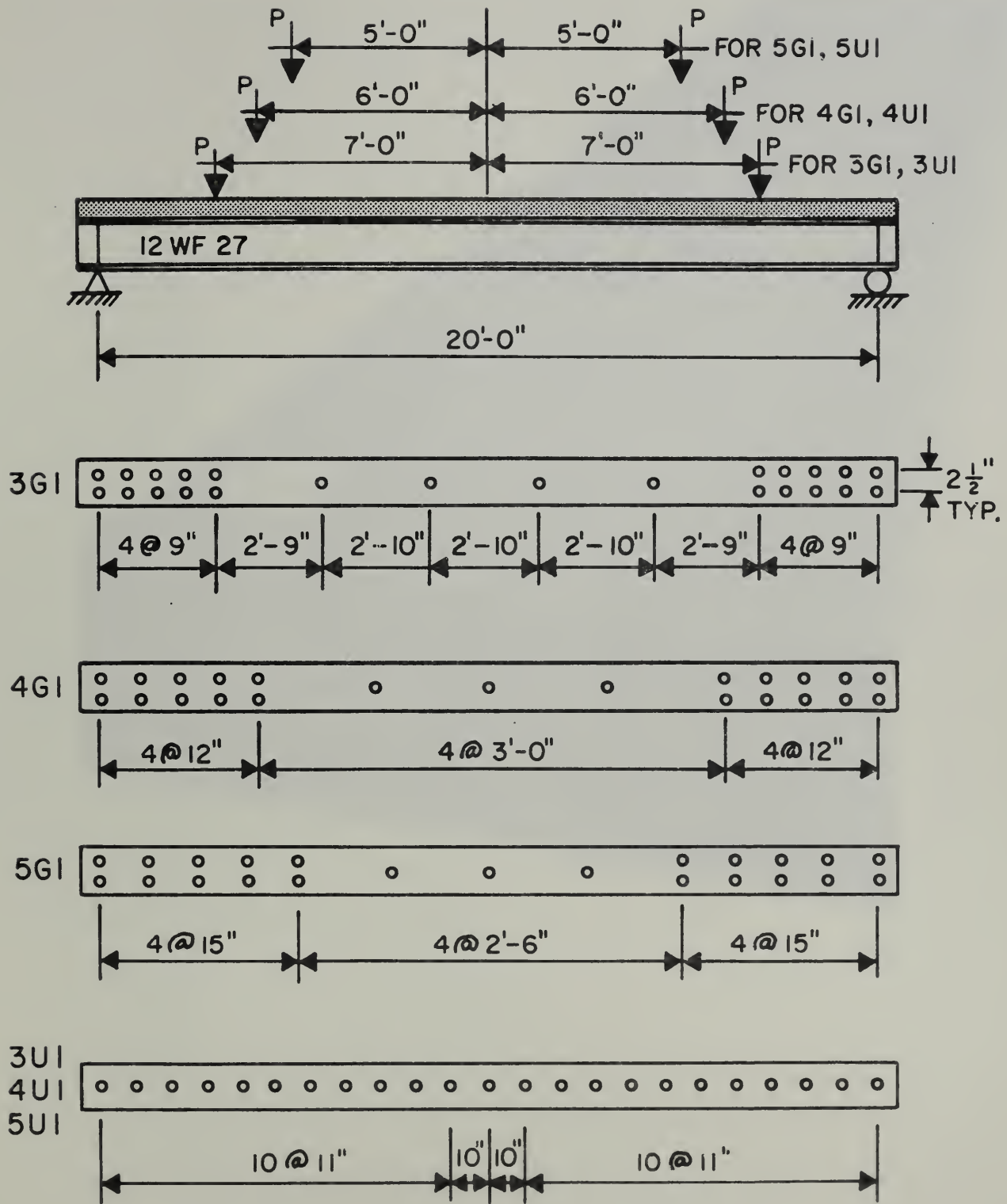


FIGURE 2.3 Loading Arrangements and Shear Connector Spacing

Handwritten text at the top of the page, possibly a title or header.

Handwritten text in the middle section of the page.

Handwritten text in the lower middle section of the page.

Handwritten text in the lower section of the page.

Handwritten text at the bottom of the page, possibly a signature or footer.



FIGURE 2.4 Form and Reinforcement
for Beam 3G-1

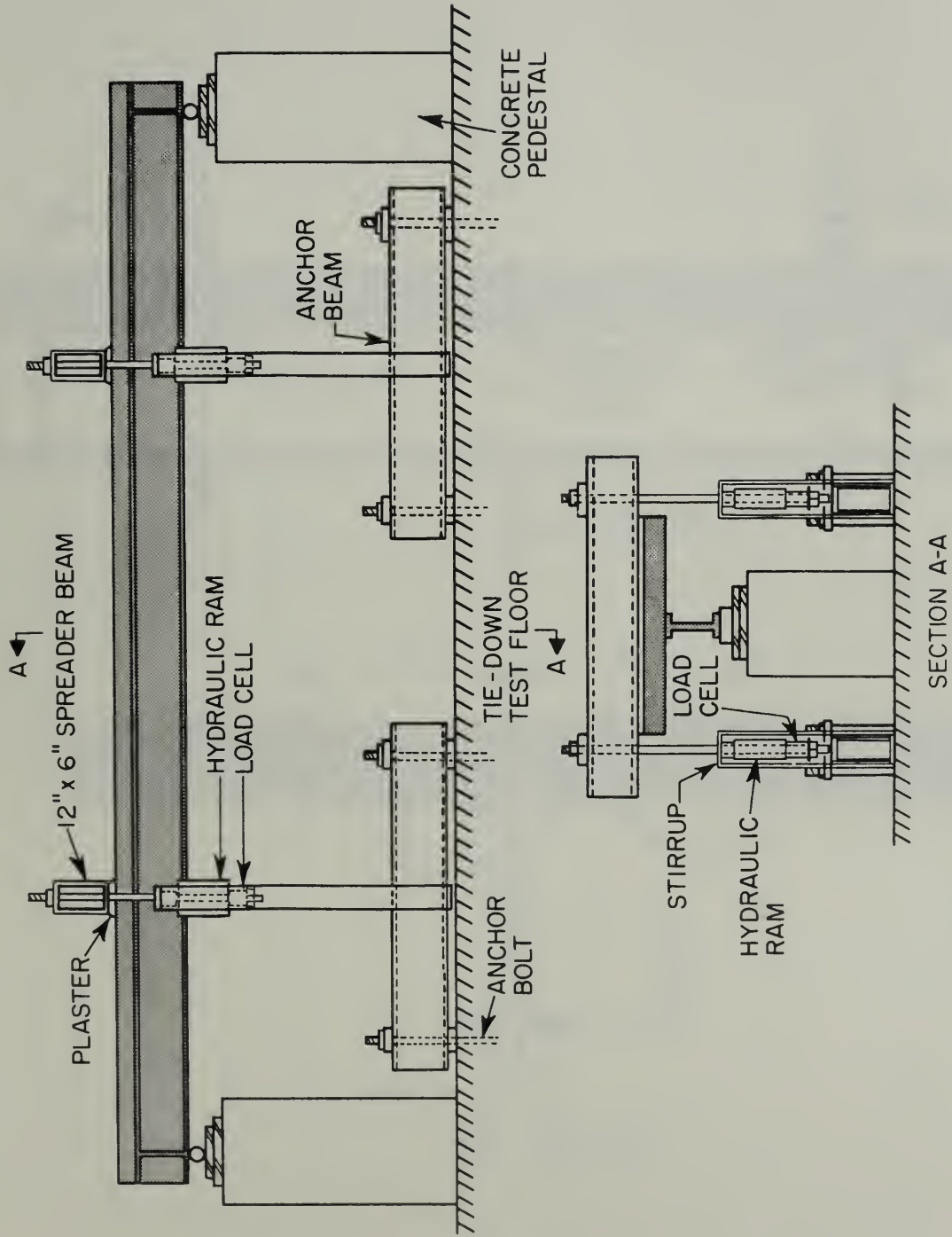


FIGURE 2.5 Test Setup

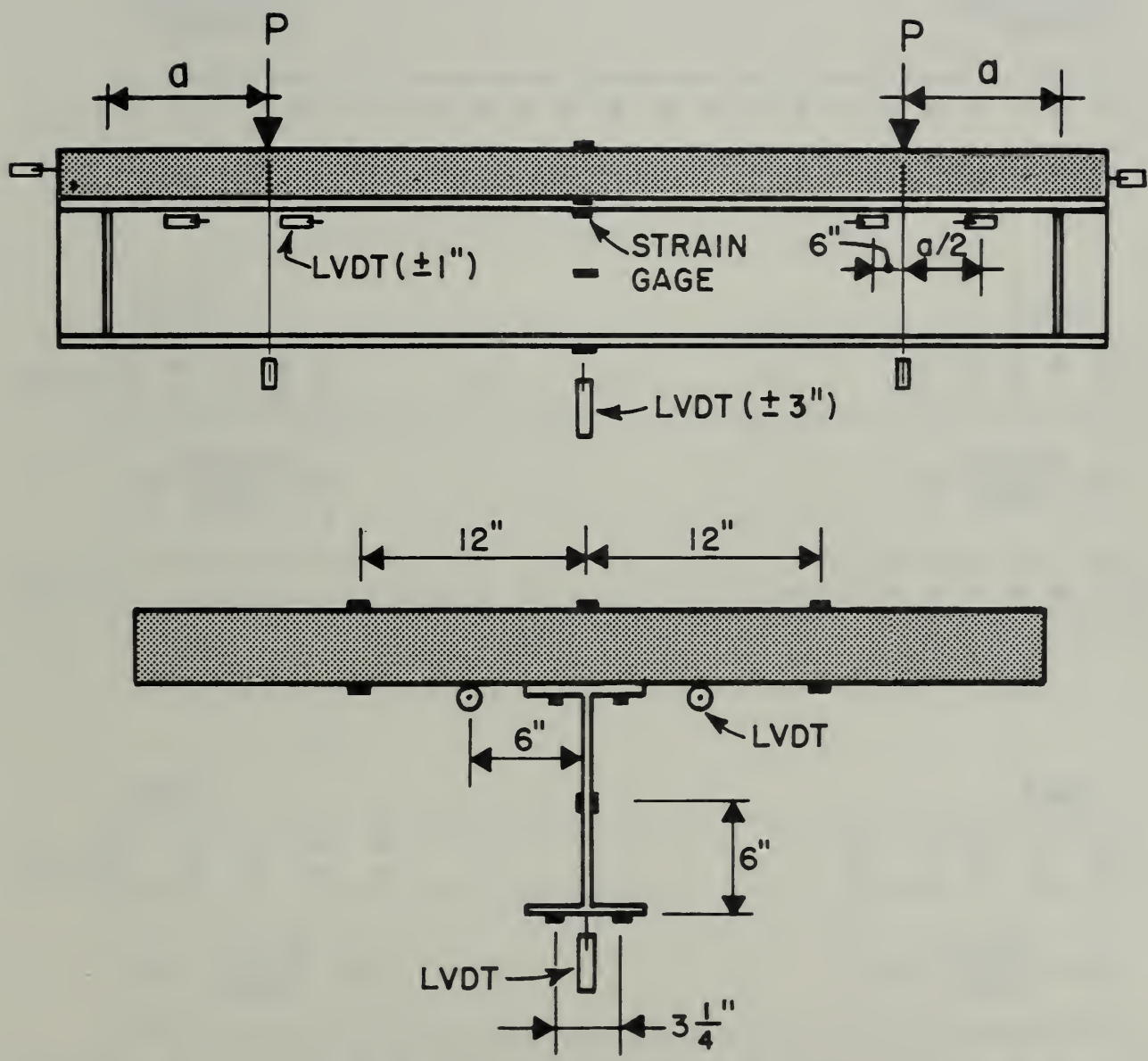


FIGURE 2.6 Location of Instrumentation

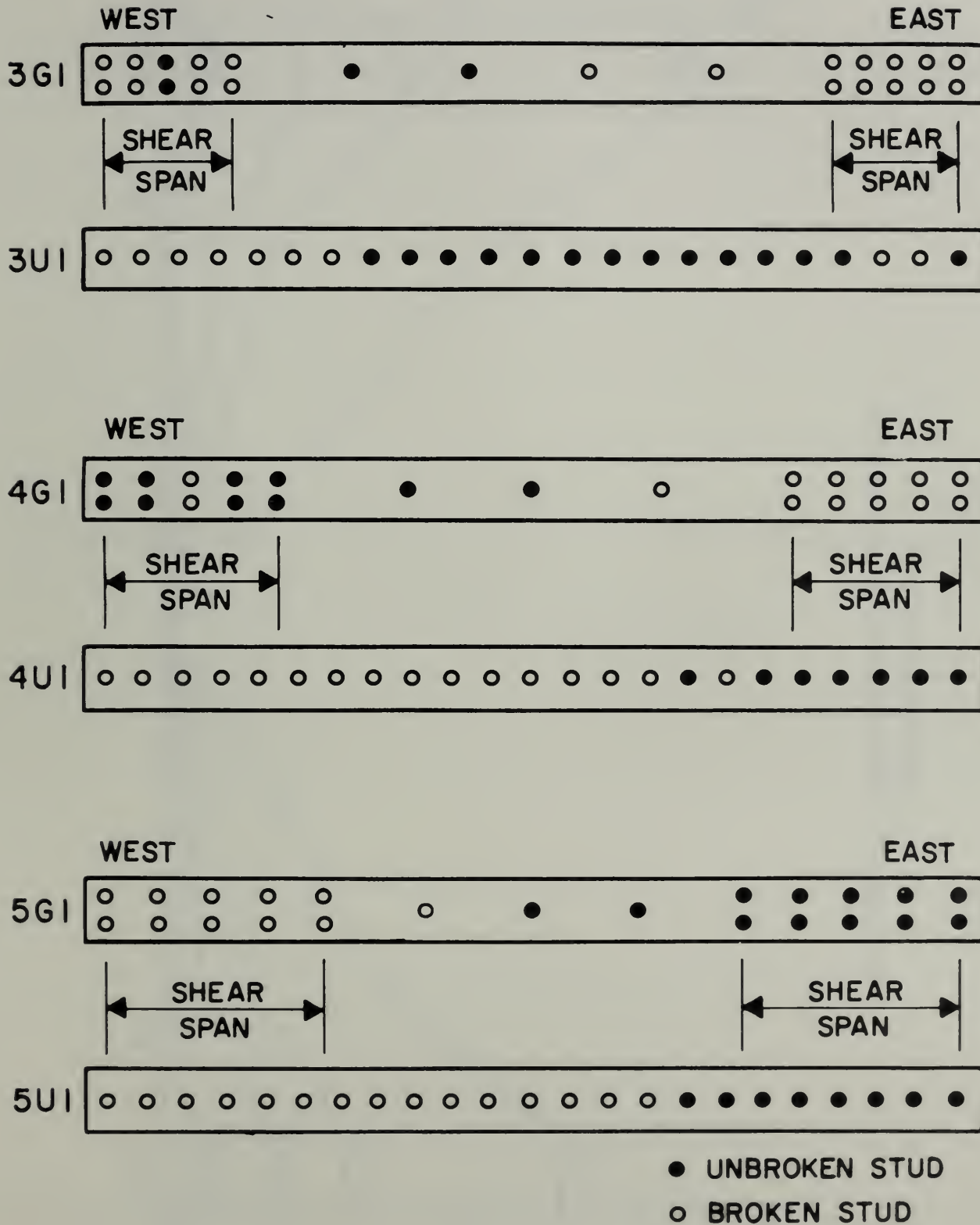


FIGURE 3.1 Location of Failed Connectors

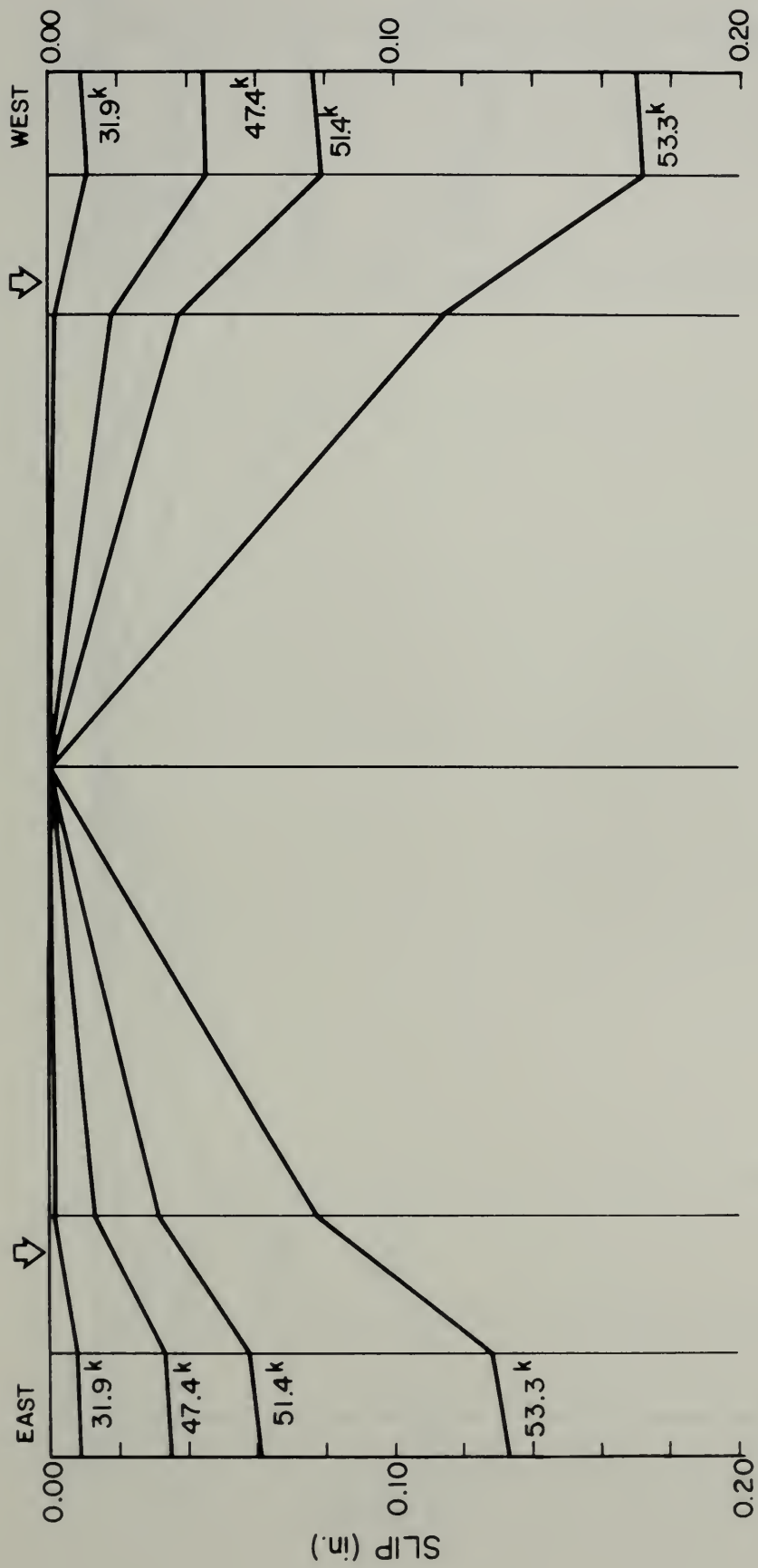


FIGURE 3.2 Experimental Slip Distribution along Beam 3G1



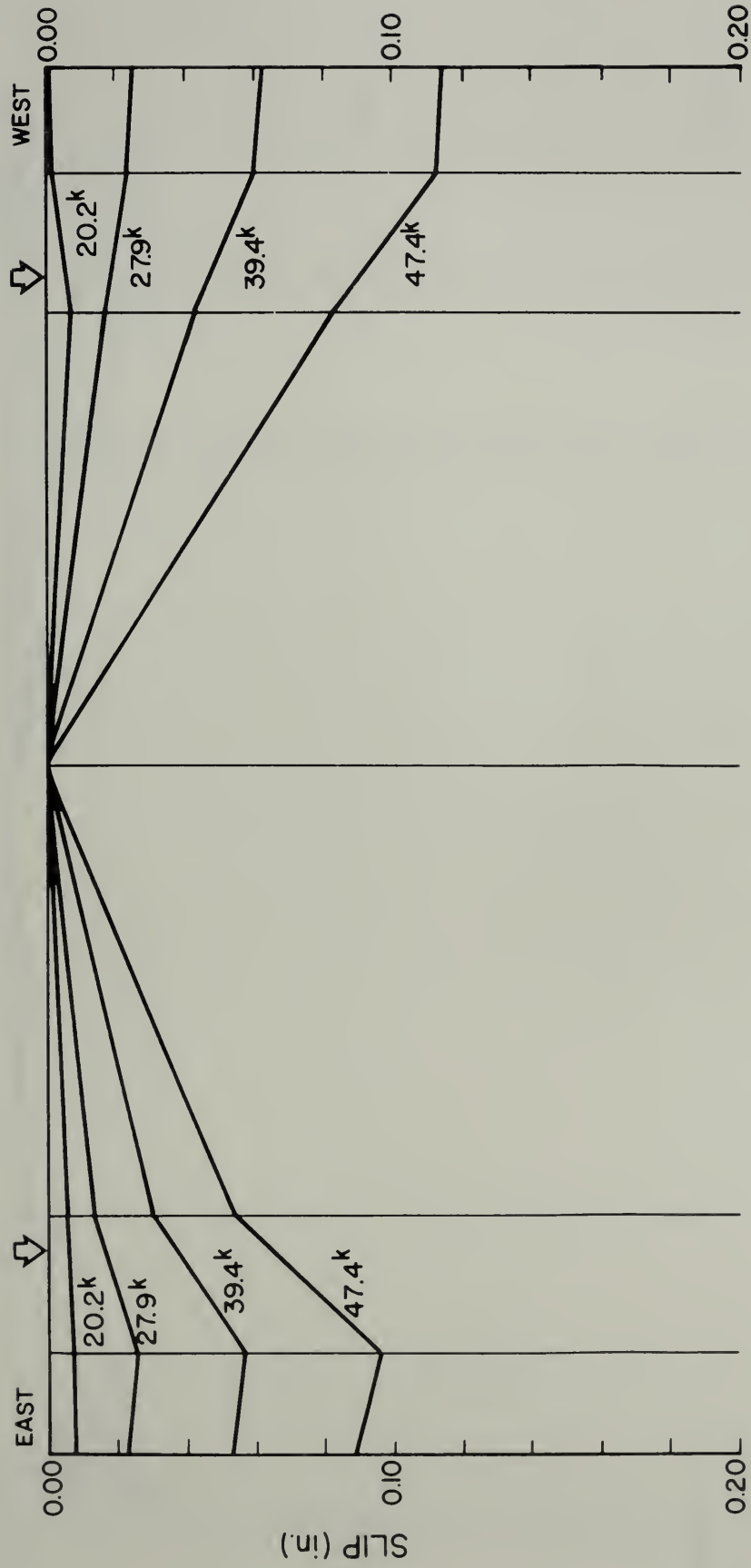


FIGURE 3.3 Experimental Slip Distribution along Beam 3U1

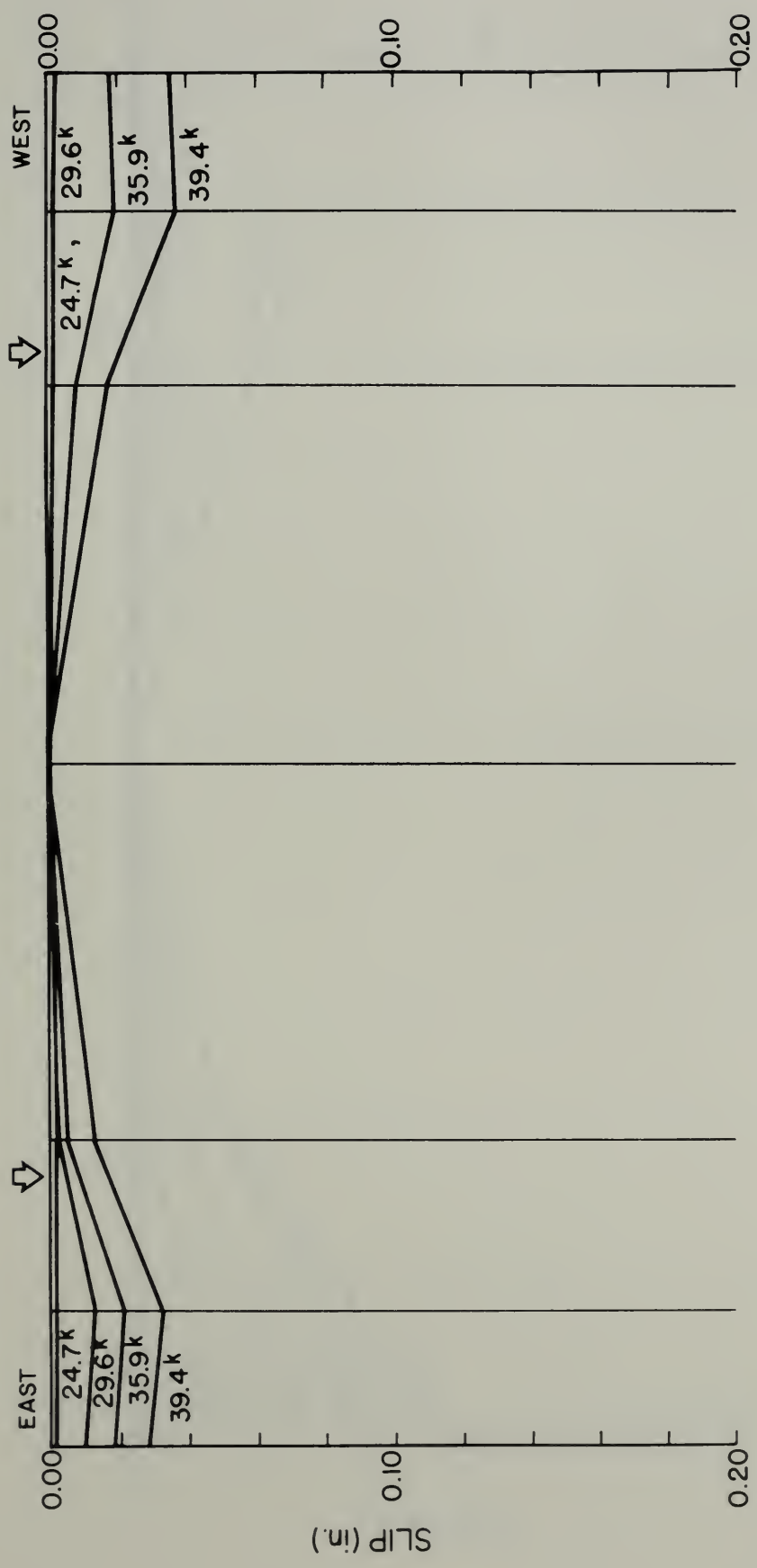


FIGURE 3.4 Experimental Slip Distribution along Beam 4G1



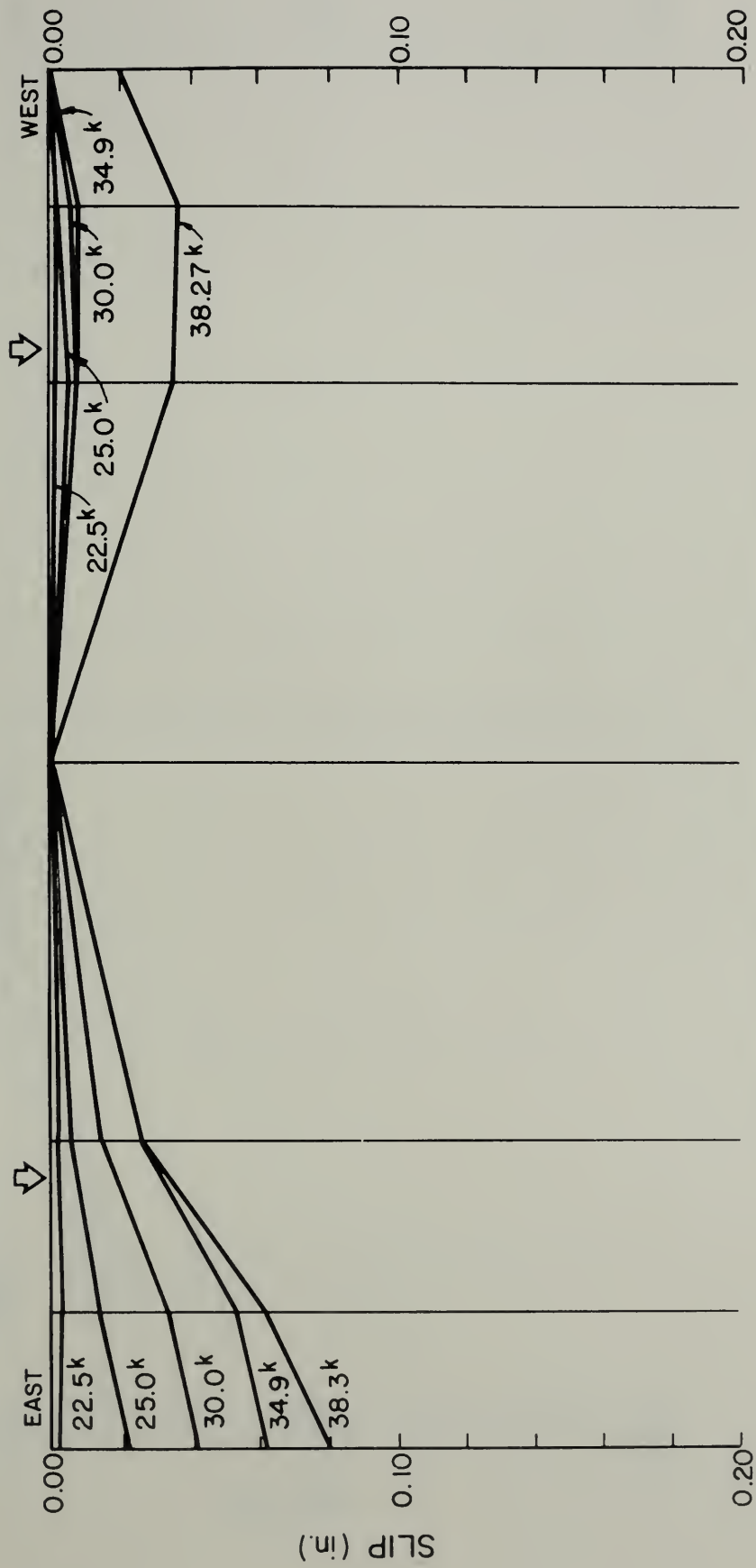
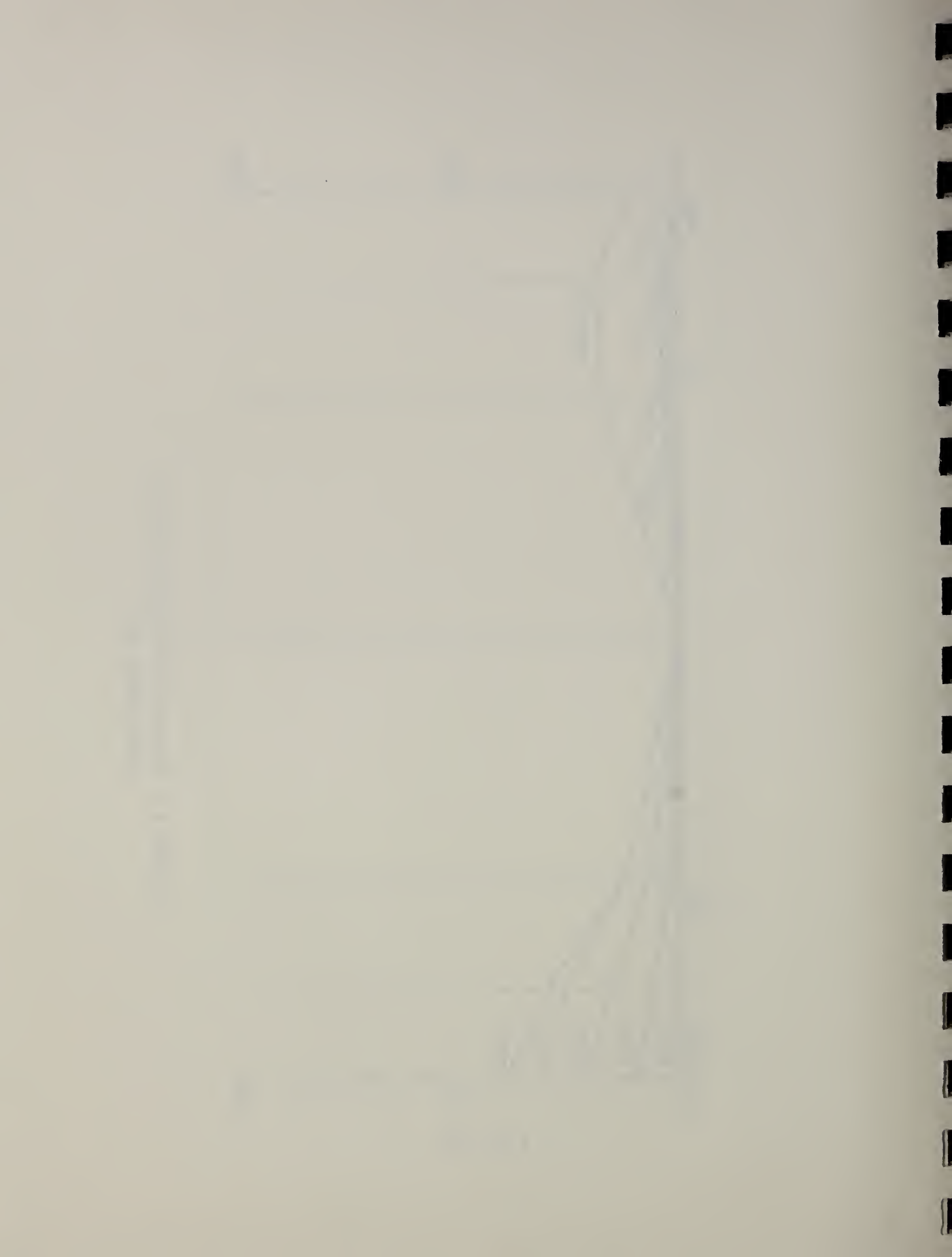


FIGURE 3.5 Experimental Slip Distribution along Beam 4U1



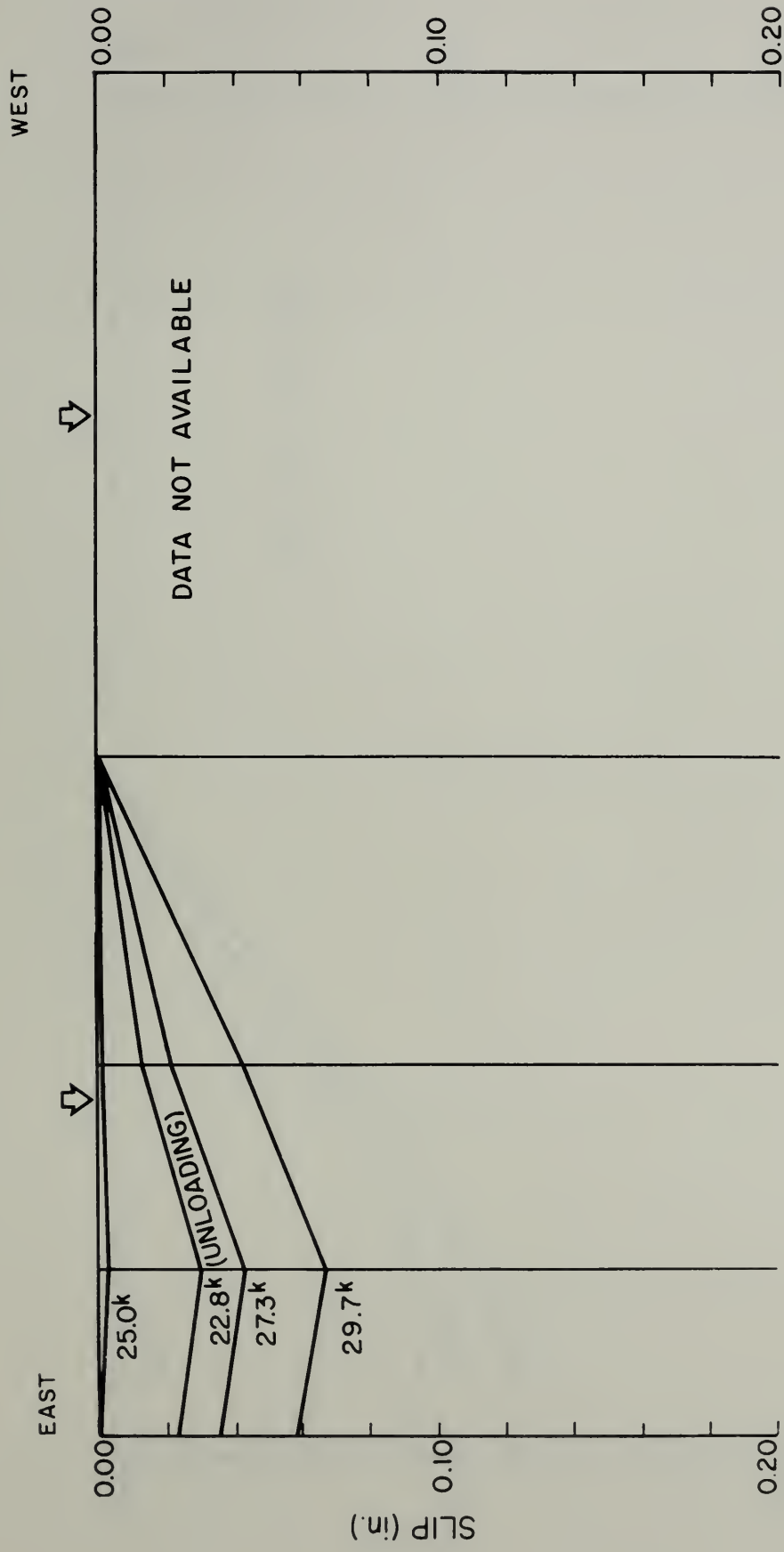


FIGURE 3.6 Experimental Slip Distribution along Beam 5G1

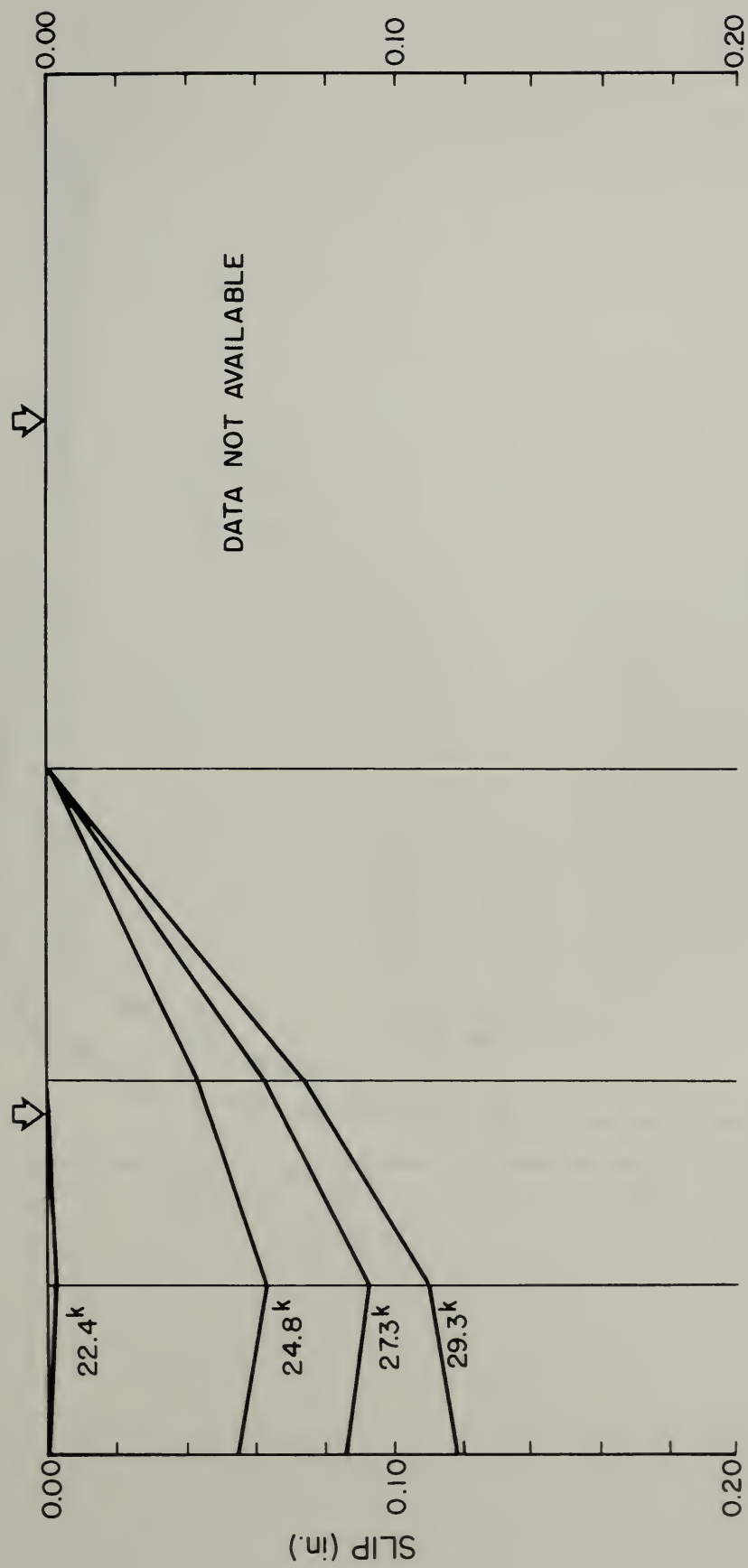
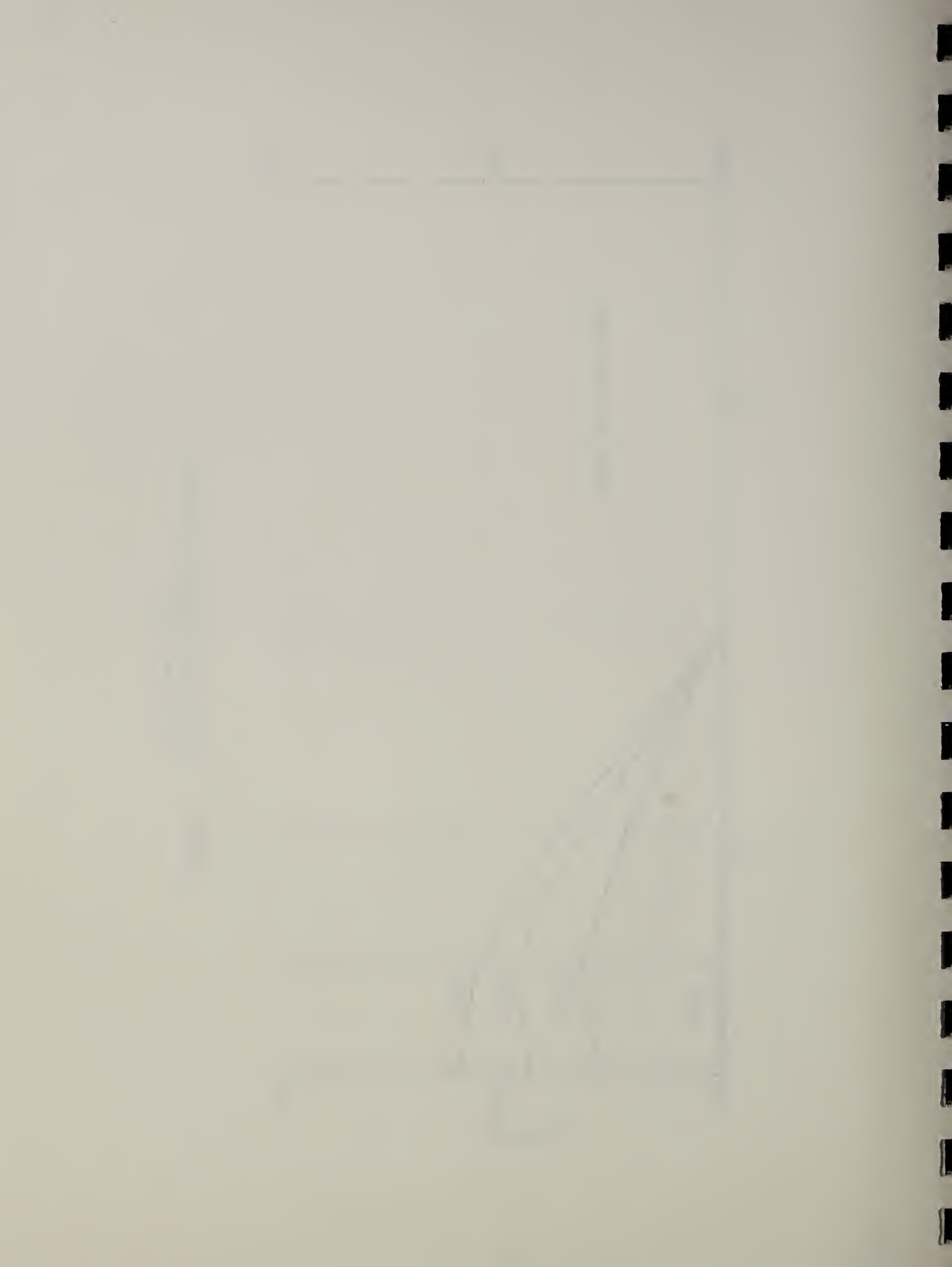


FIGURE 3.7 Experimental Slip Distribution along Beam 5U1



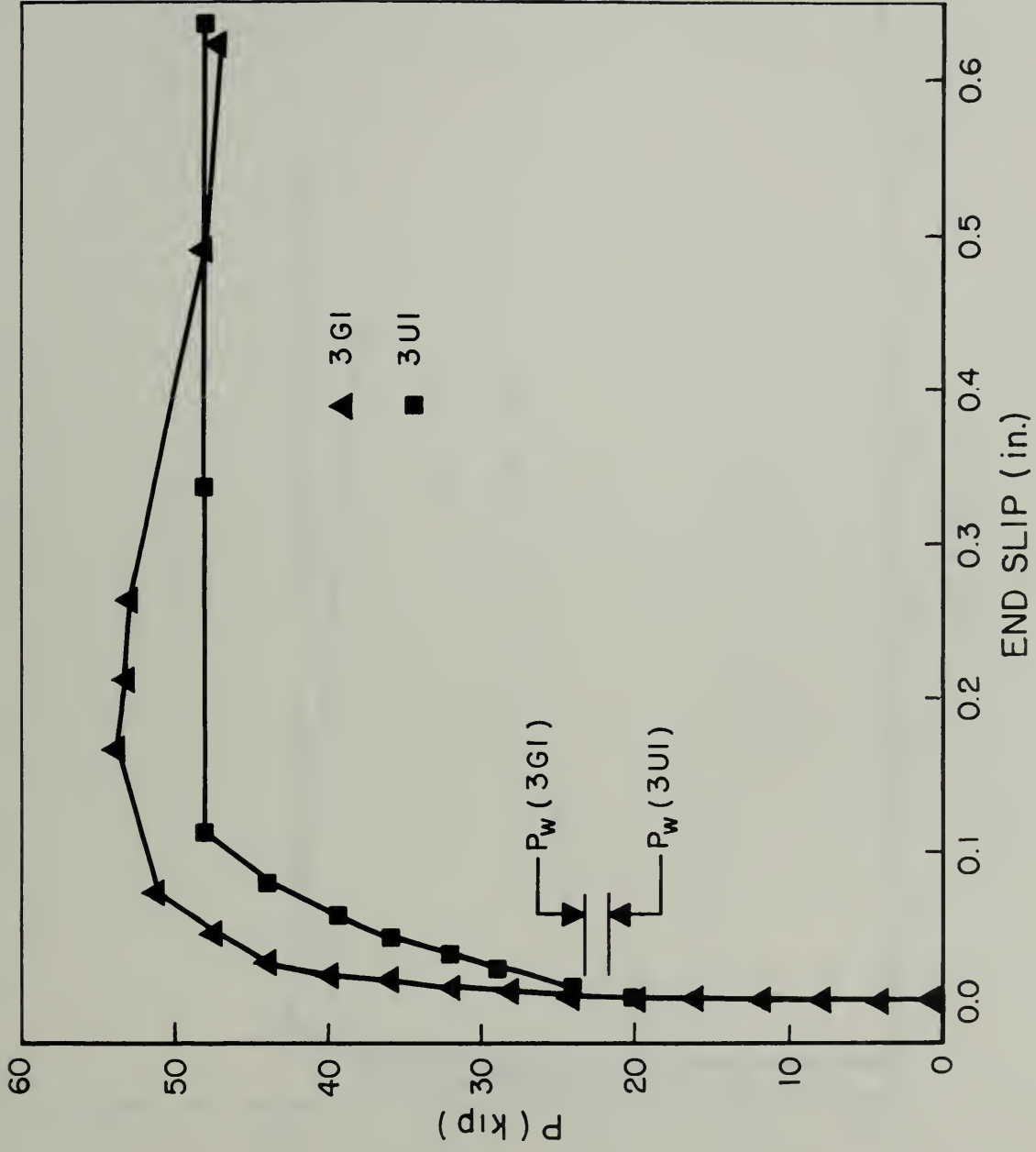
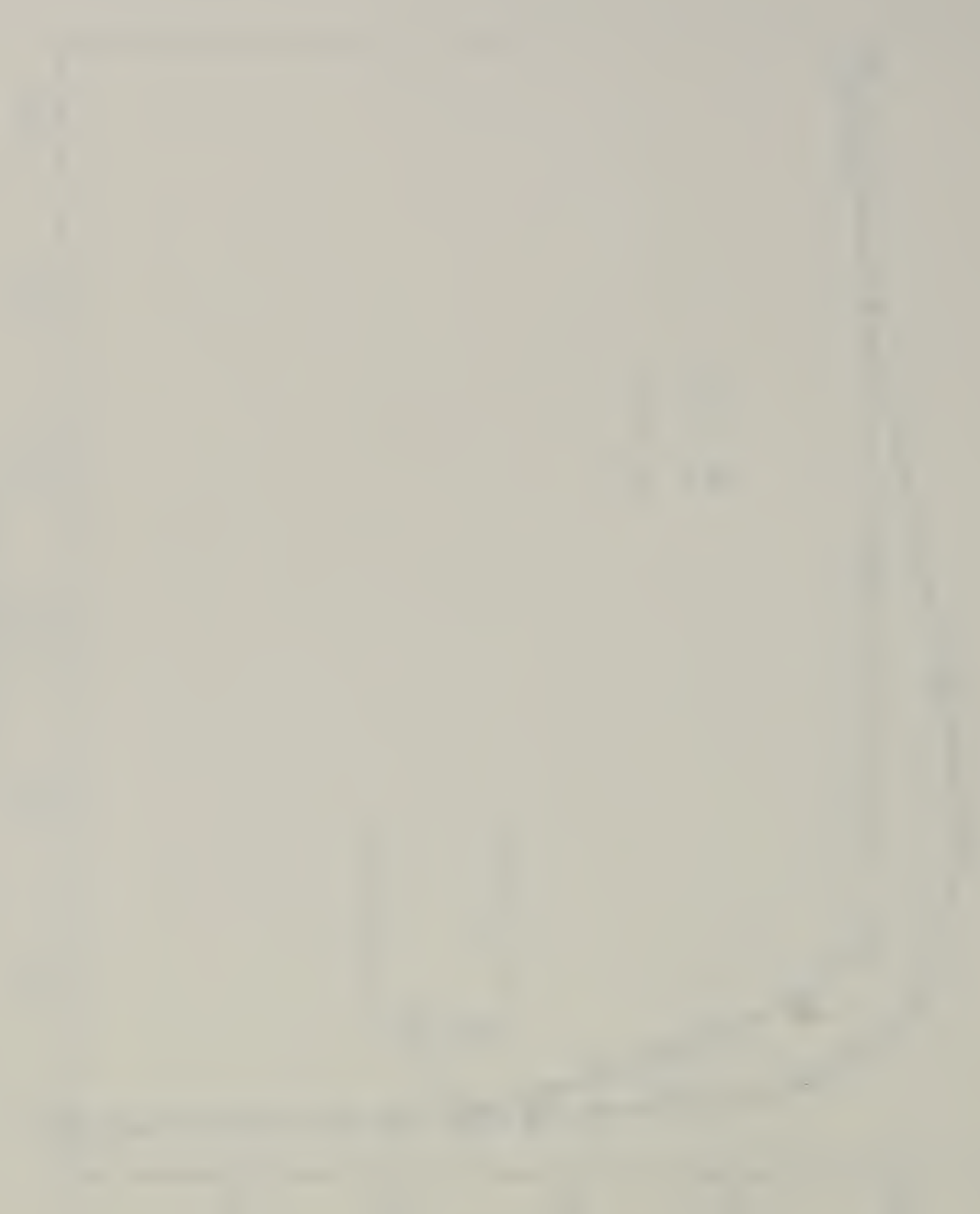


FIGURE 3.8 Load-End Slip Curves for Beams 3G1 and 3UI



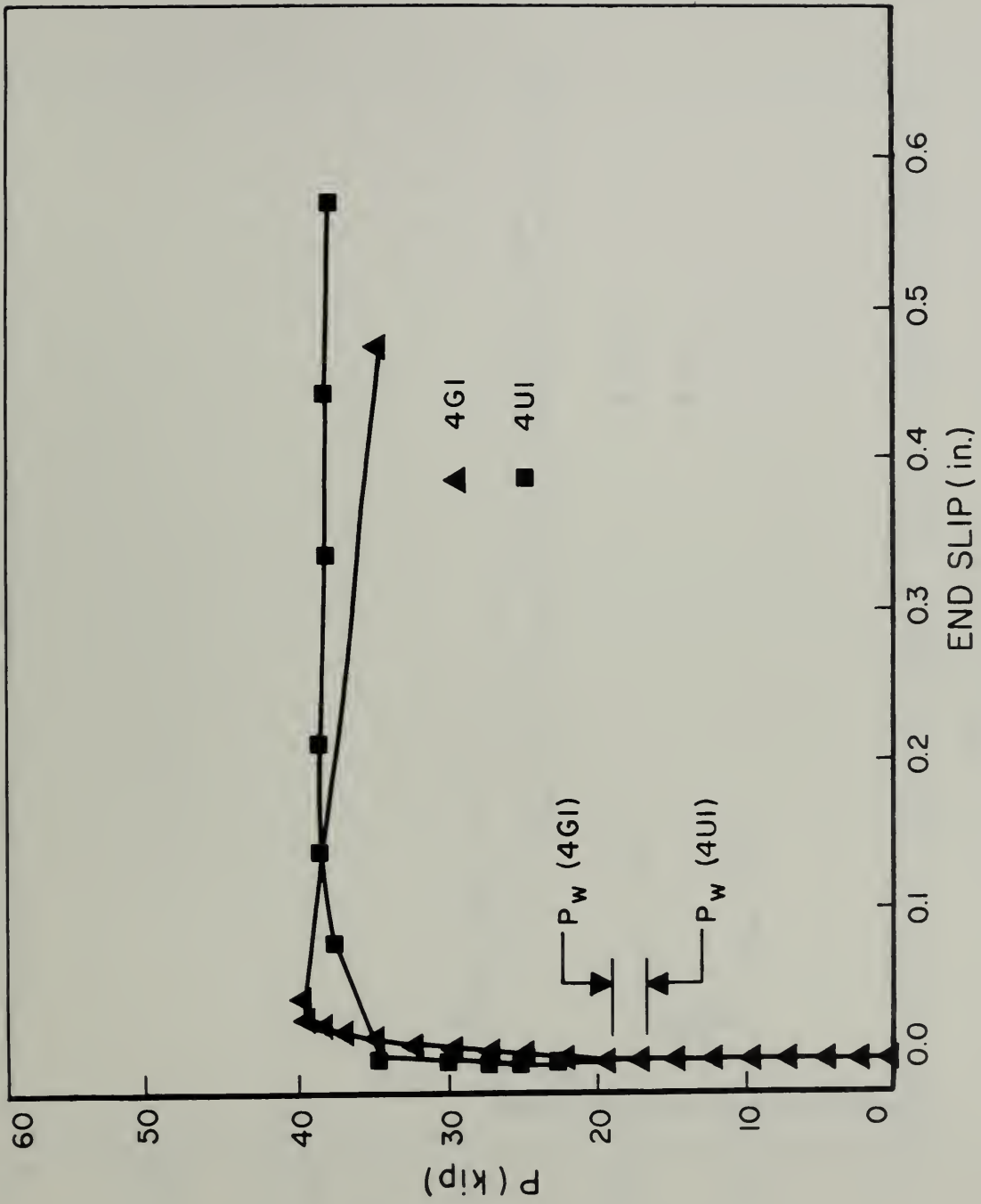
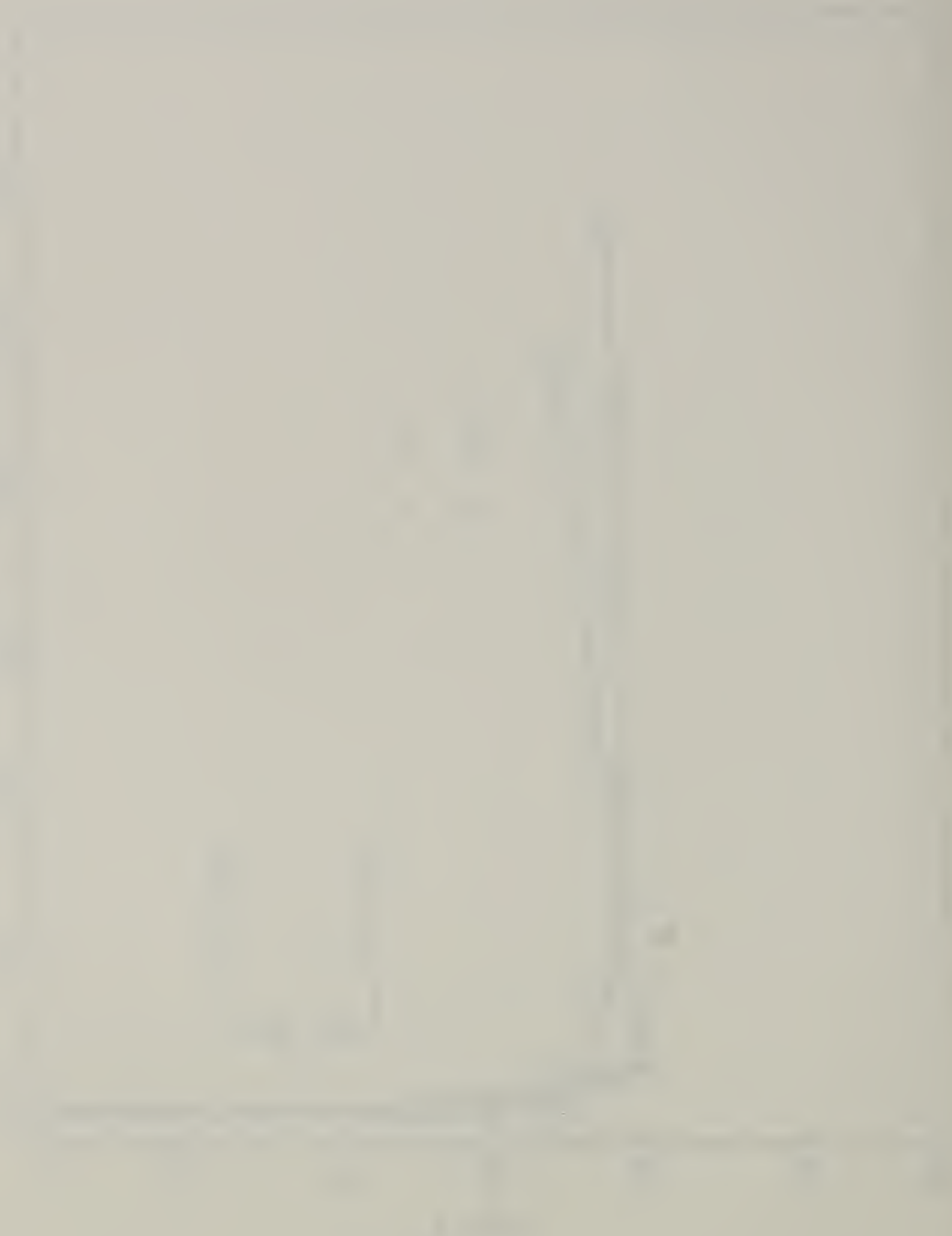


FIGURE 3.9 Load-End Slip Curves for Beams 4G1 and 4U1



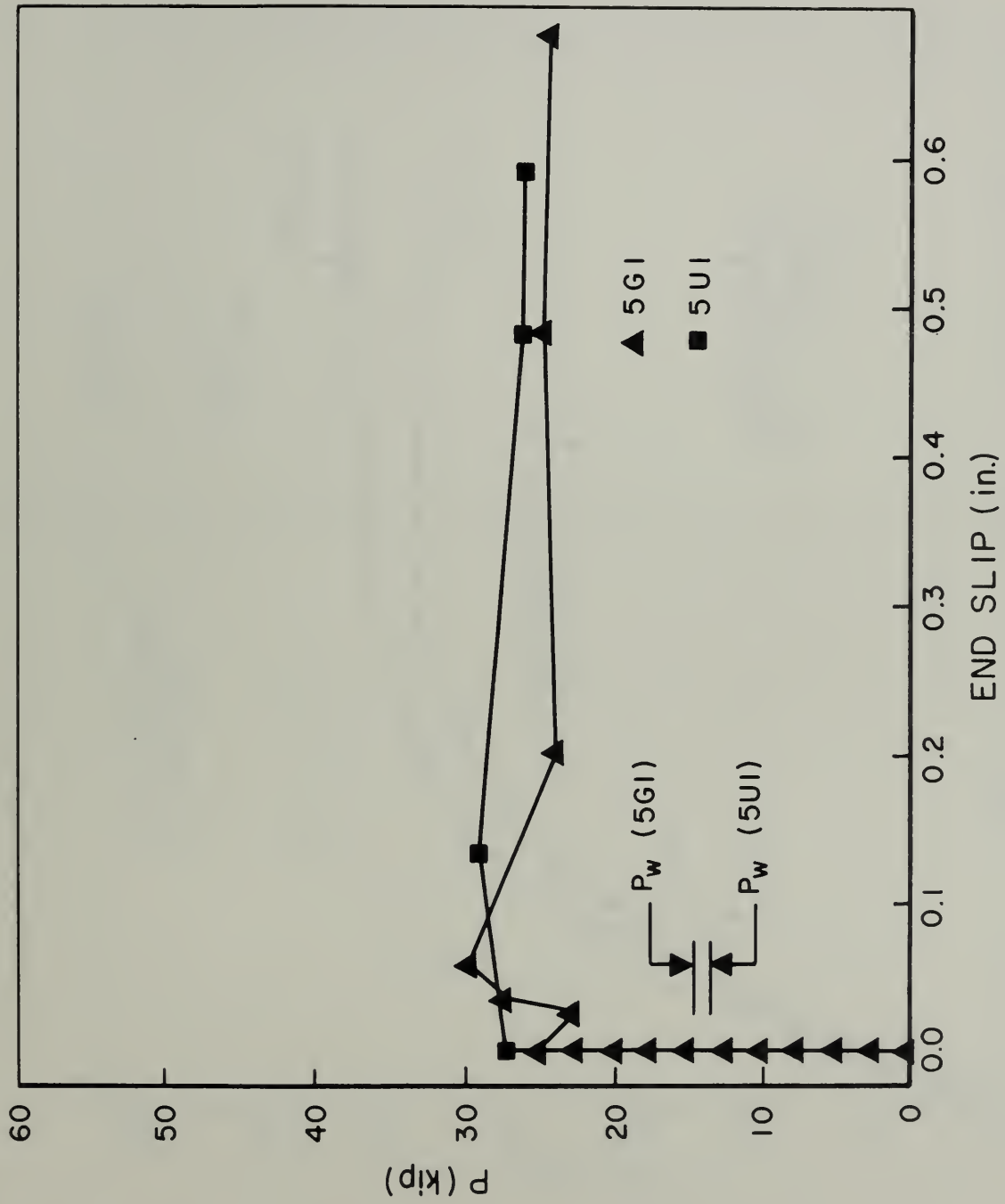
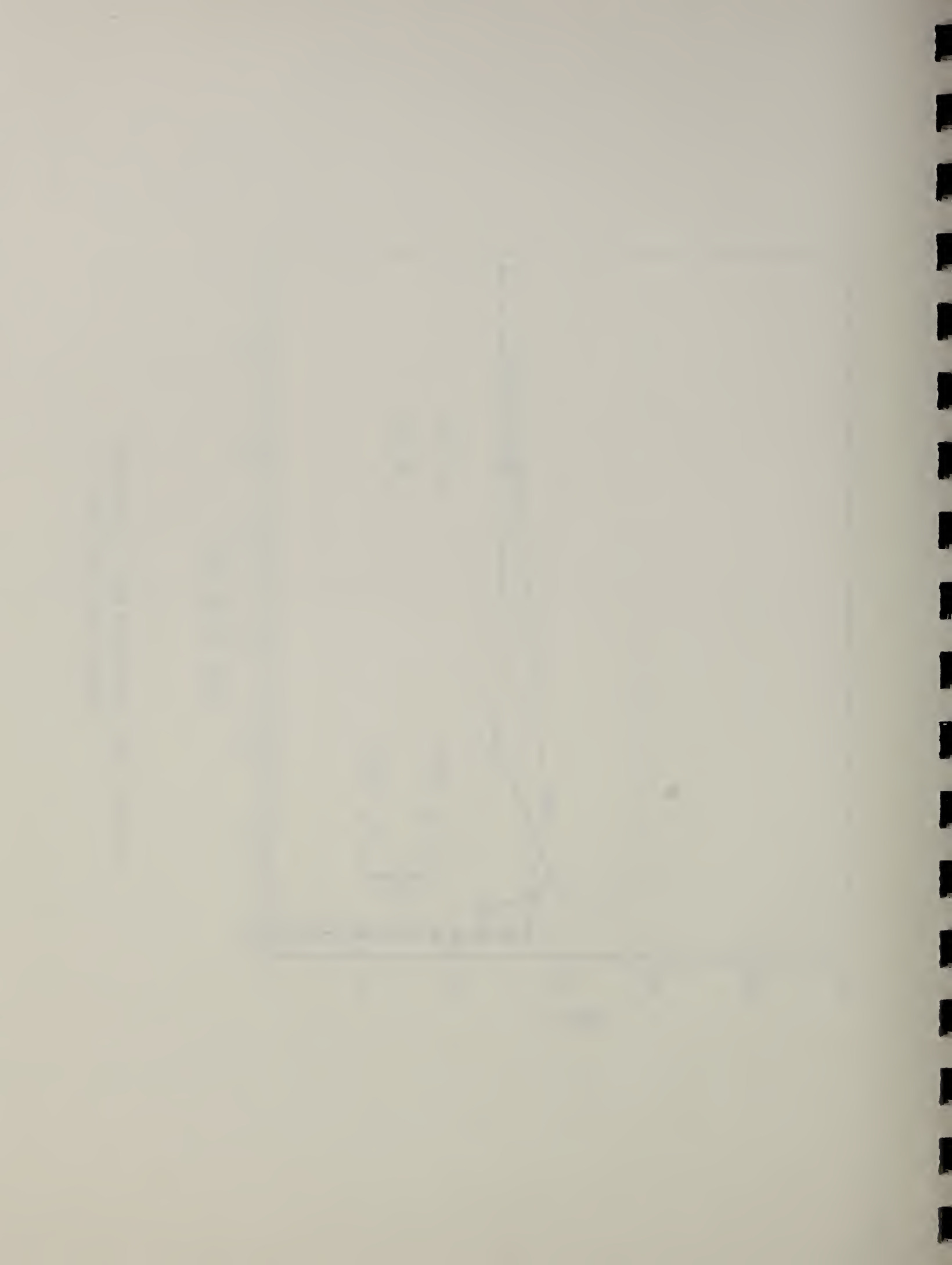


FIGURE 3.10 Load-End Slip Curves for Beams 5G1 and 5U1



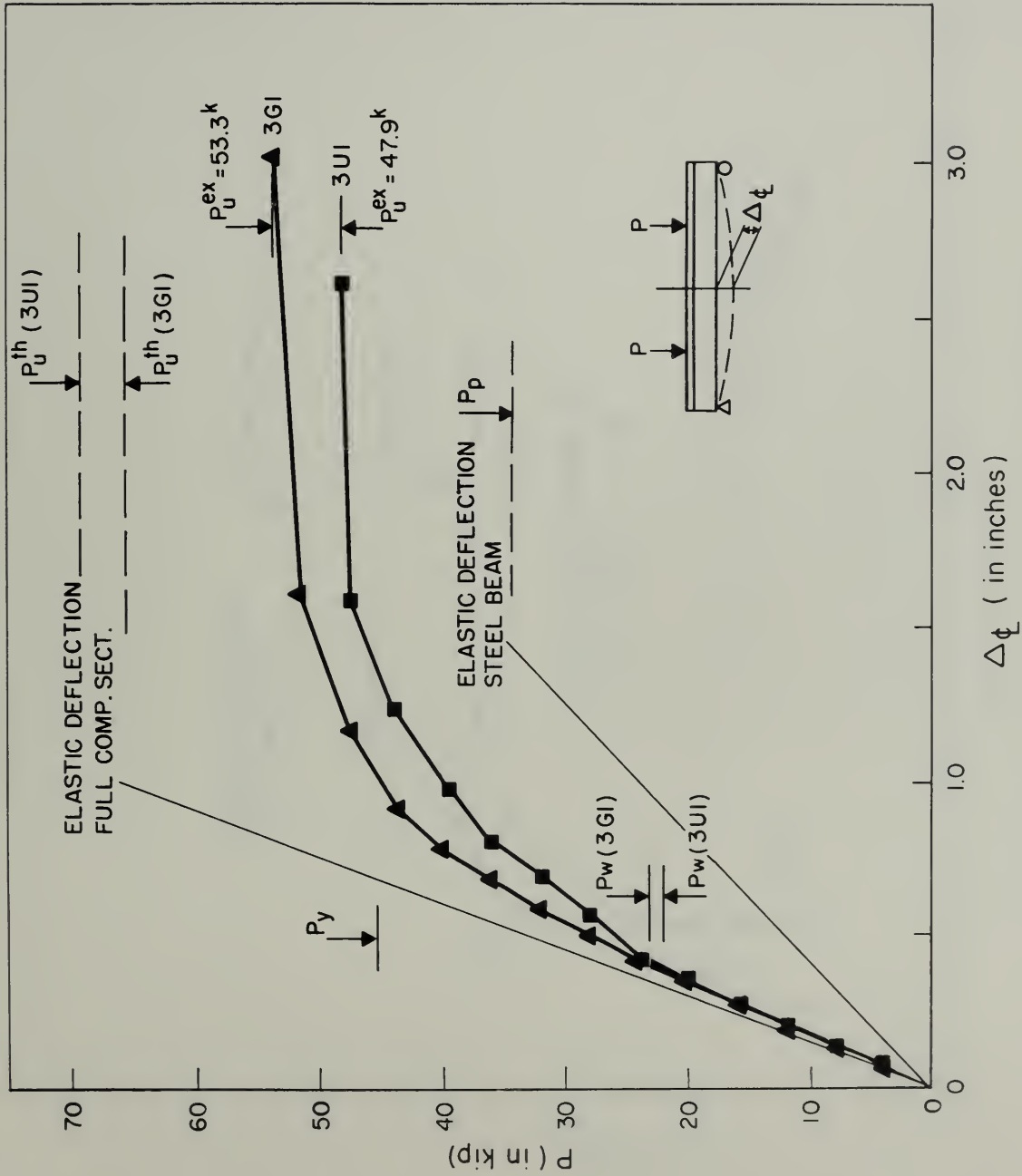


FIGURE 3.11 Load-Midspan Deflection Curves for Beams 3G1 and 3U1

Handwritten notes, possibly bleed-through from the reverse side of the page. The text is extremely faint and illegible.

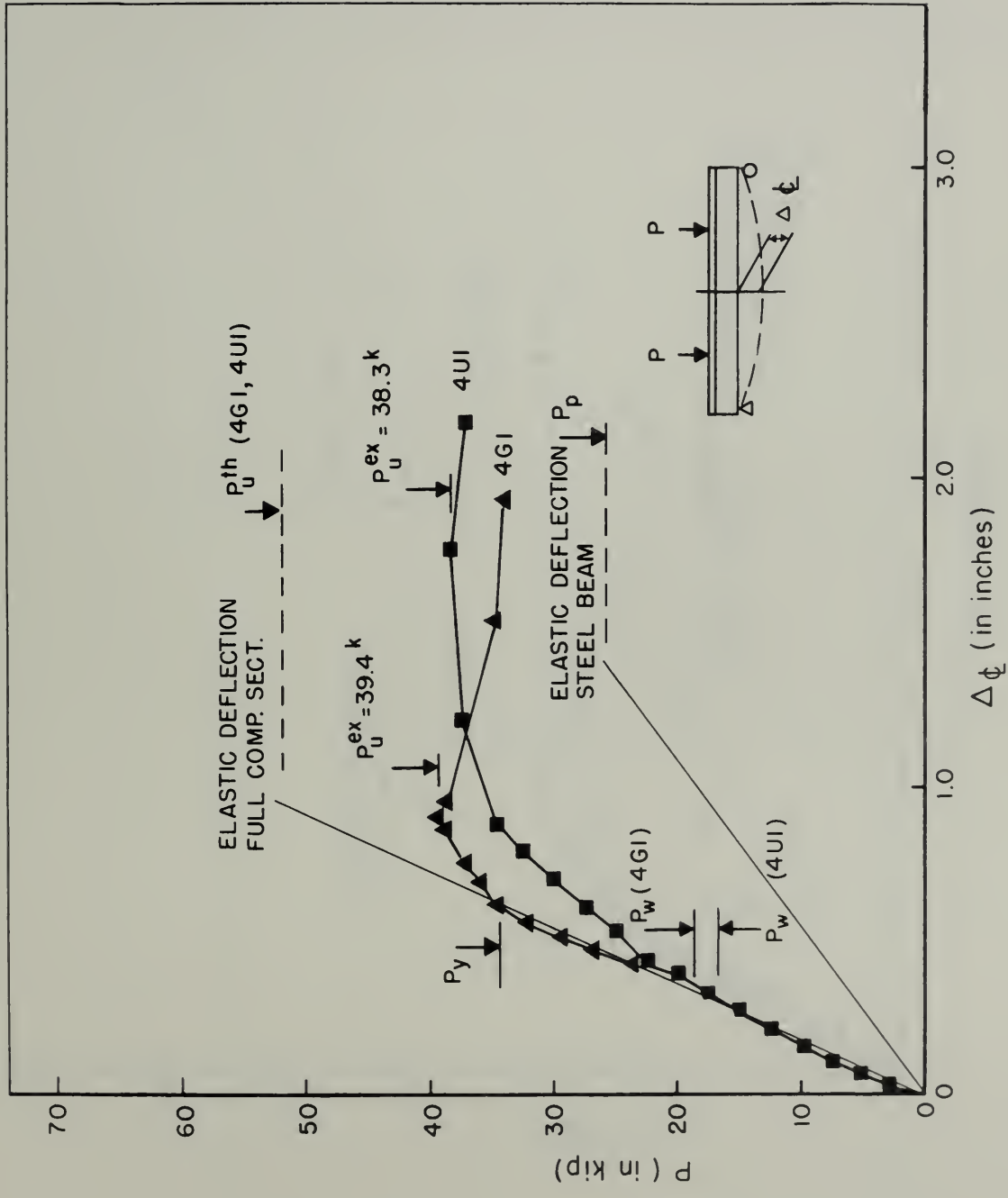
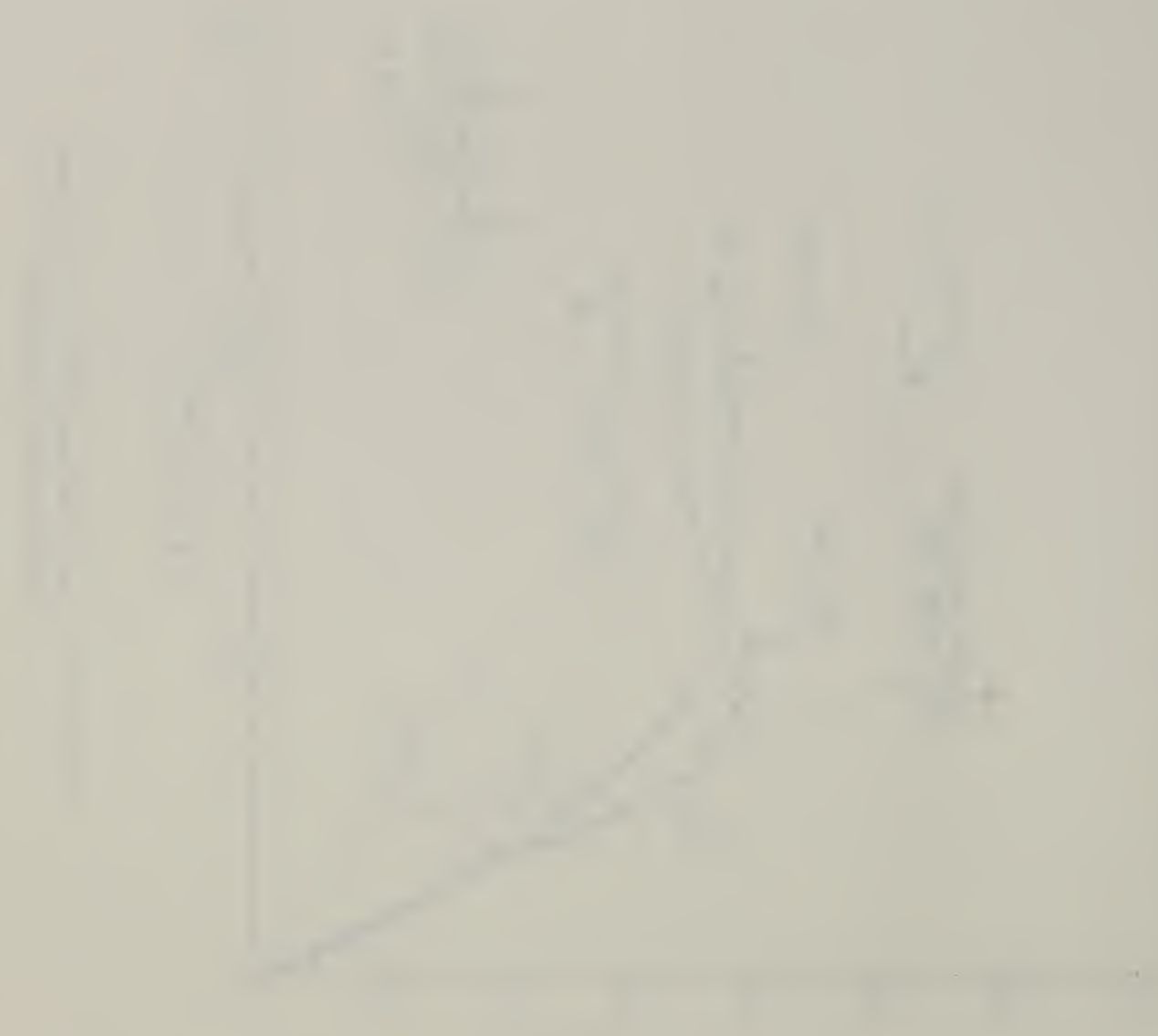


FIGURE 3.12 Load-Midspan Deflection Curves for Beams 4G1 and 4U1



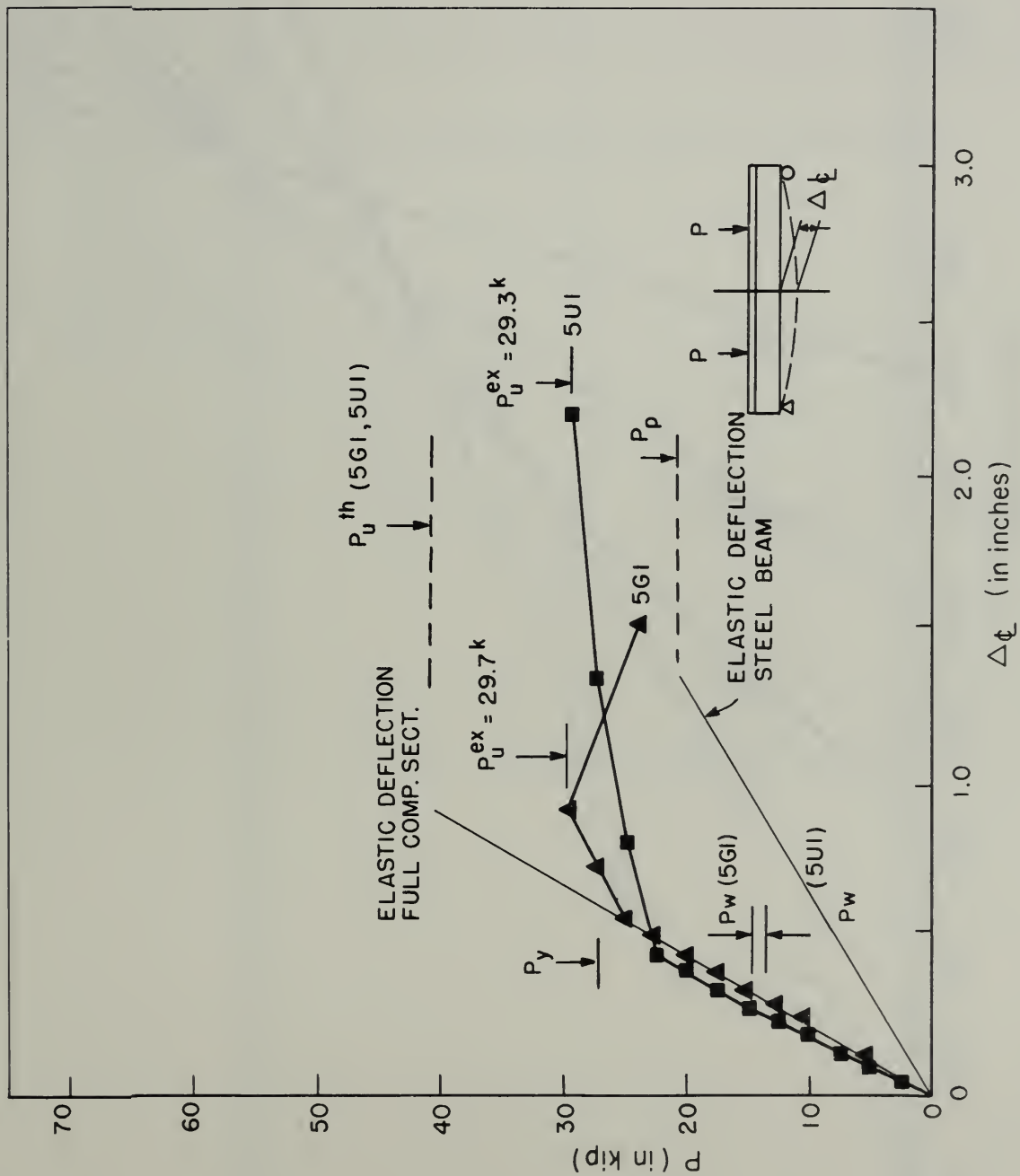
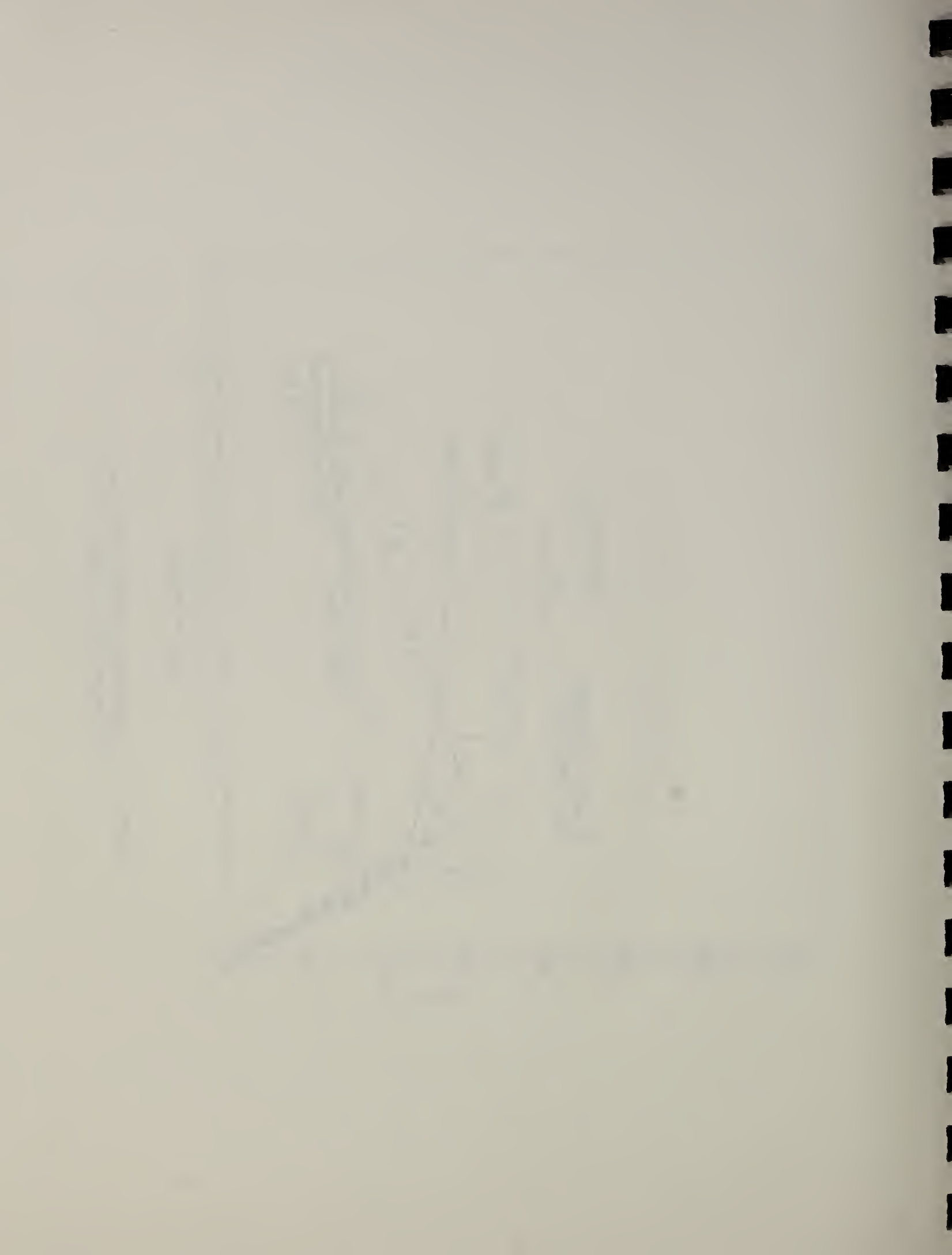


FIGURE 3.13 Load-Midspan Deflection Curves for Beams 5G1 and 5U1



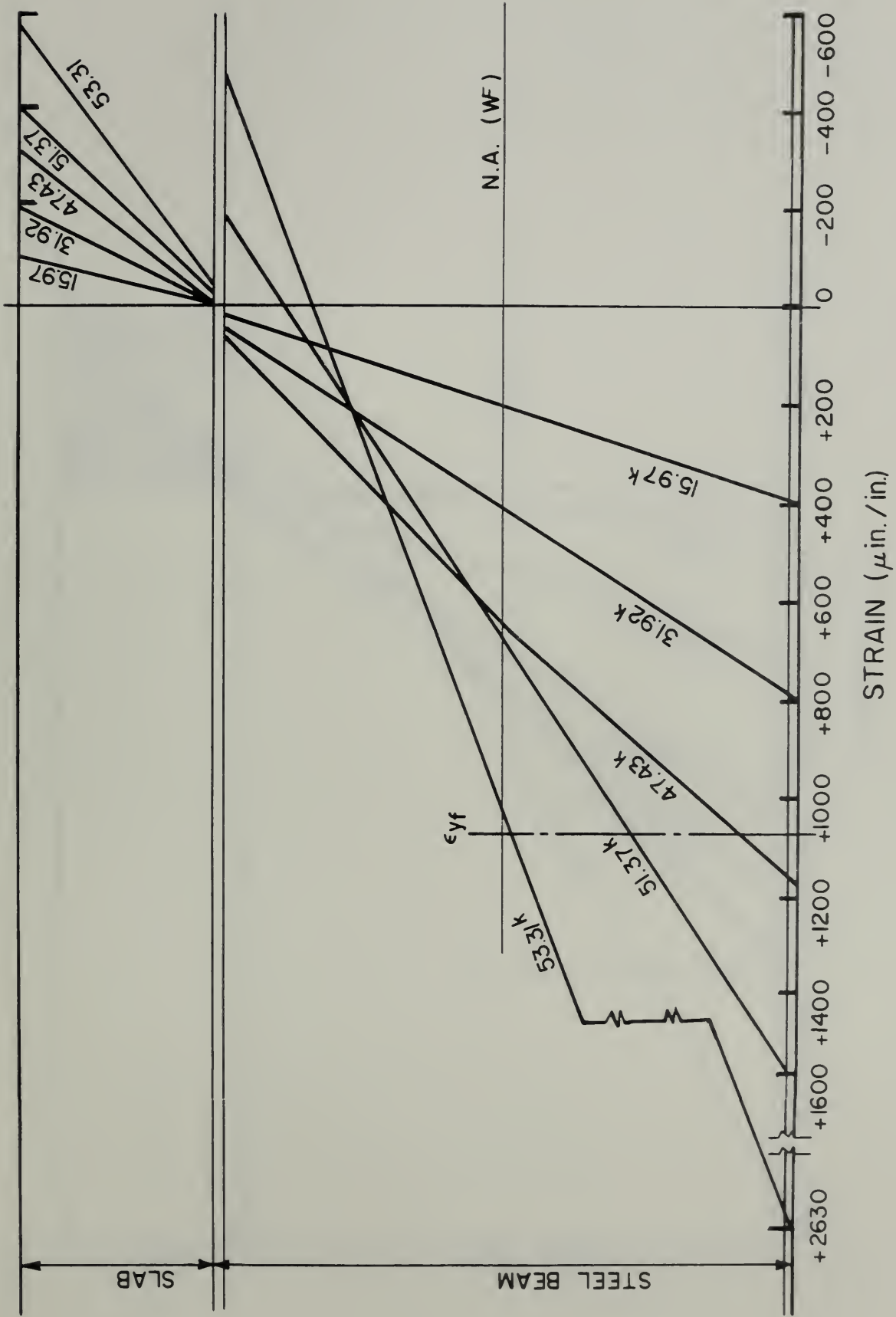


FIGURE 3.14 Midspan Strain Distributions for Beam 3G1



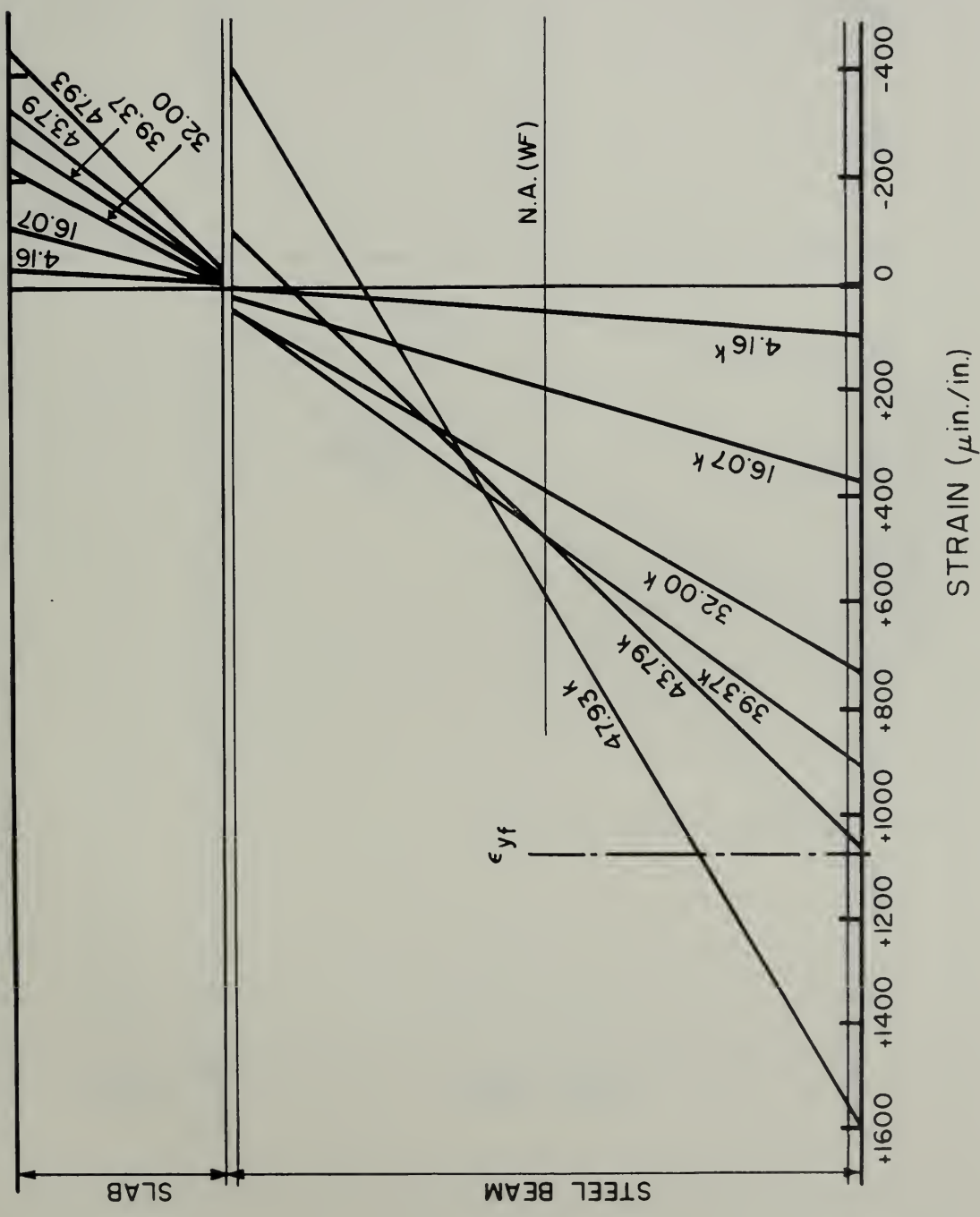
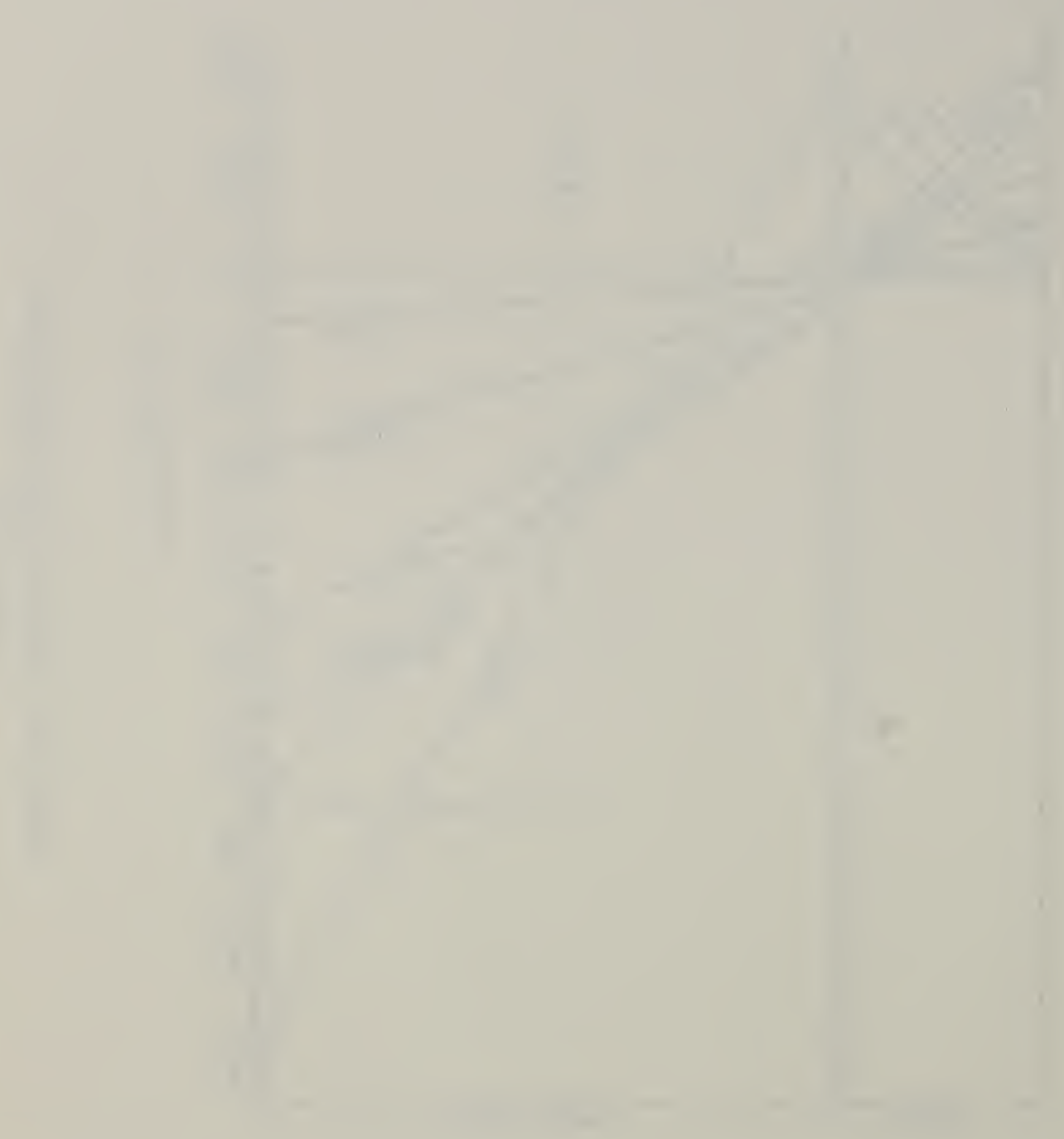


FIGURE 3.15 Midspan Strain Distributions for Beam 3U1



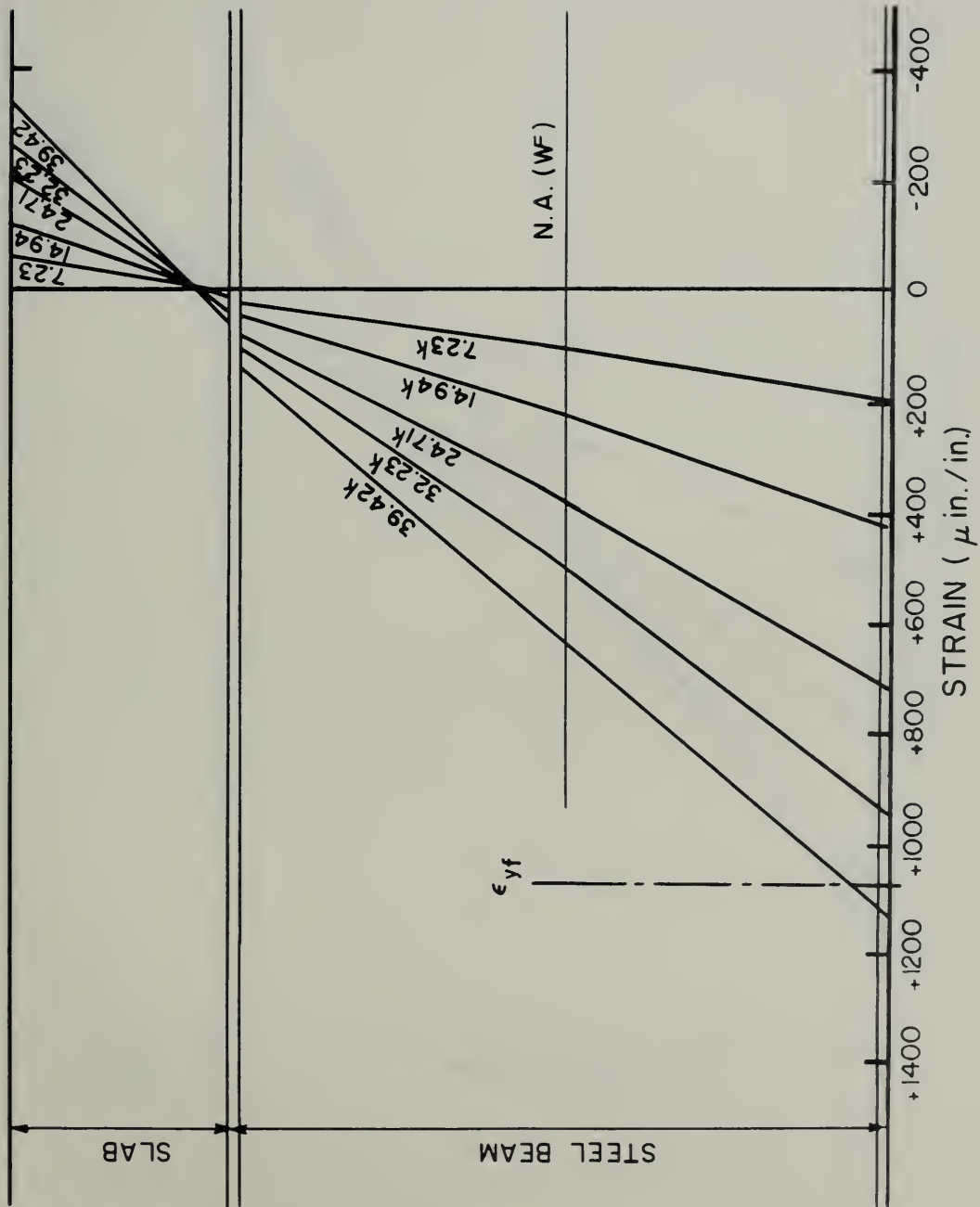
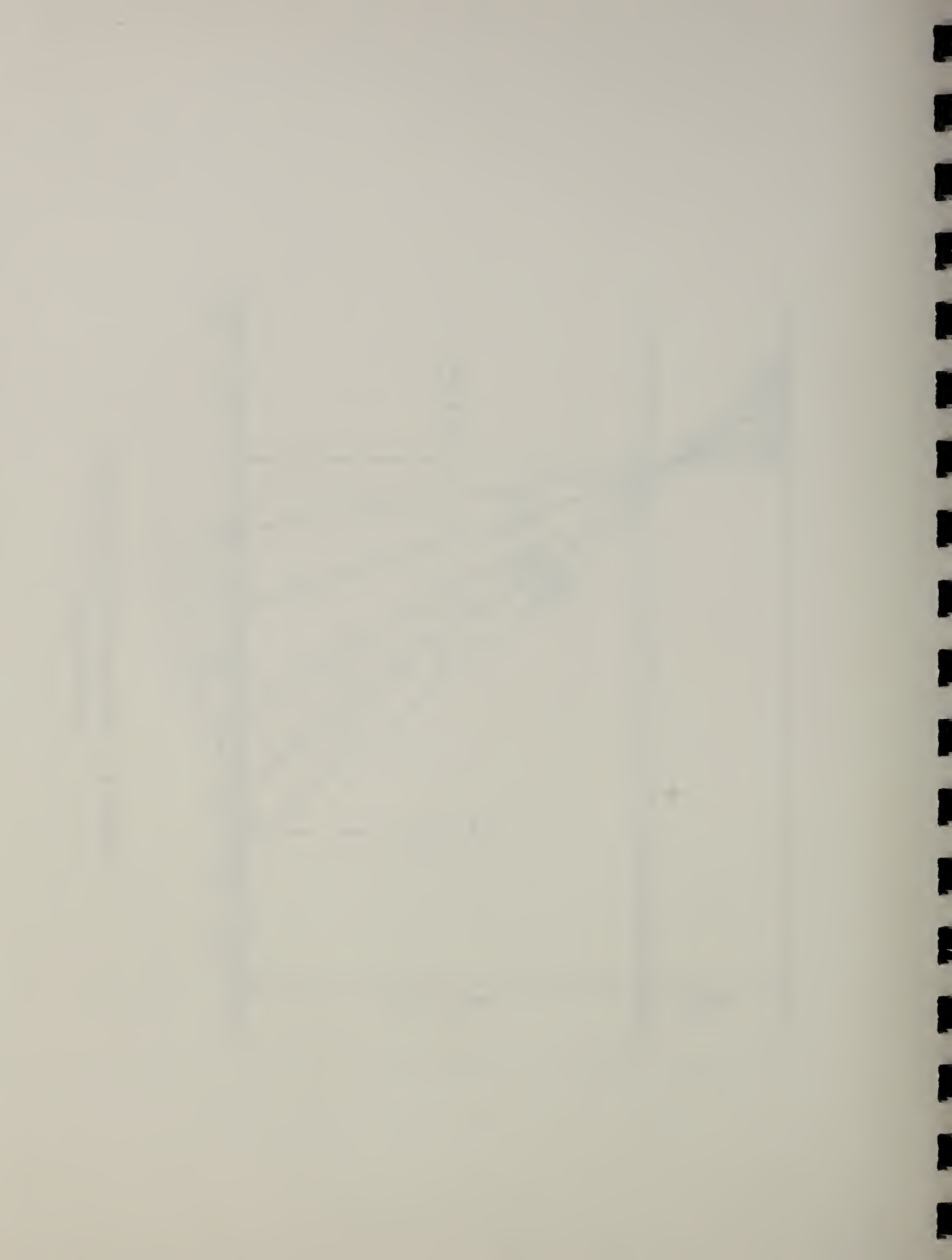


FIGURE 3.16 Midspan Strain Distributions for Beam 4G1



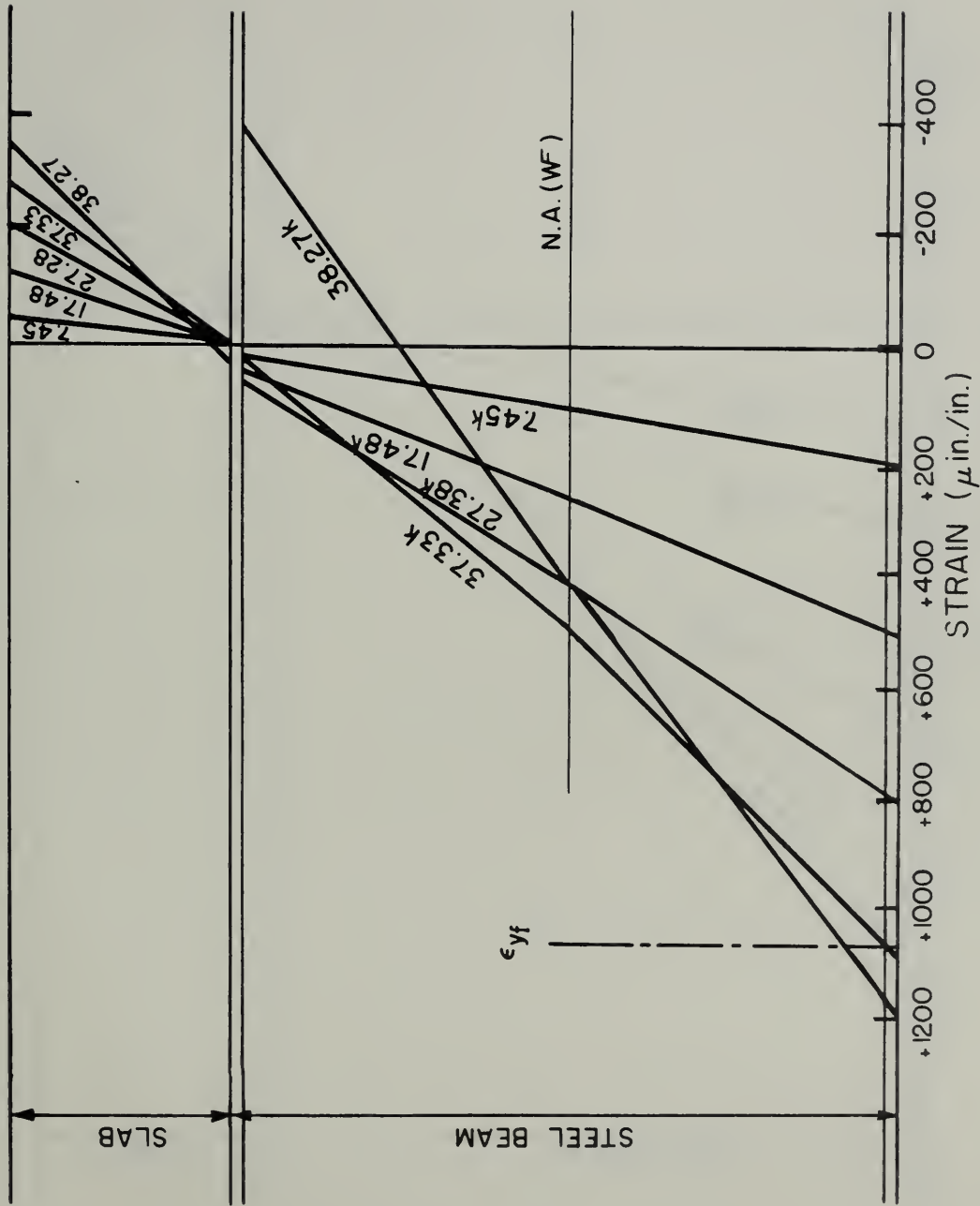


FIGURE 3.17 Midspan Strain Distributions for Beam 4U1



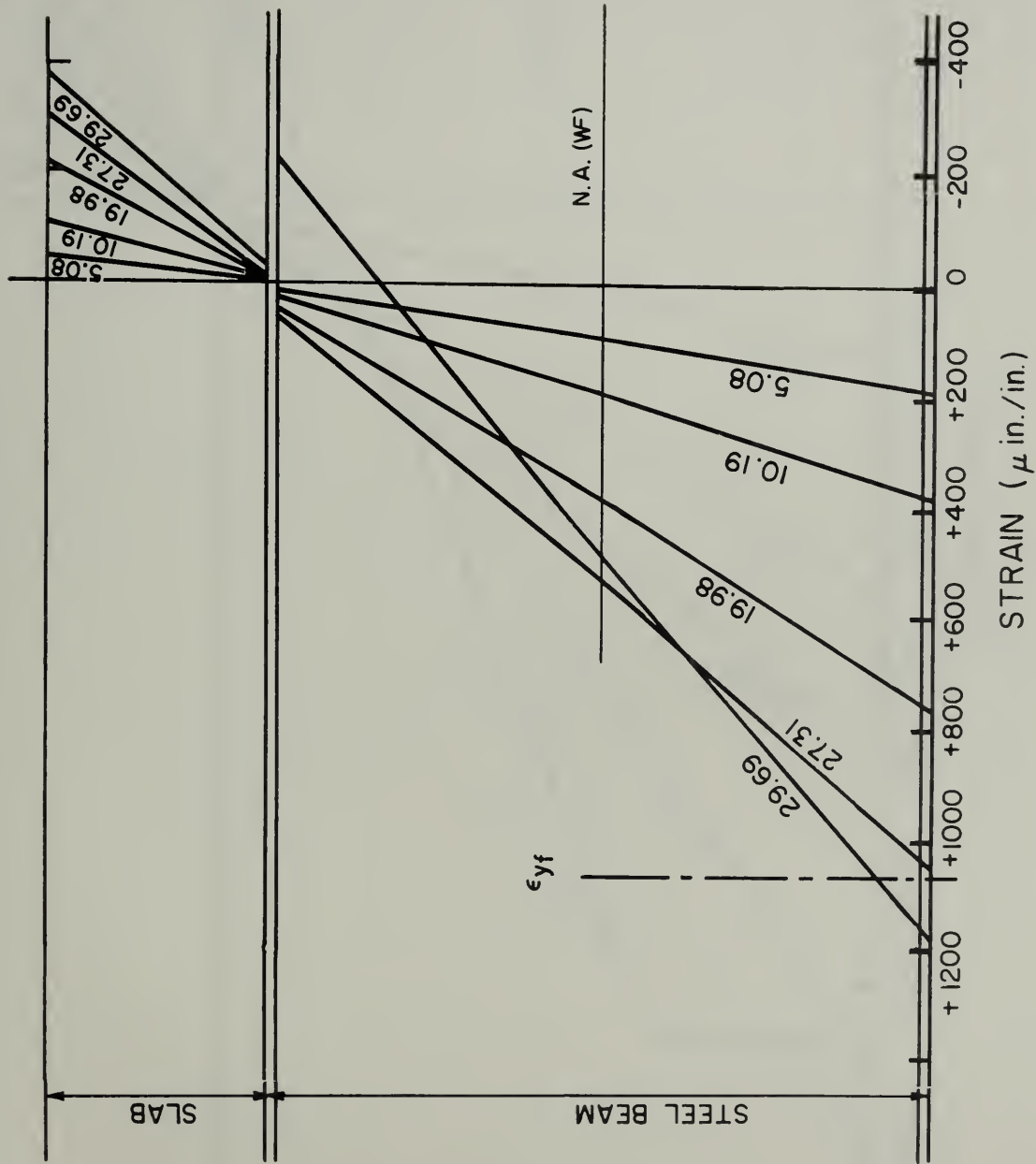


FIGURE 3.18 Midspan Strain Distributions for Beam 5G1

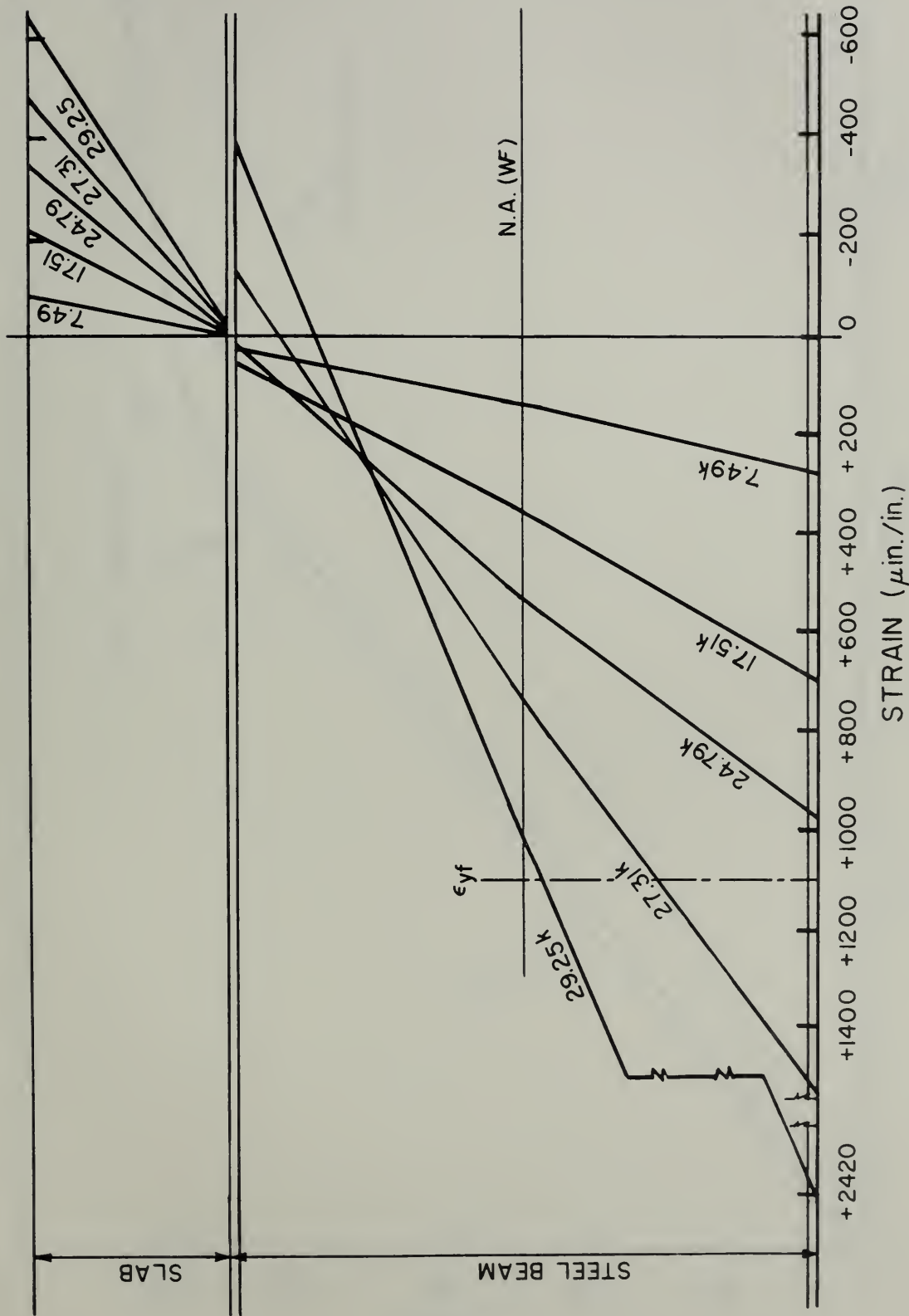


FIGURE 3.19 Midspan Strain Distributions for Beam 5U1



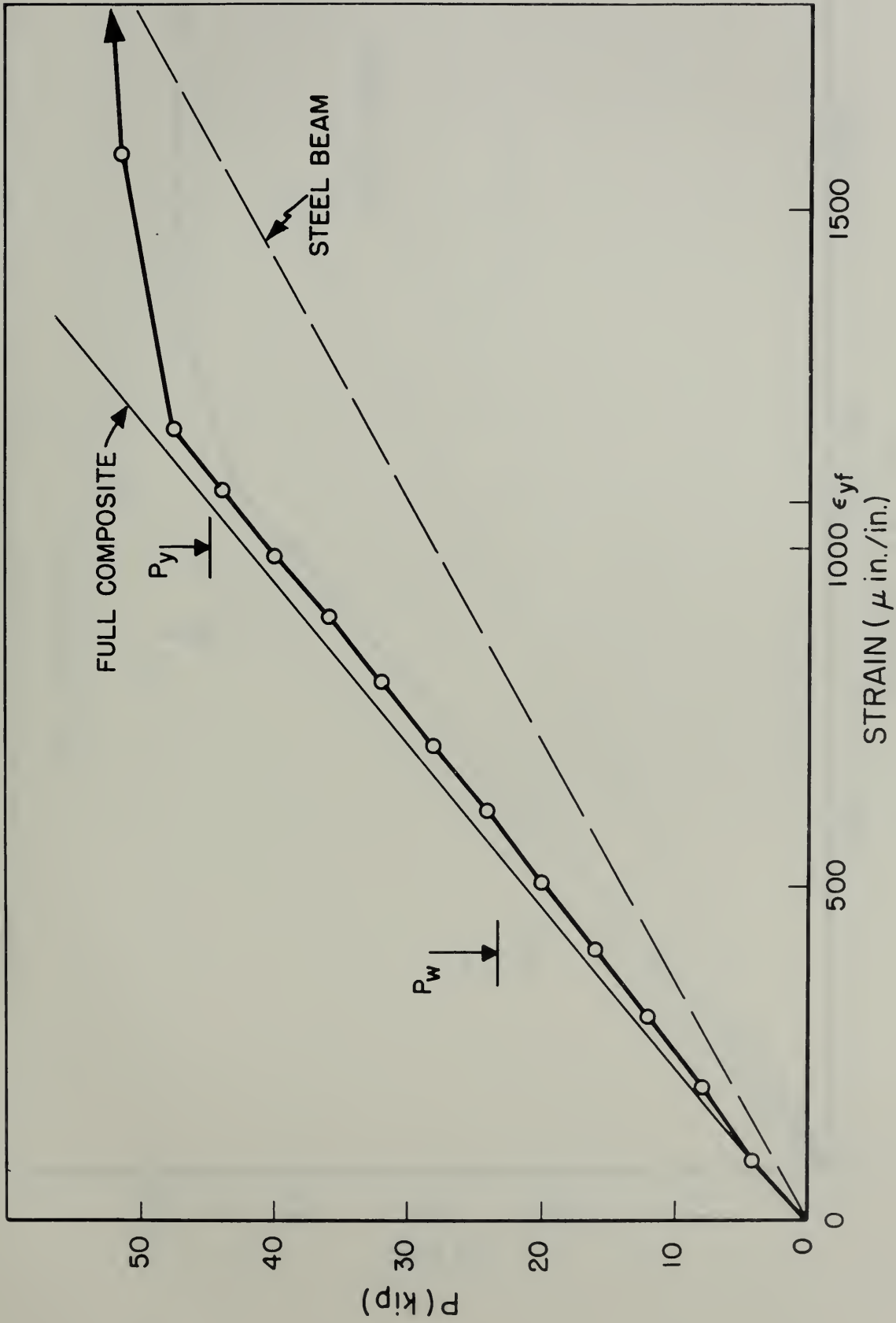


FIGURE 3.20 Load-Tension Flange Strain Curve for Beam 3G1



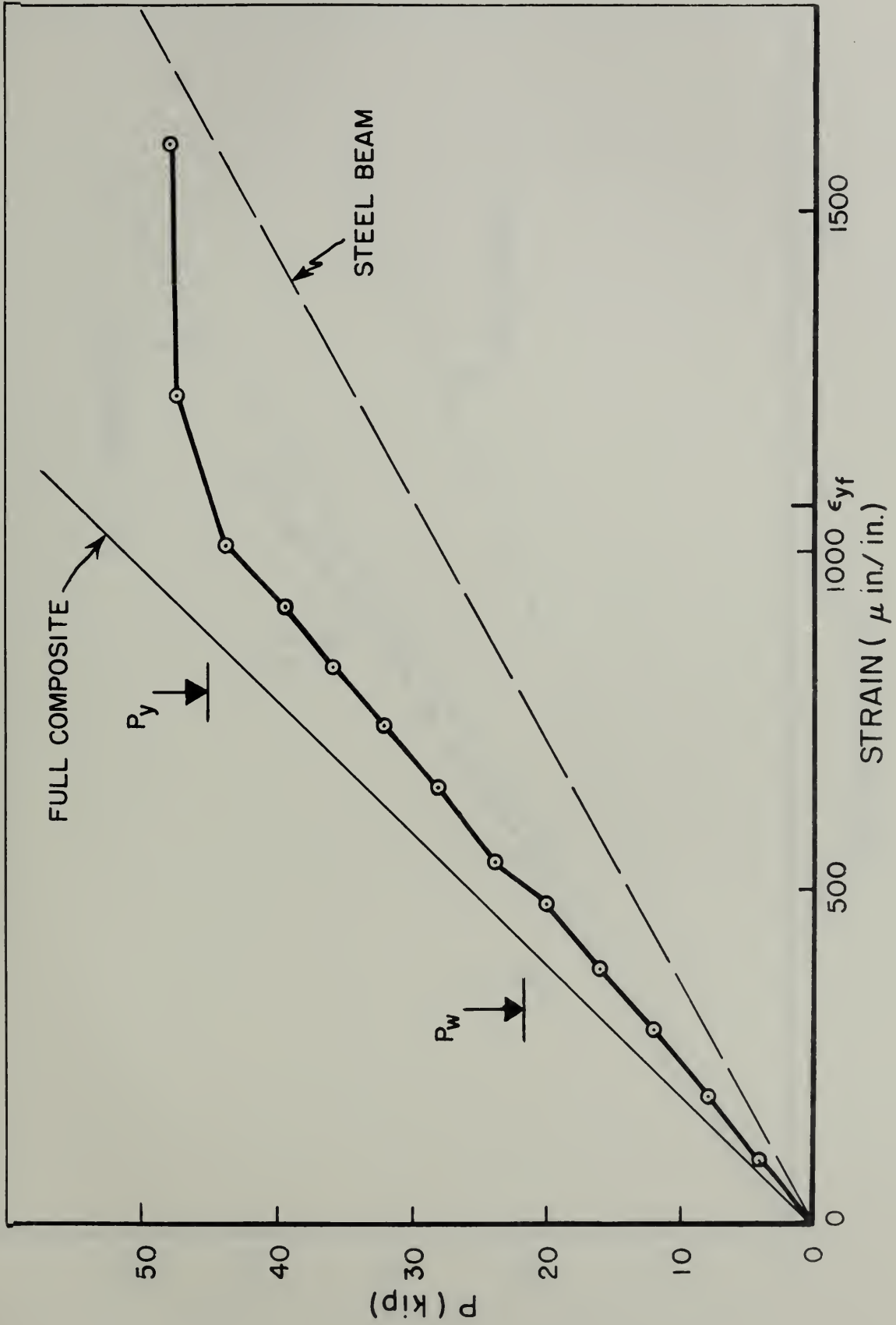


FIGURE 3.21 Load-Tension Flange Strain Curve for Beam 3U1



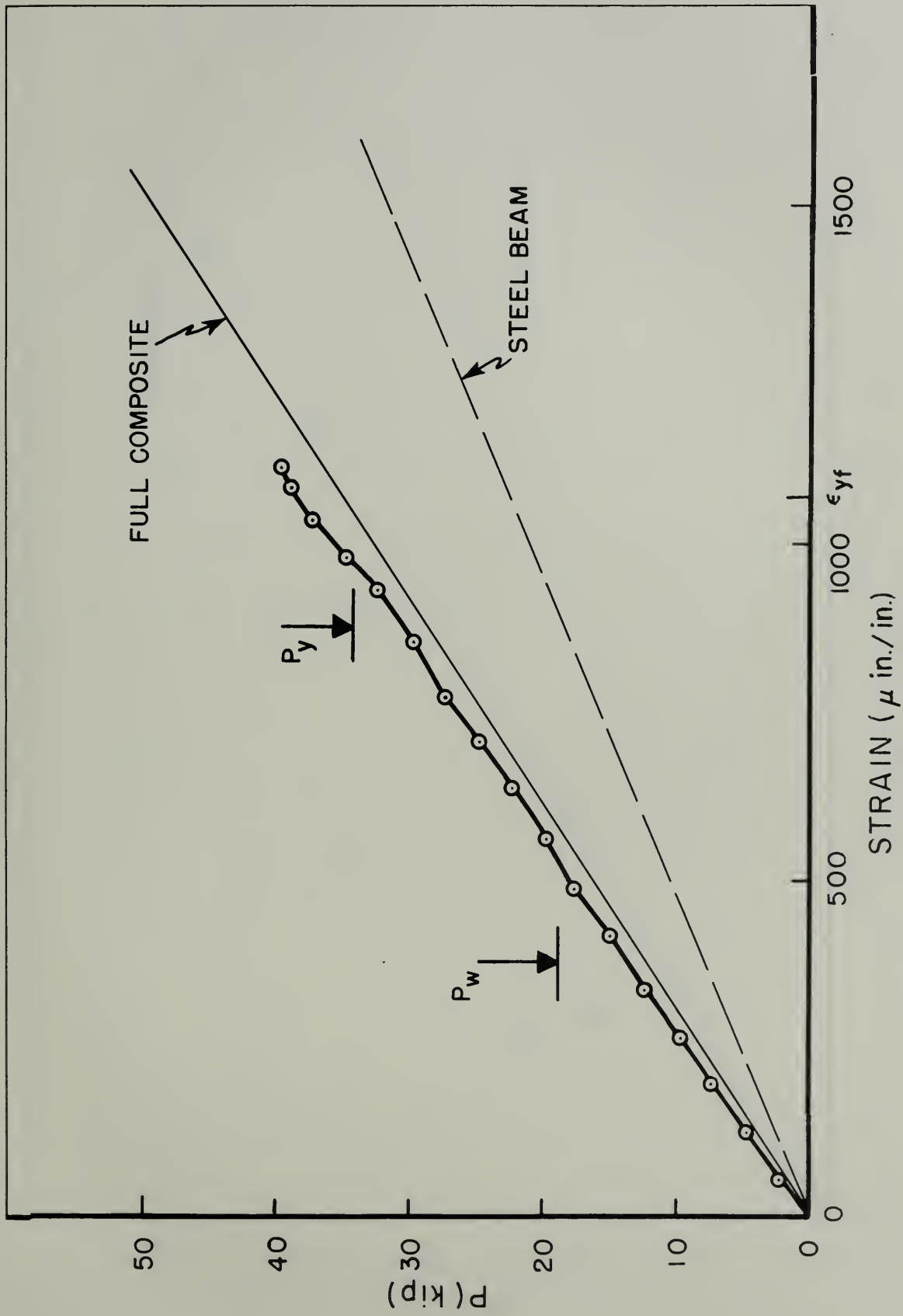
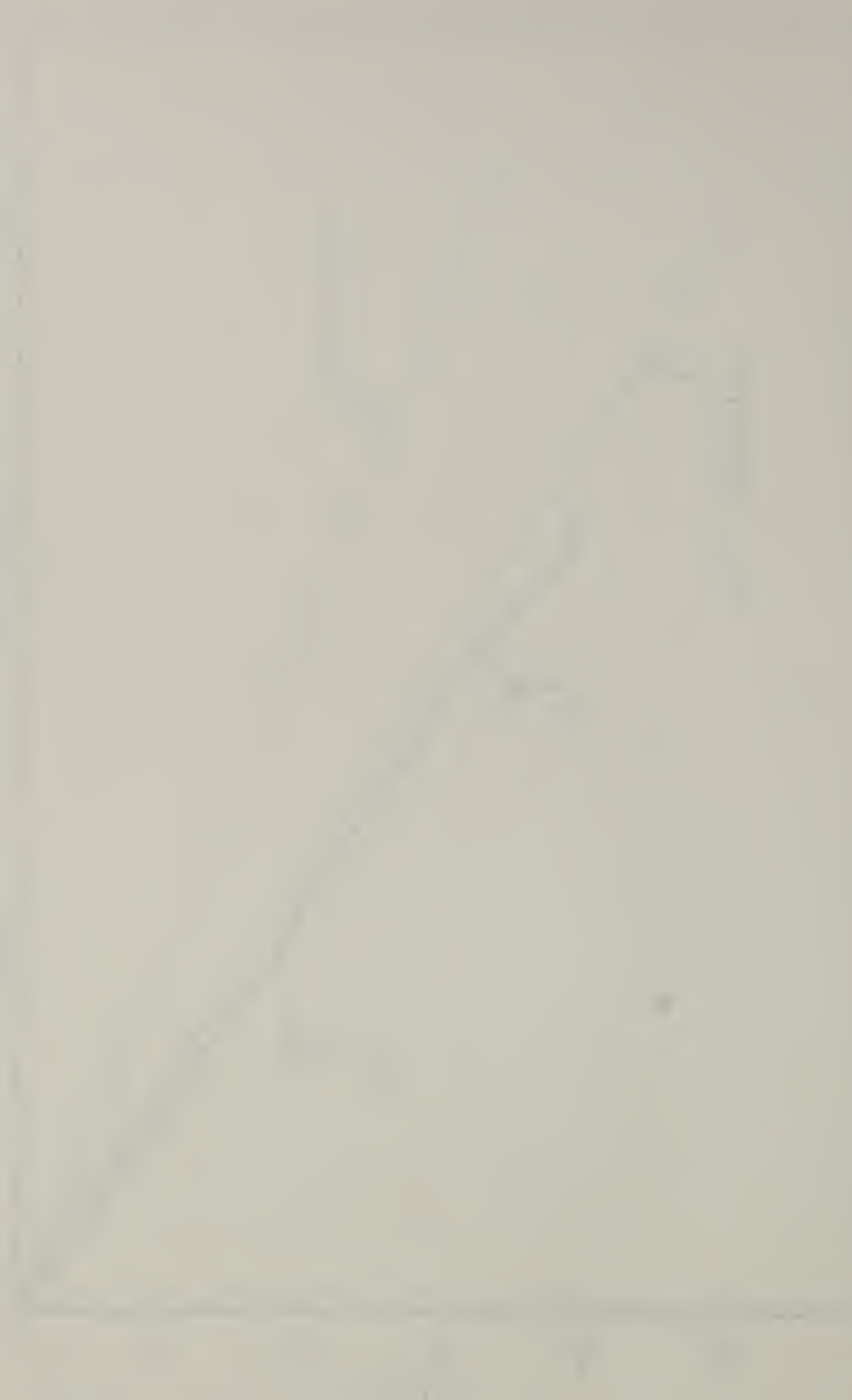


FIGURE 3.22 Load-Tension Flange Strain Curve for Beam 4G1



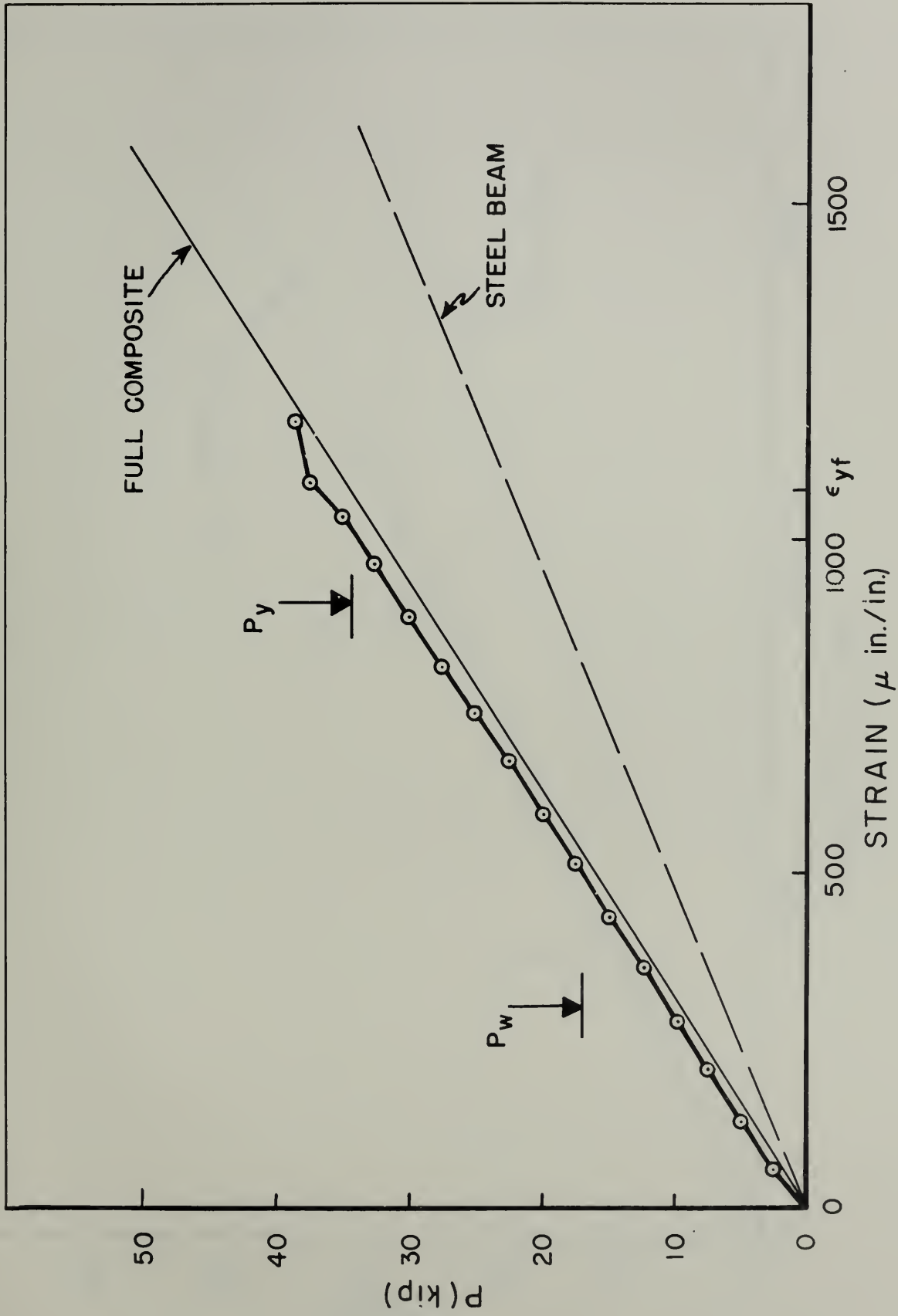


FIGURE 3.23 Load-Tension Flange Strain Curve for Beam 4U1



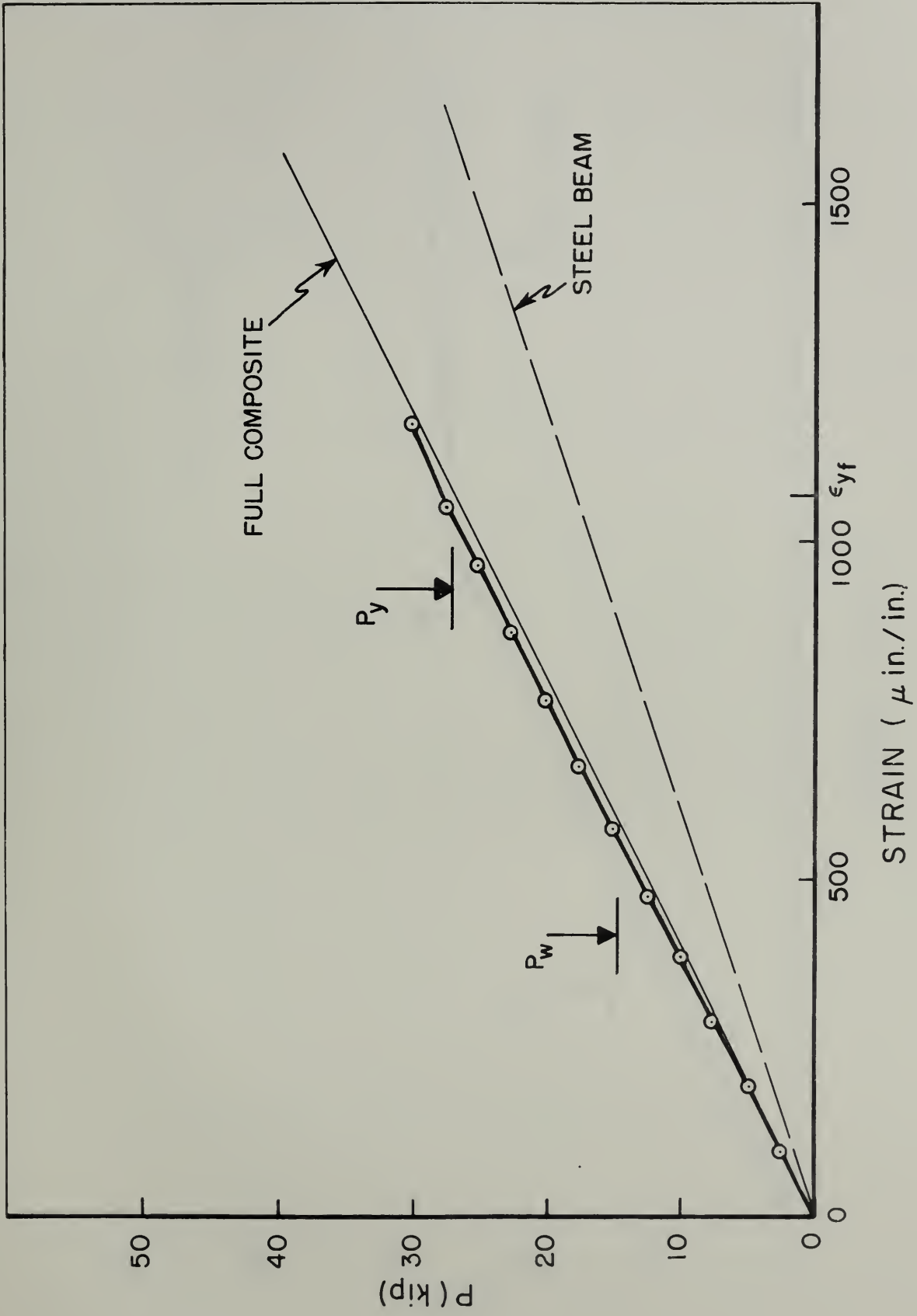
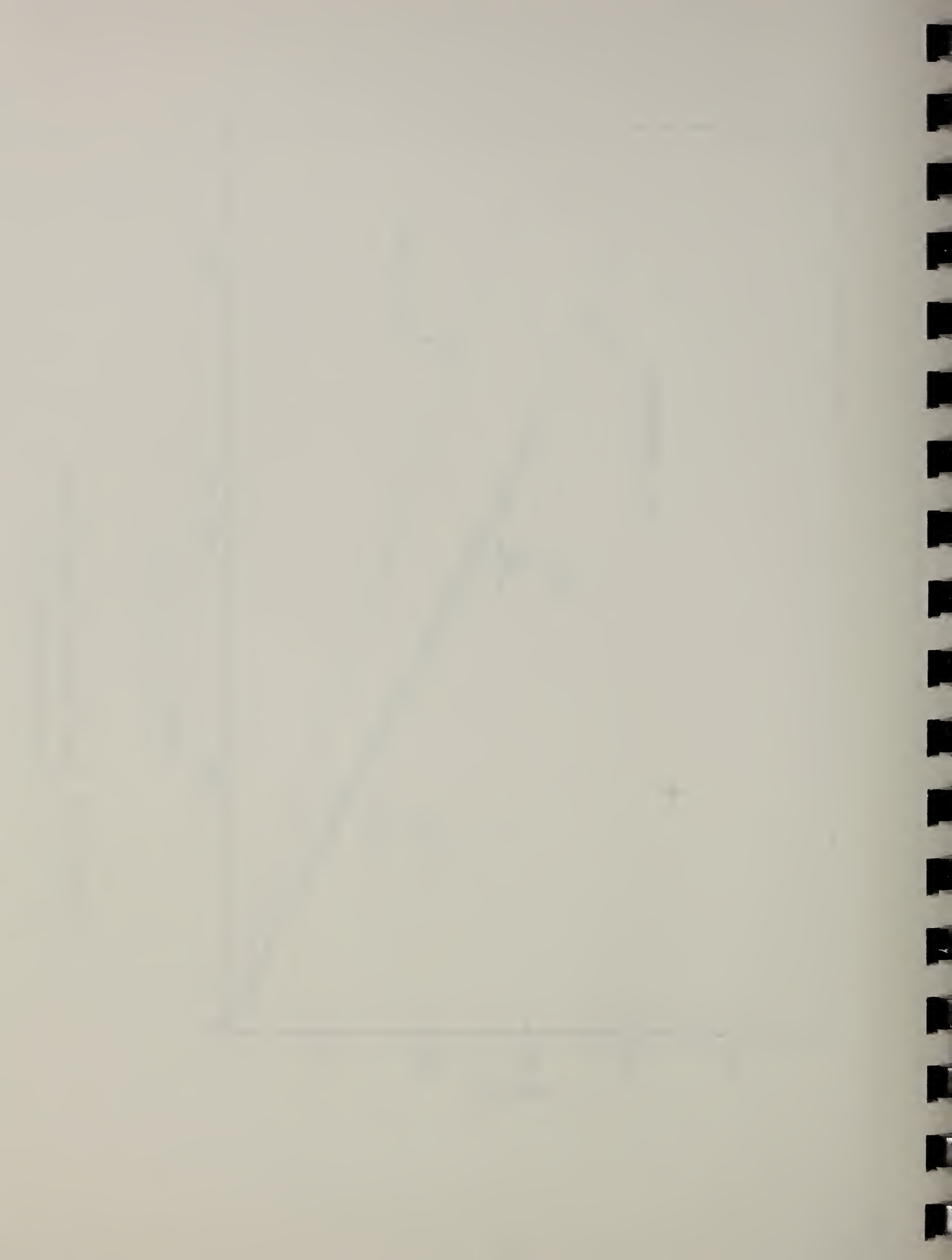


FIGURE 3.24 Load-Tension Flange Strain Curve for Beam 5G1



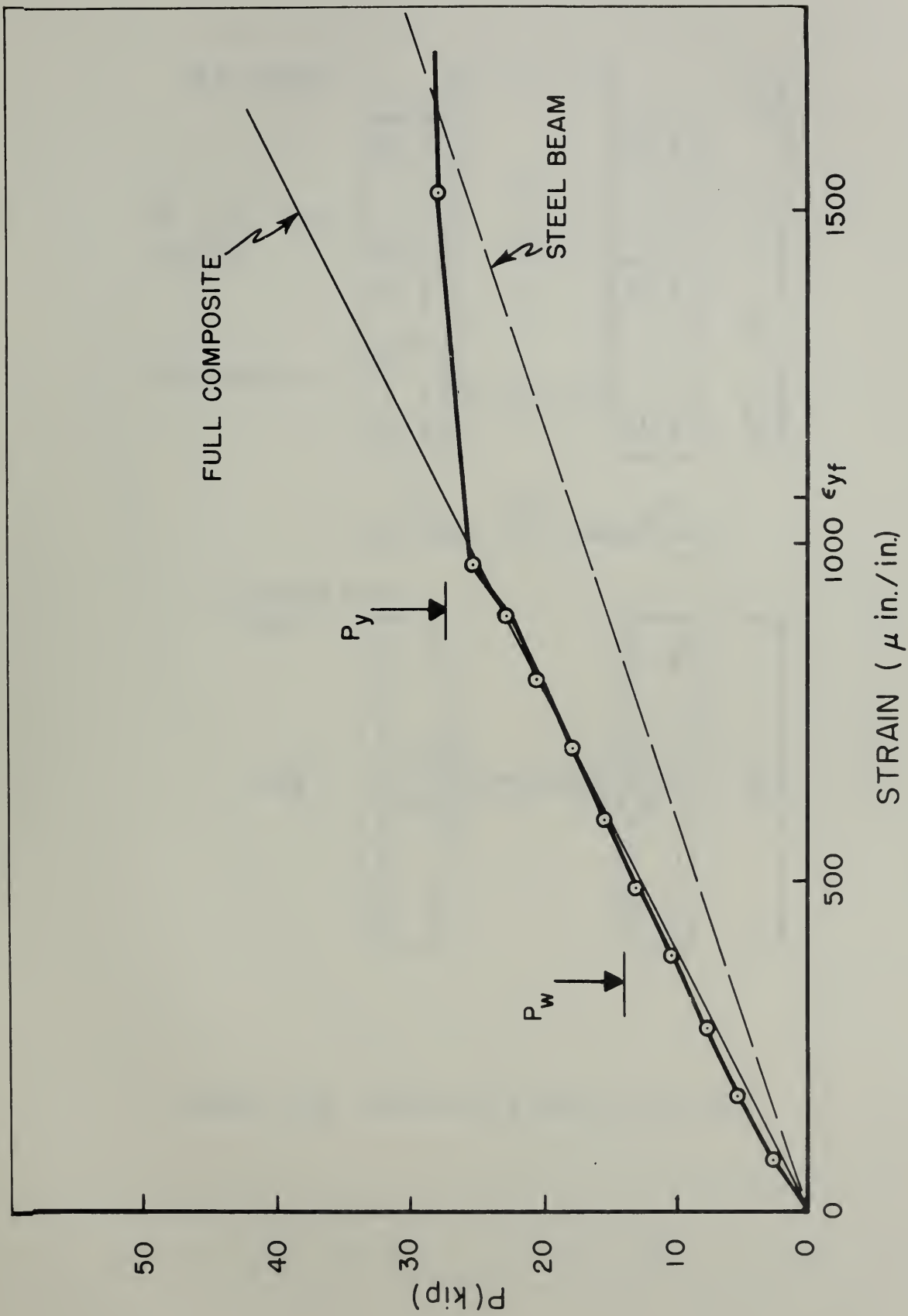


FIGURE 3.25 Load-Tension Flange Strain Curve for Beam 5U1



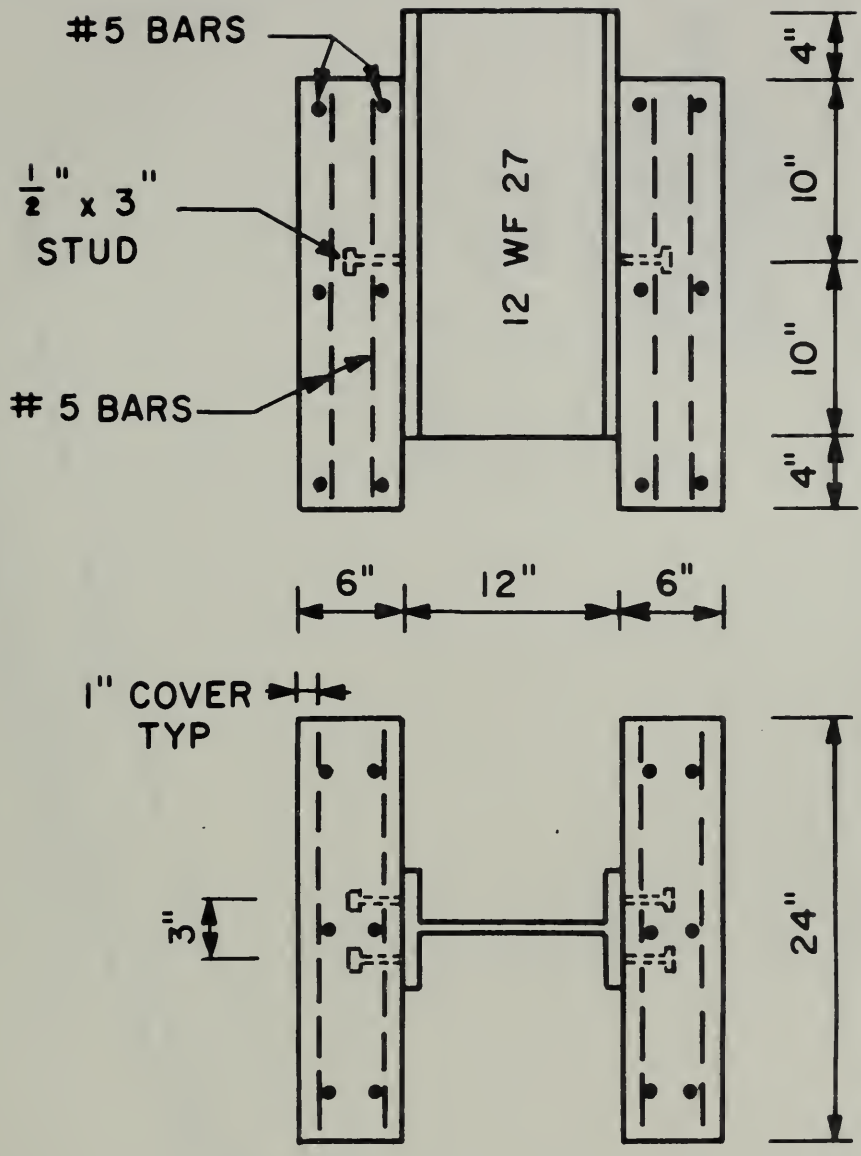
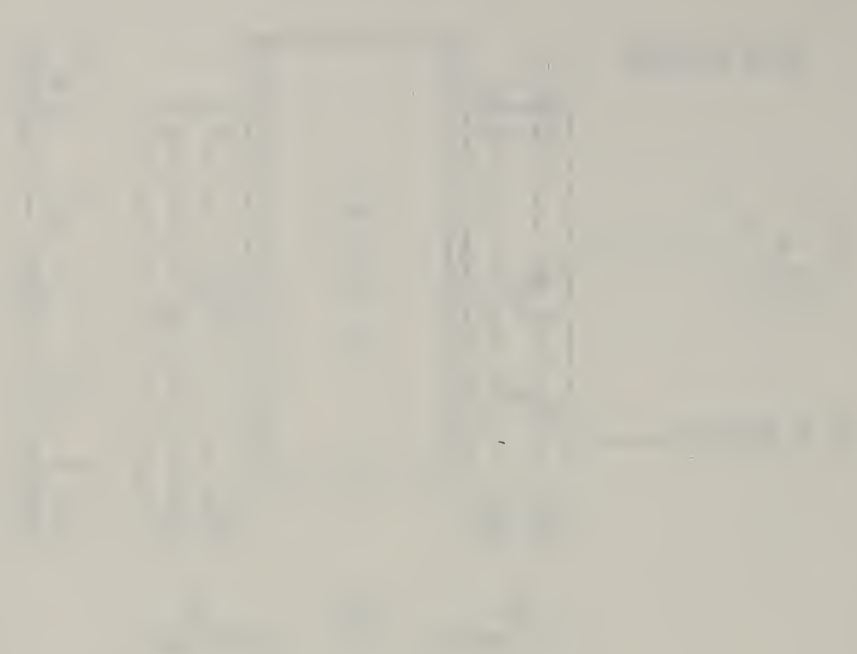


FIGURE 3.26 Details of Pushout Specimen



Faint text or a caption located below the diagrams, which is mostly illegible.

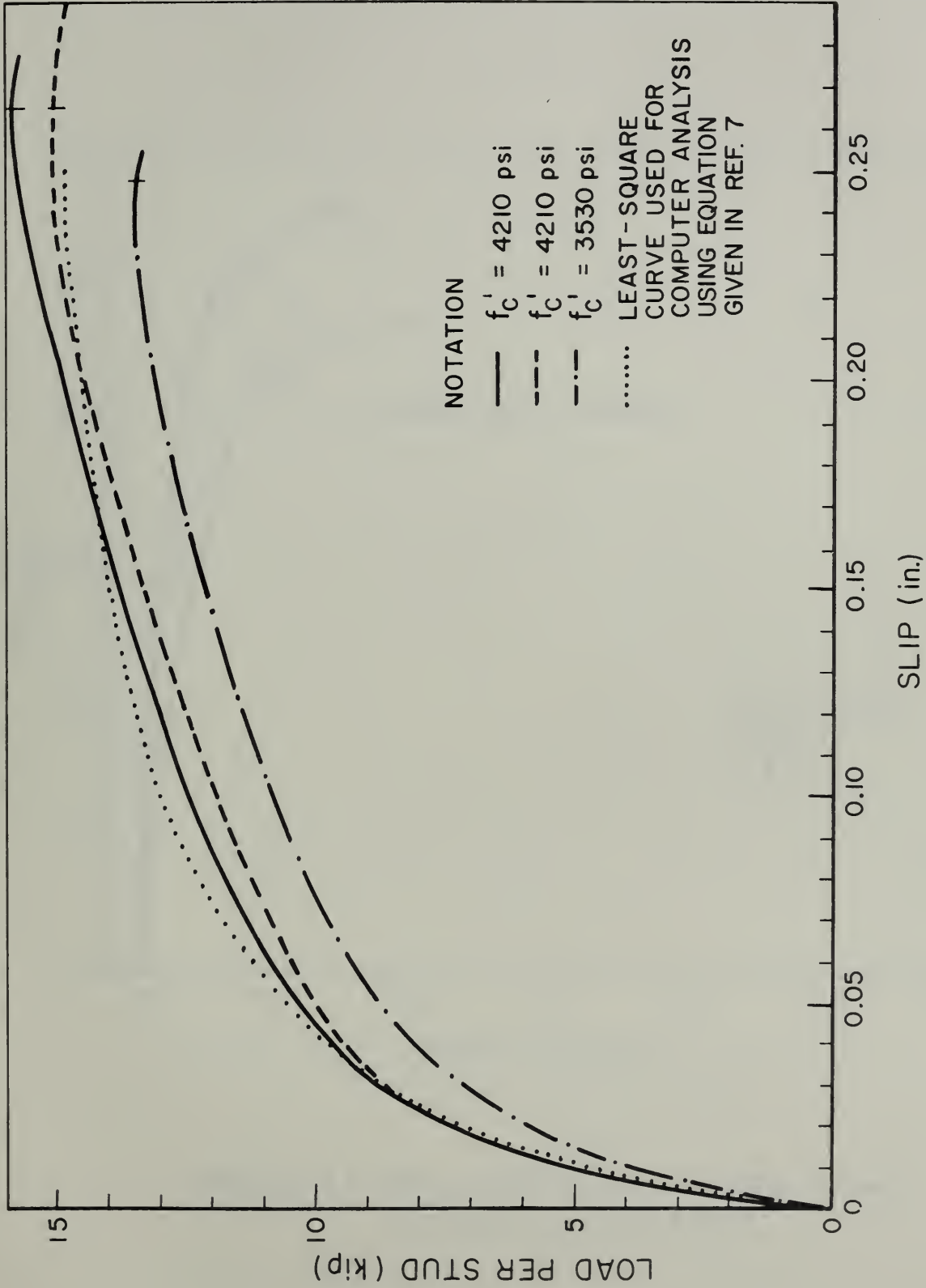
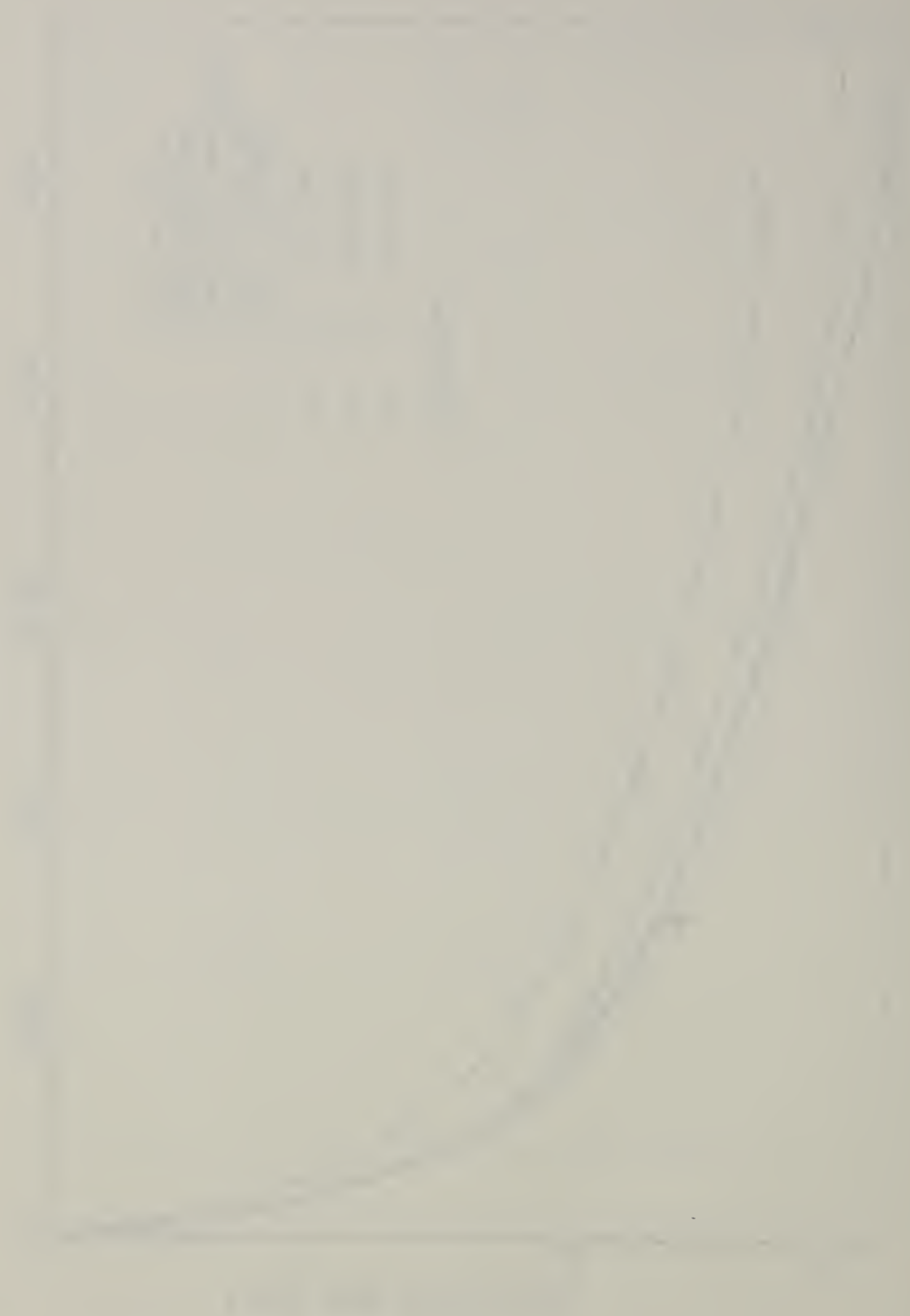


FIGURE 3.27 Load-Slip Curves of Pushout Specimens



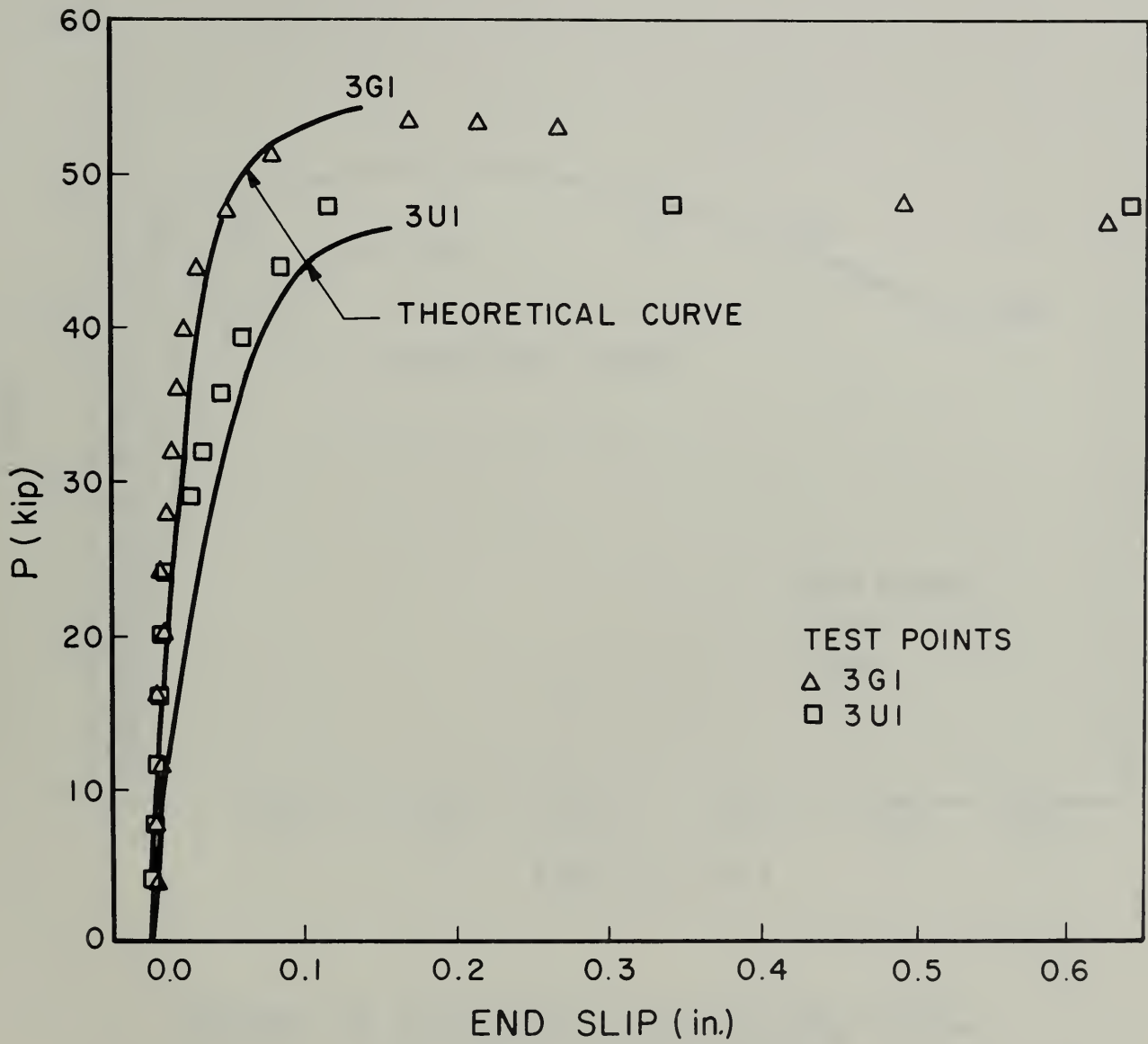
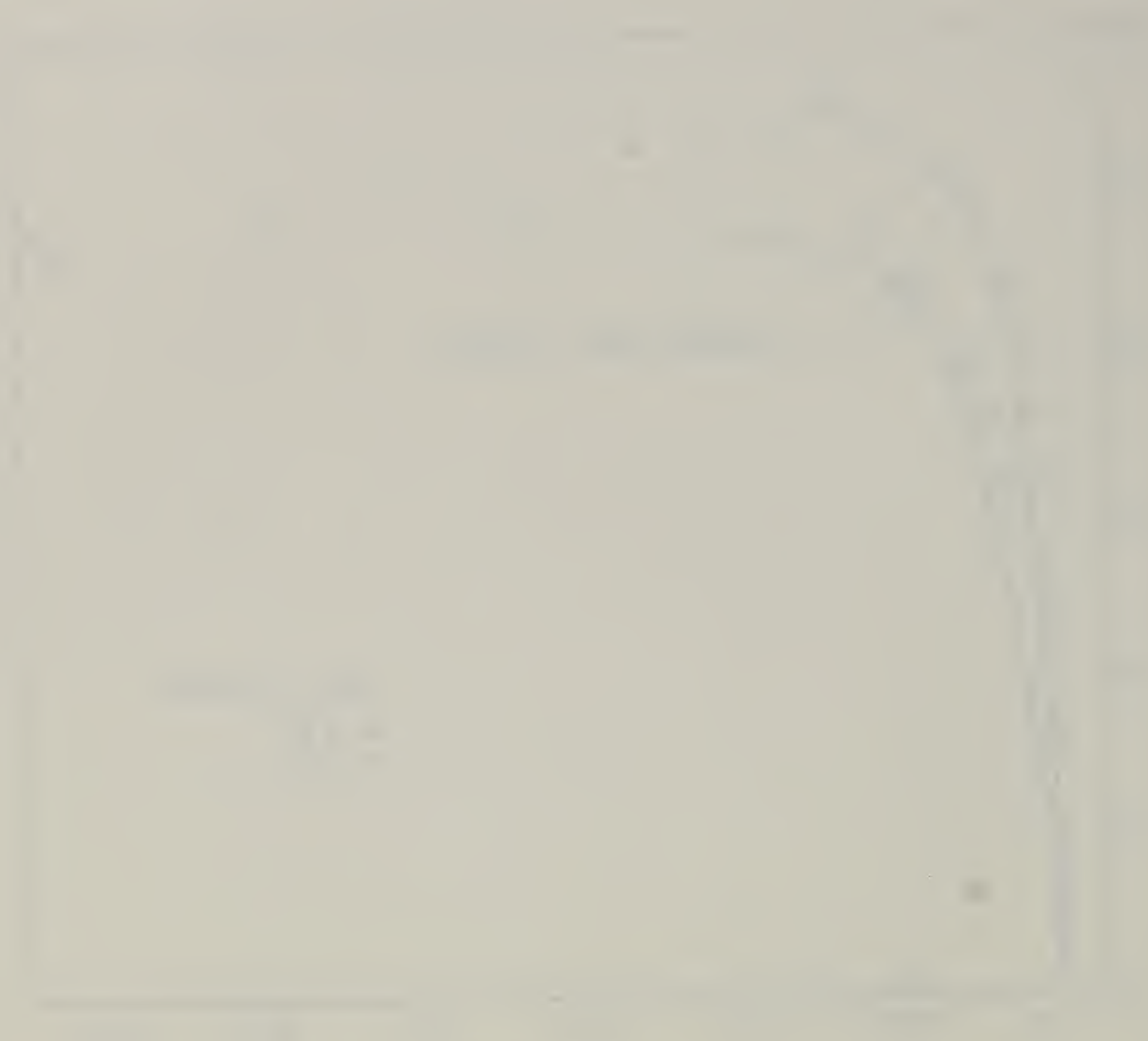


FIGURE 4.1 Theoretical Load-End Slip Curves for Beams 3G1 and 3U1



Faint text at the bottom of the page, possibly a title or a reference, which is illegible due to the low contrast and blurriness.

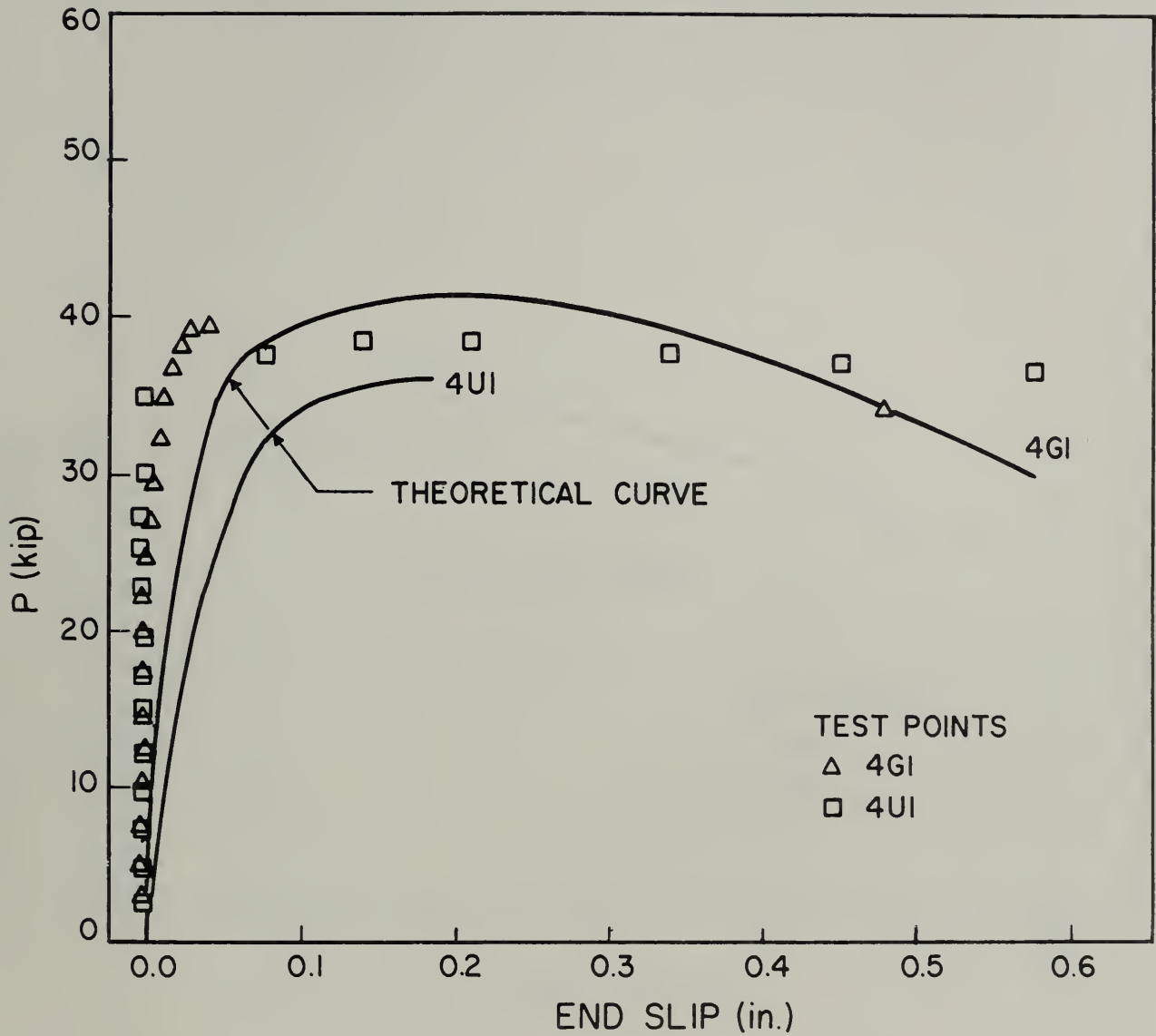


FIGURE 4.2 Theoretical Load-End Slip Curves for Beams 4G1 and 4U1



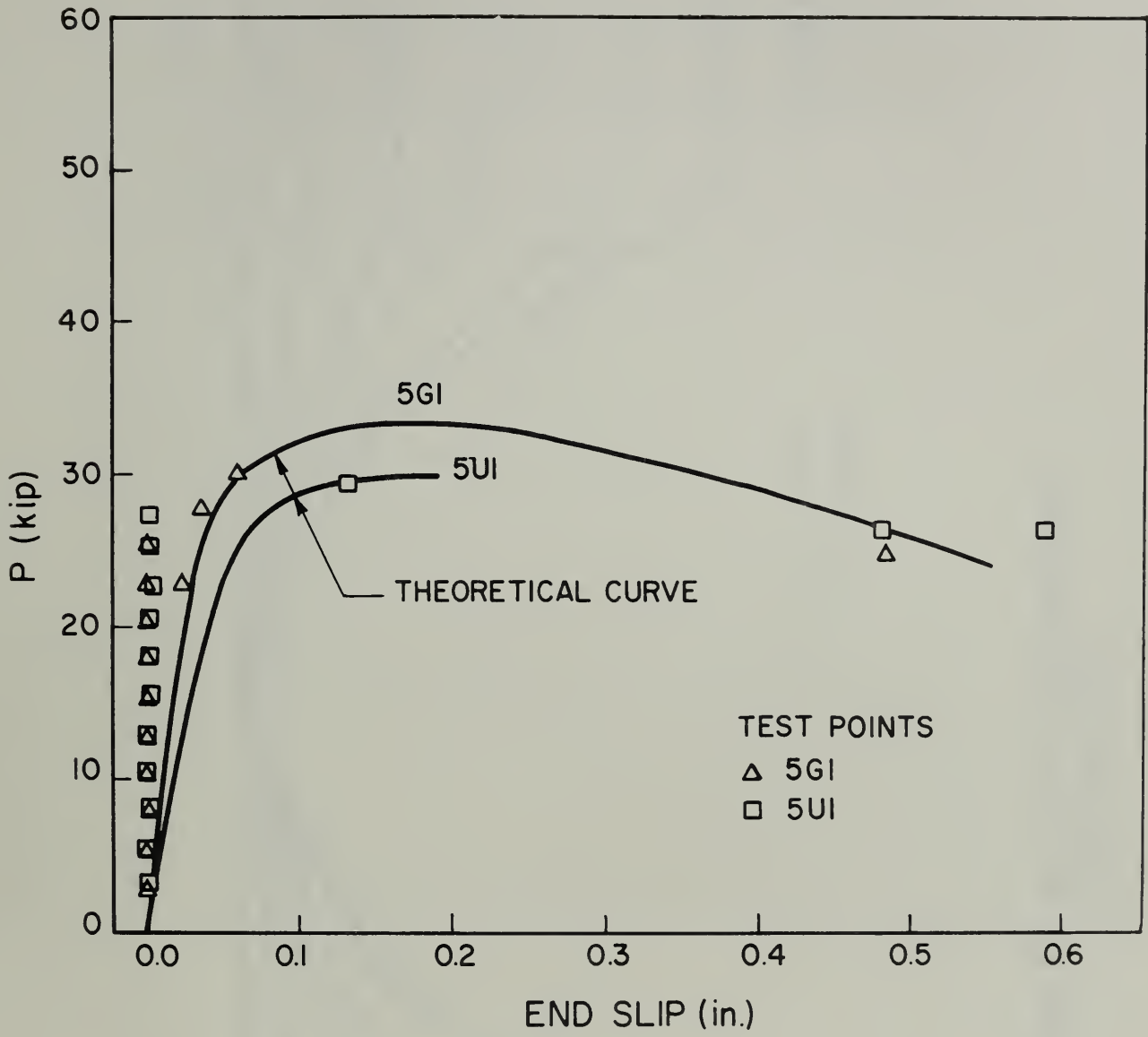


FIGURE 4.3 Theoretical Load-End Slip Curves for Beams 5G1 and 5U1



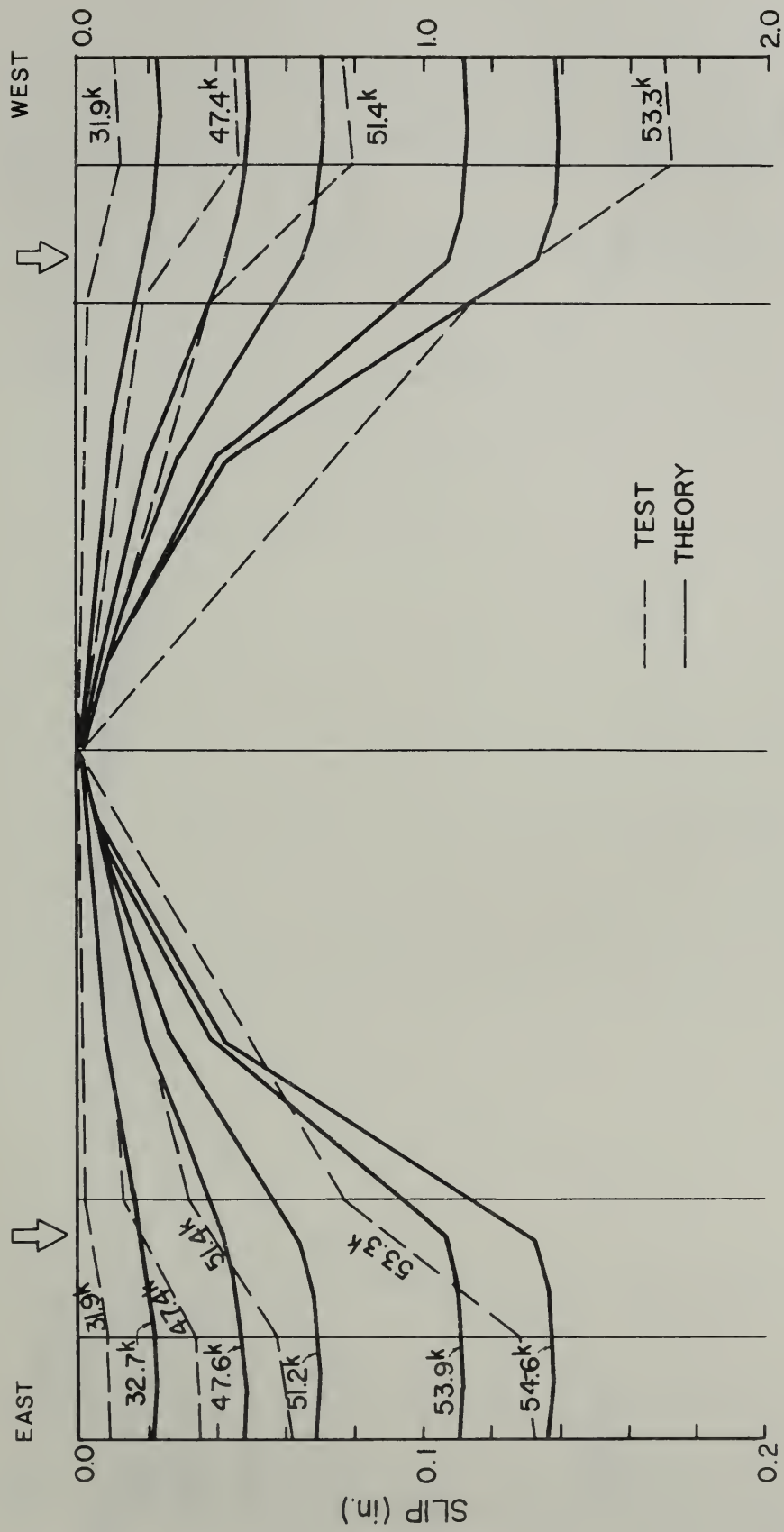
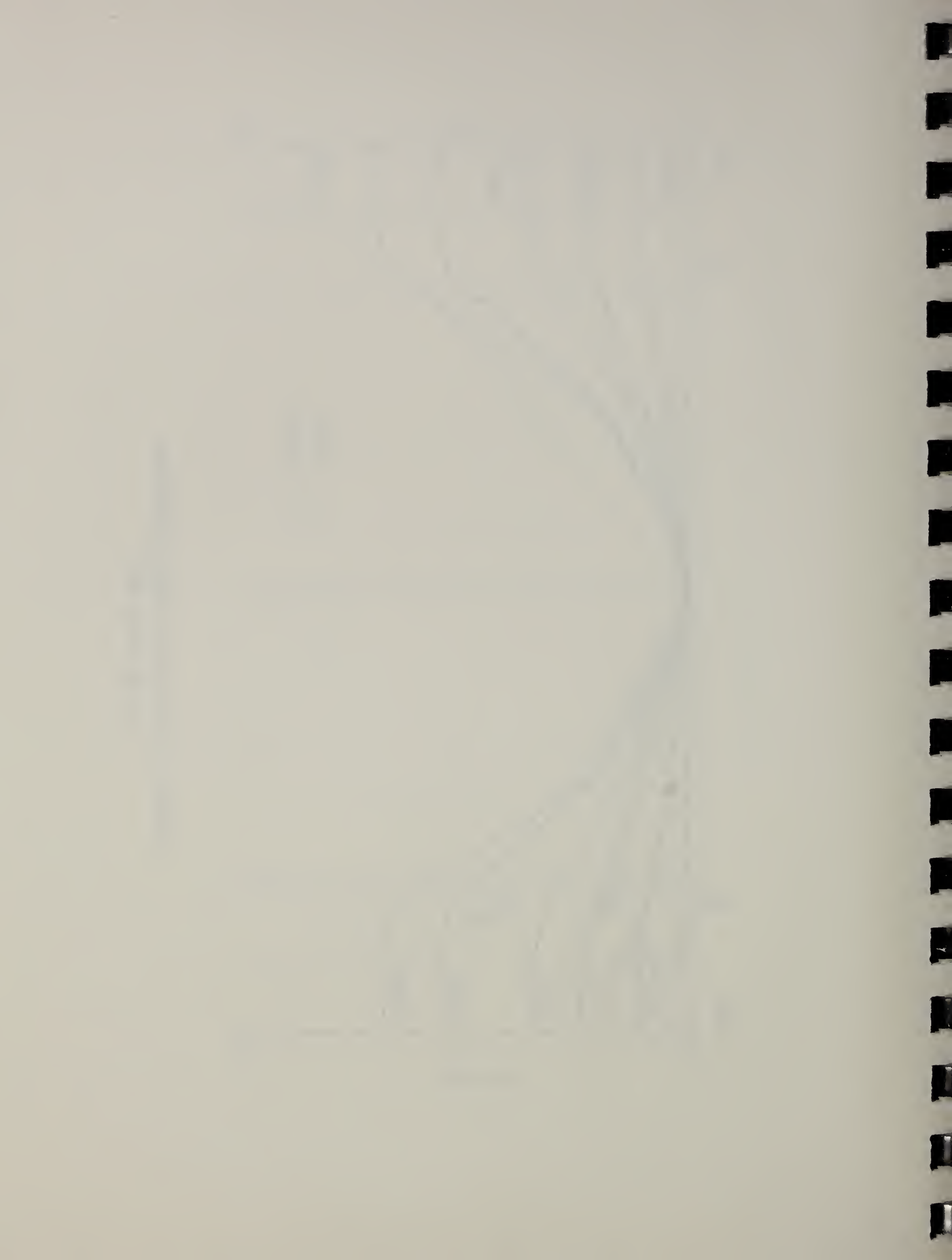


FIGURE 4.4 Theoretical Slip Distribution along Beam 3G1



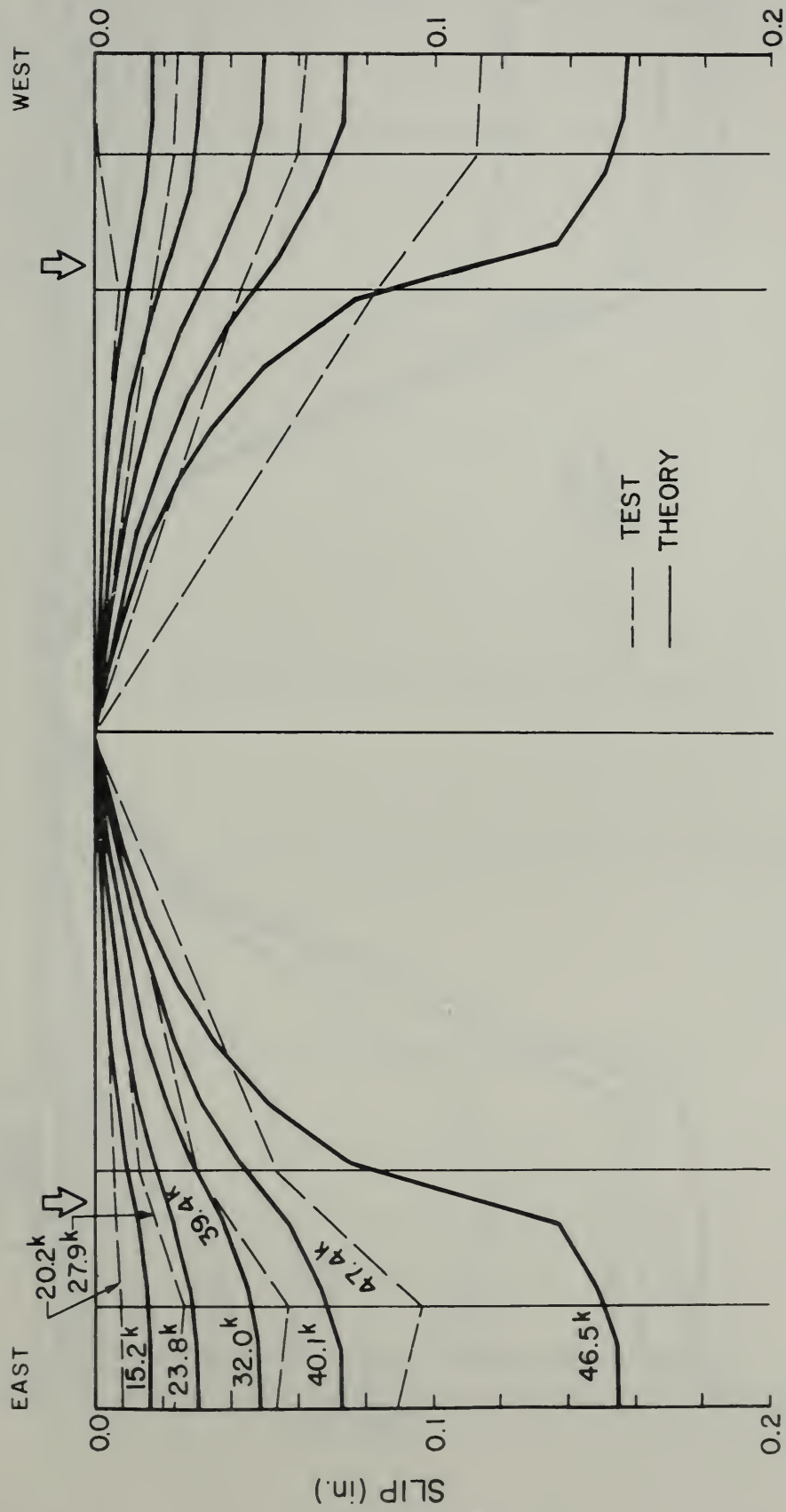


FIGURE 4.5 Theoretical Slip Distribution
along Beam 3U1

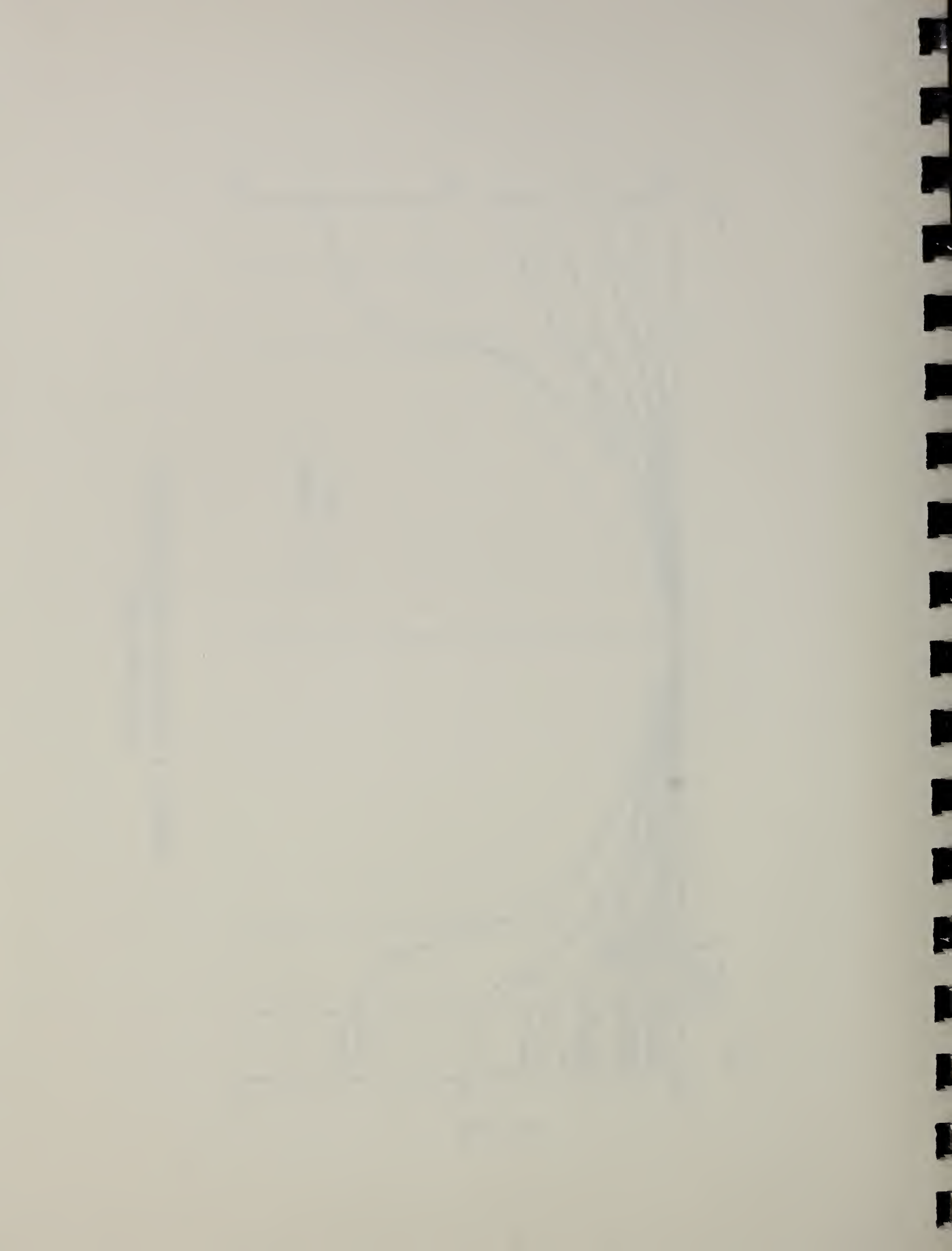




FIGURE 4.6 Theoretical Slip Distribution along Beam 4G1



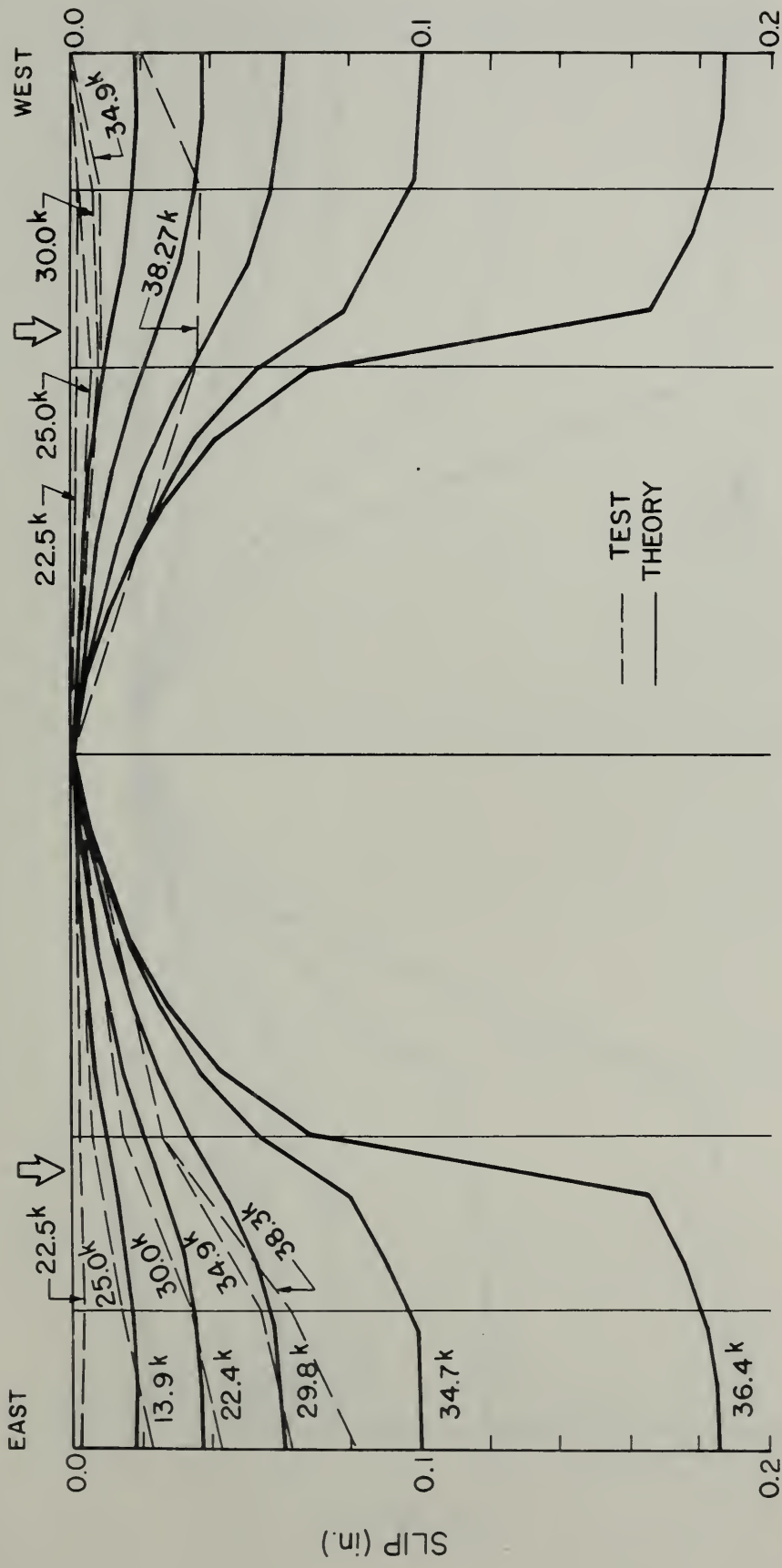


FIGURE 4.7 Theoretical Slip Distribution along Beam 4U1



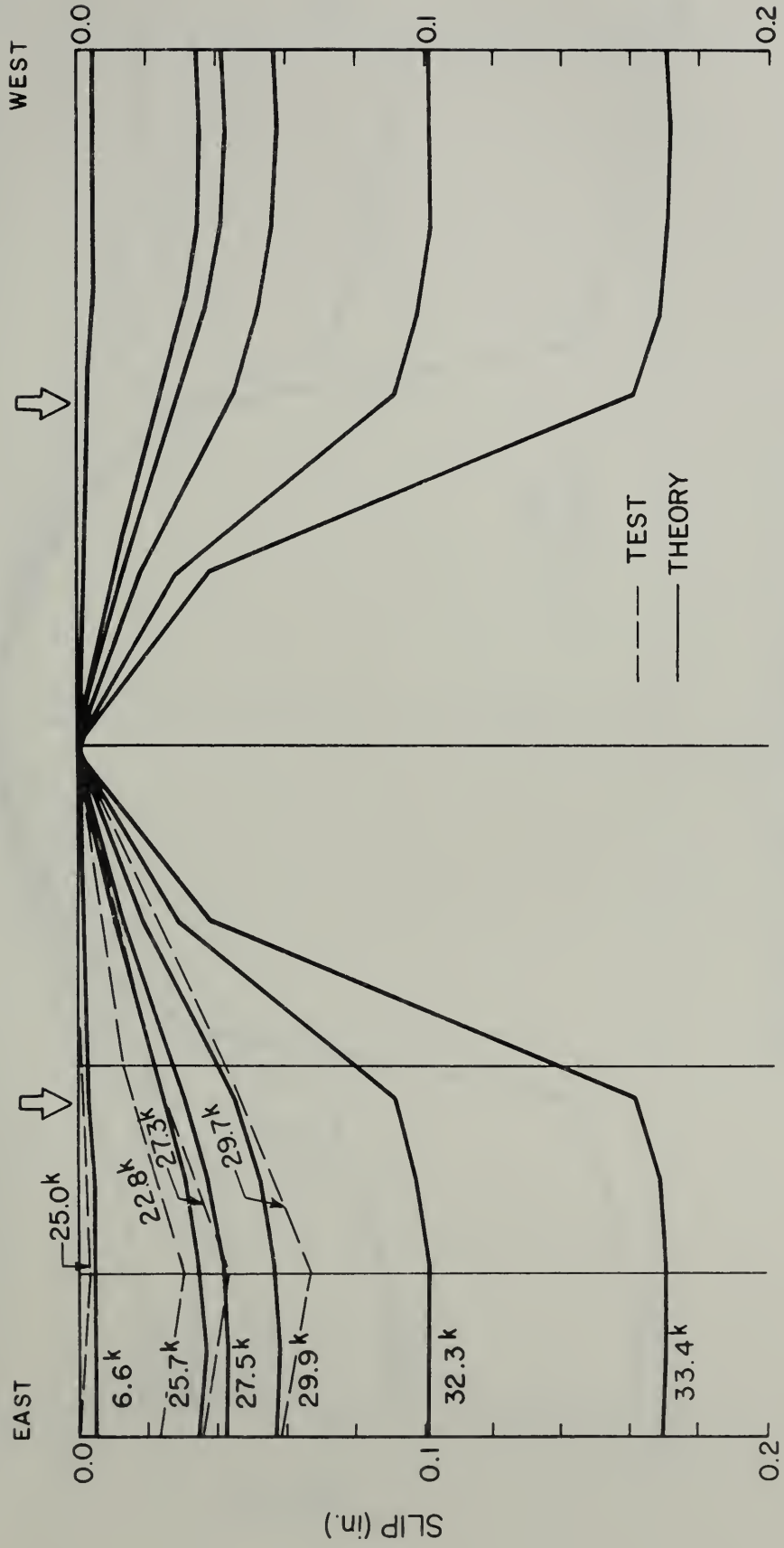


FIGURE 4.8 Theoretical Slip Distribution along Beam 5G1



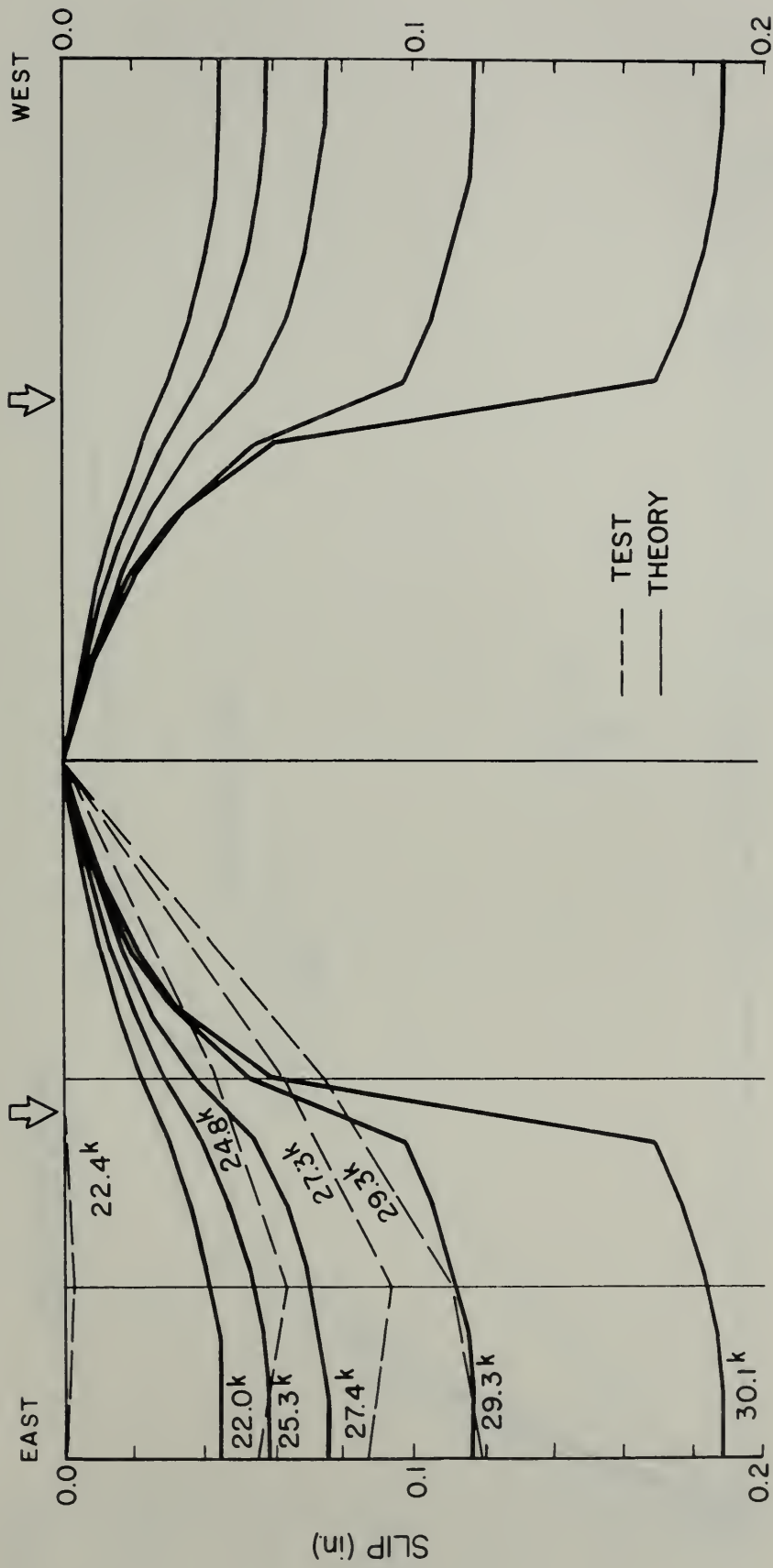


FIGURE 4.9 Theoretical Slip Distribution along Beam 5U1



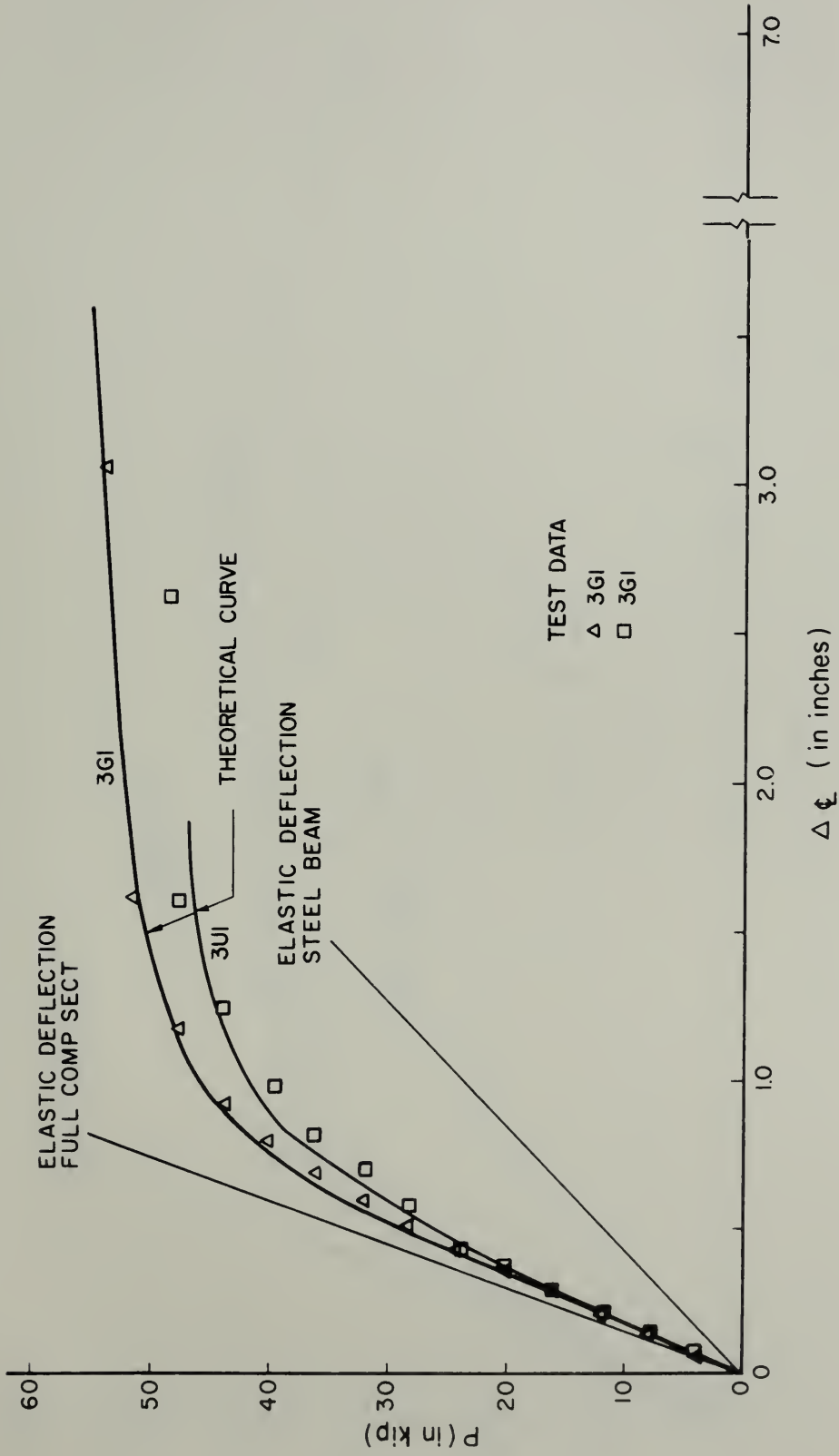
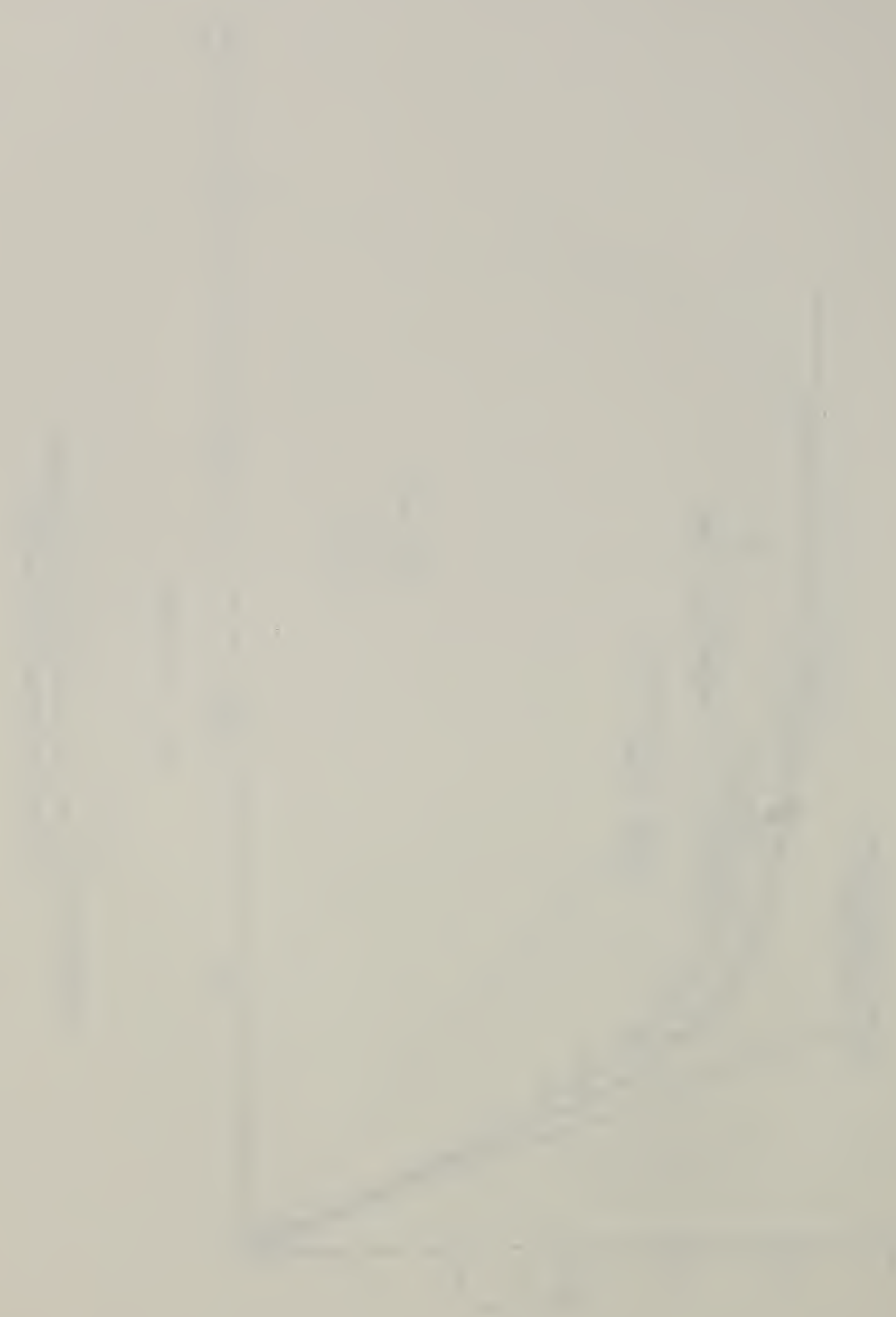


FIGURE 4.10 Theoretical Load-Midspan Deflection Curves for Beams 3G1 and 3U1



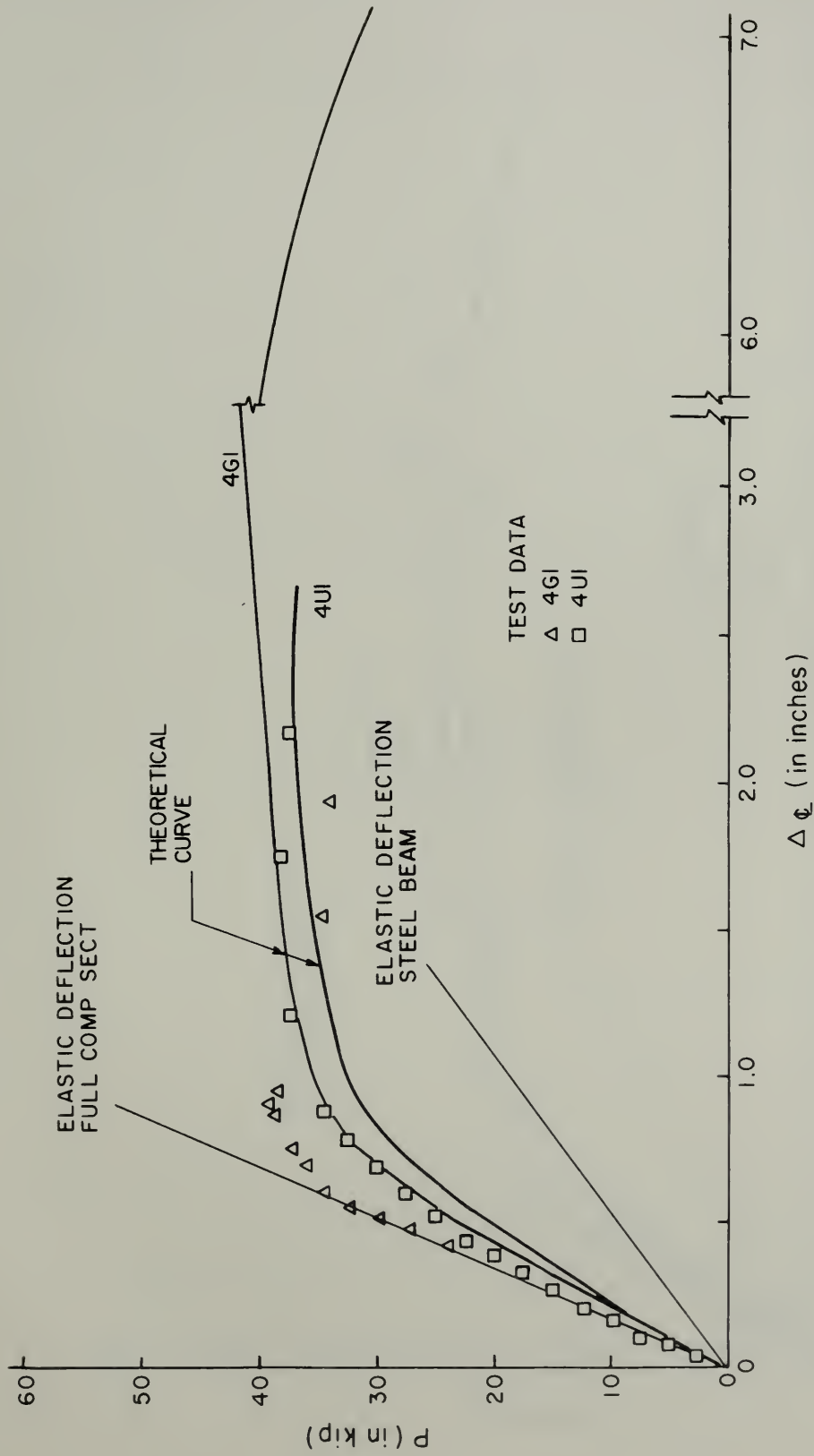
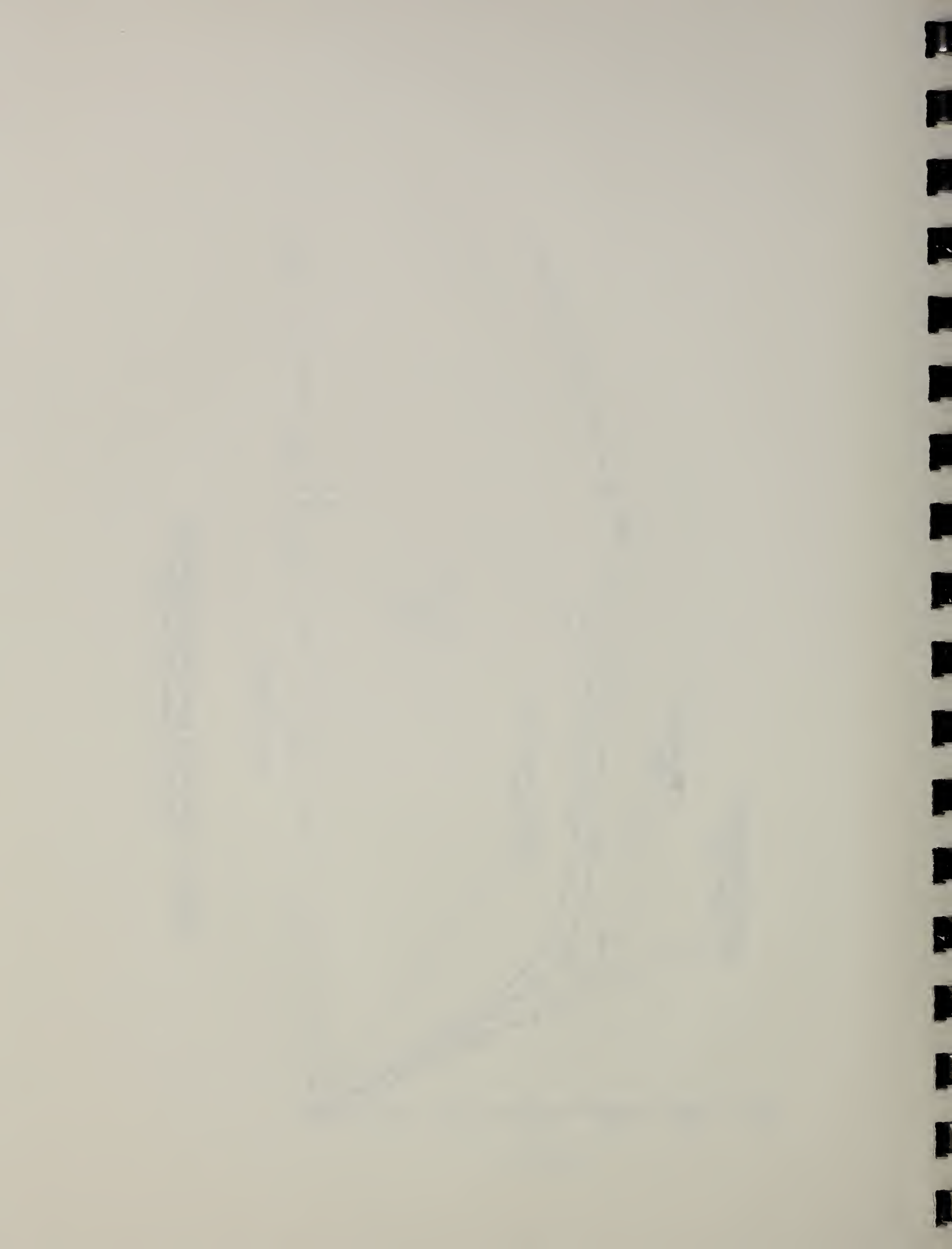


FIGURE 4.11 Theoretical Load-Midspan Deflection Curves for Beams 4G1 and 4U1



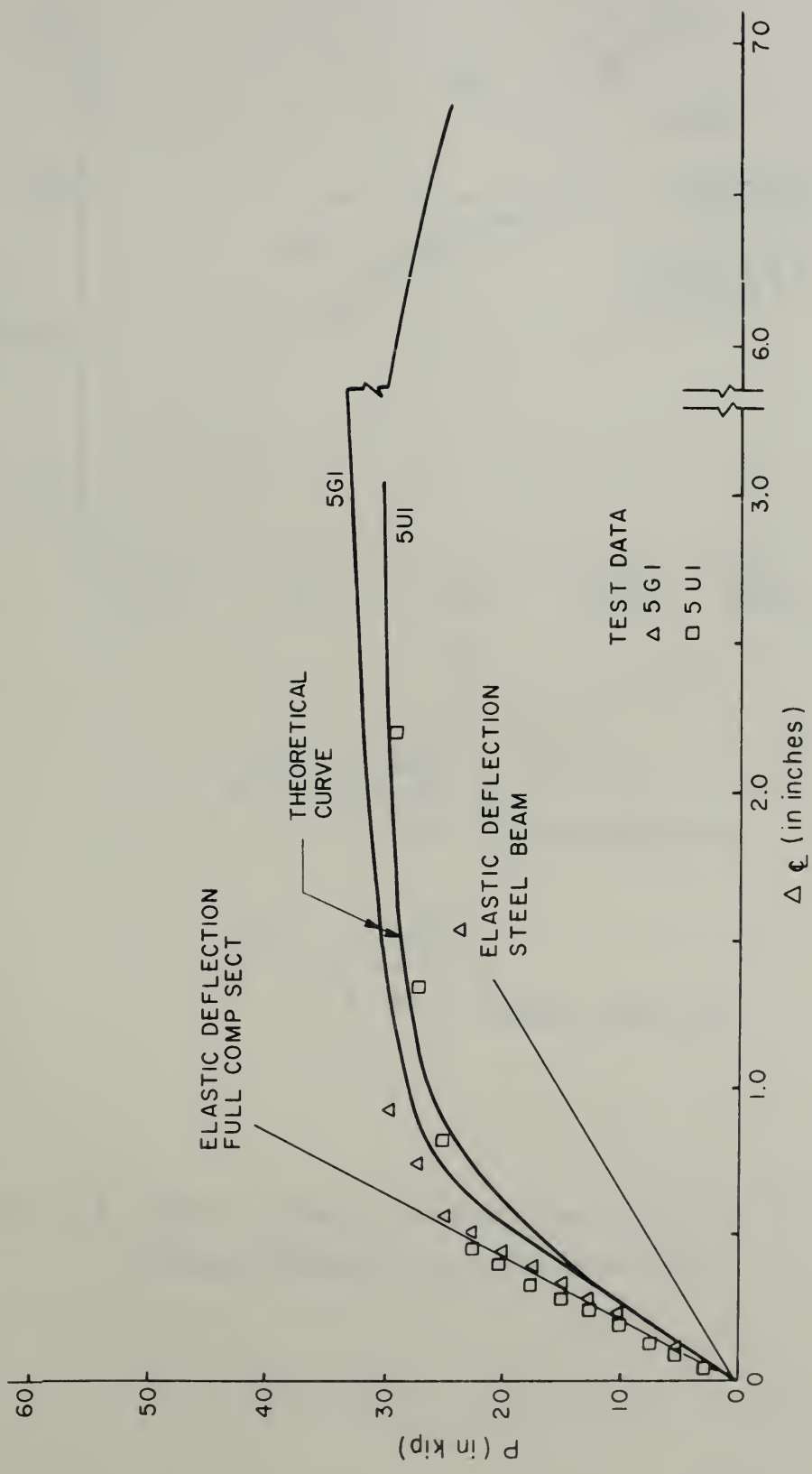
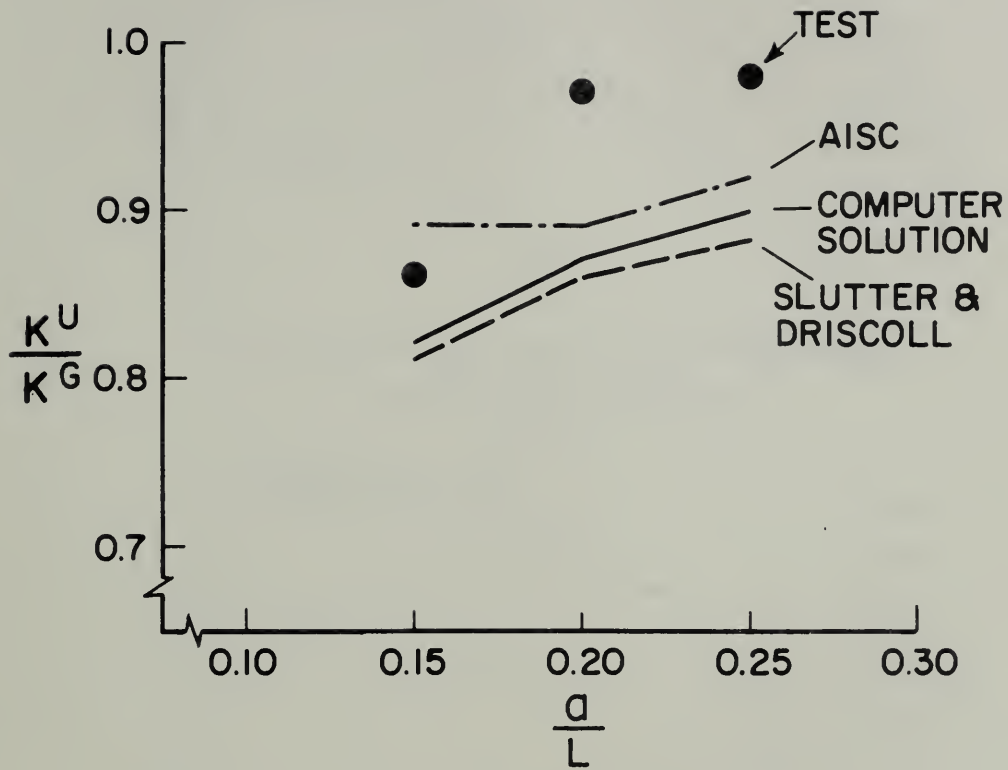


FIGURE 4.12 Theoretical Load-Midspan Deflection Curves for Beams 5G1 and 5U1

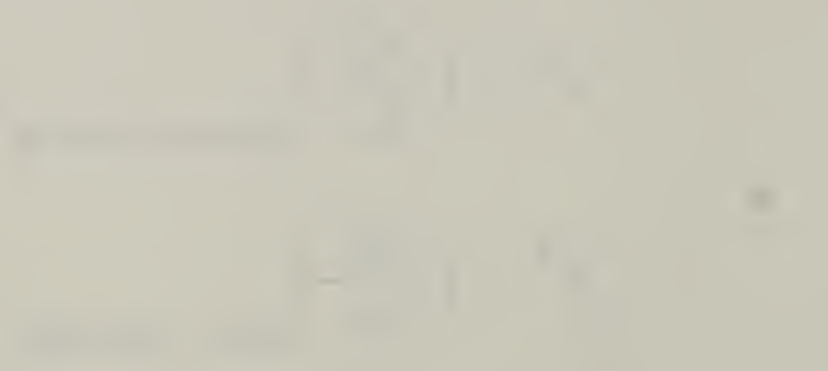
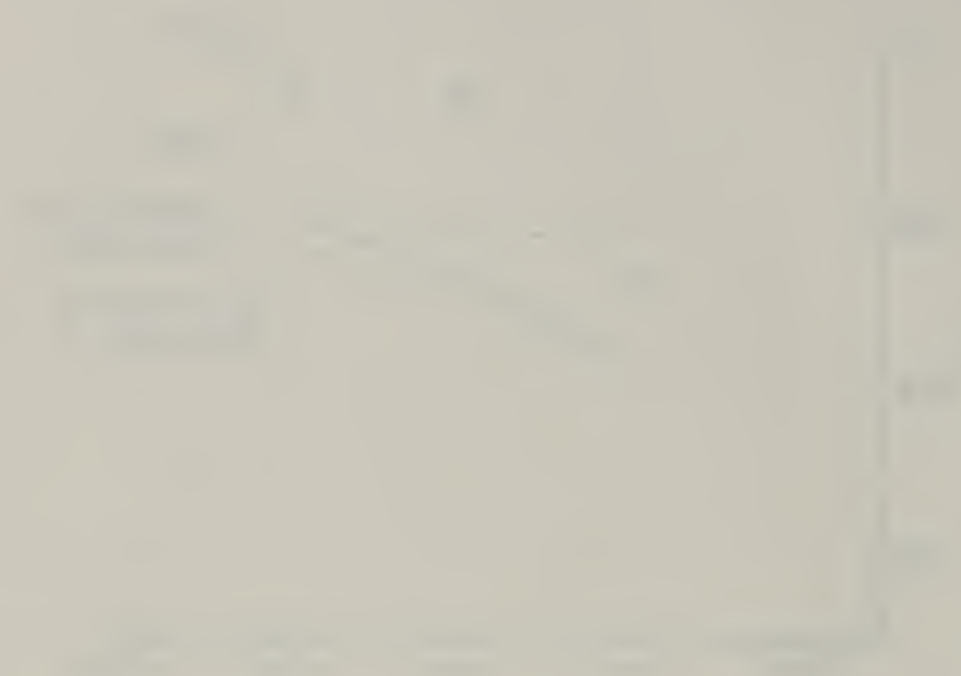




$$K^U = \left(\frac{M_U^{ex}}{M_U} \right) \text{Uniform Spacing}$$

$$K^G = \left(\frac{M_U^{ex}}{M_U} \right) \text{Group Spacing}$$

FIGURE 4.13 Effect of Shear Connector Spacing on Ultimate Strength vs. Shear-Span Ratio



Faint, illegible text or a caption located at the bottom of the page, possibly describing the diagrams above.

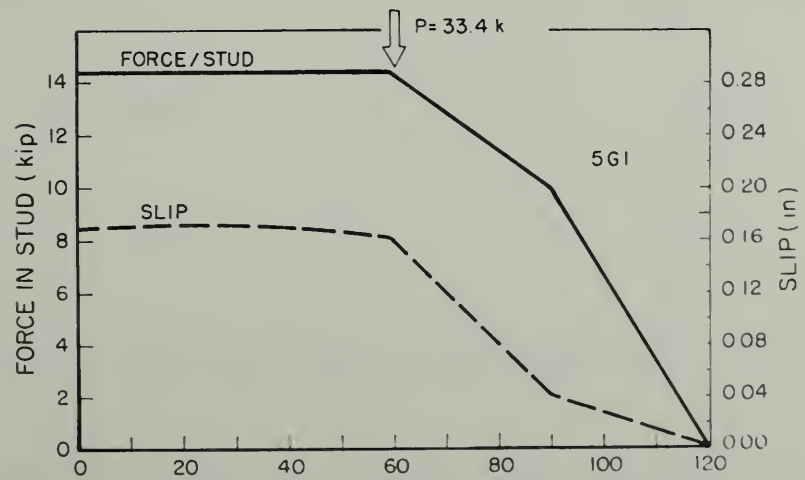
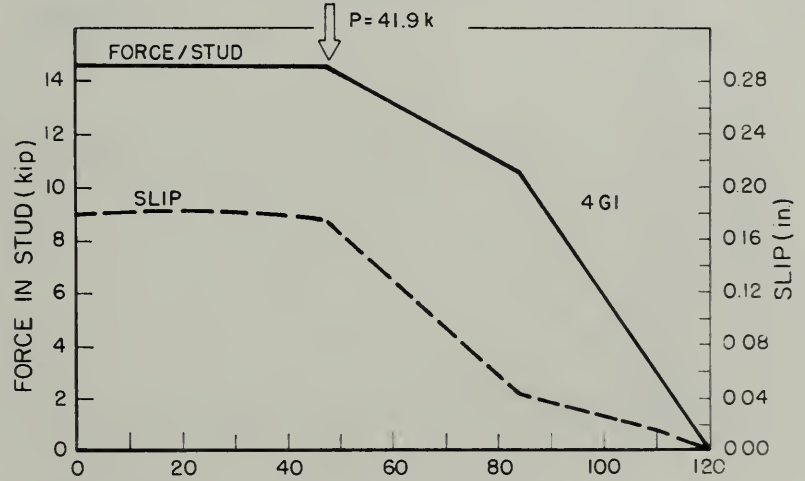
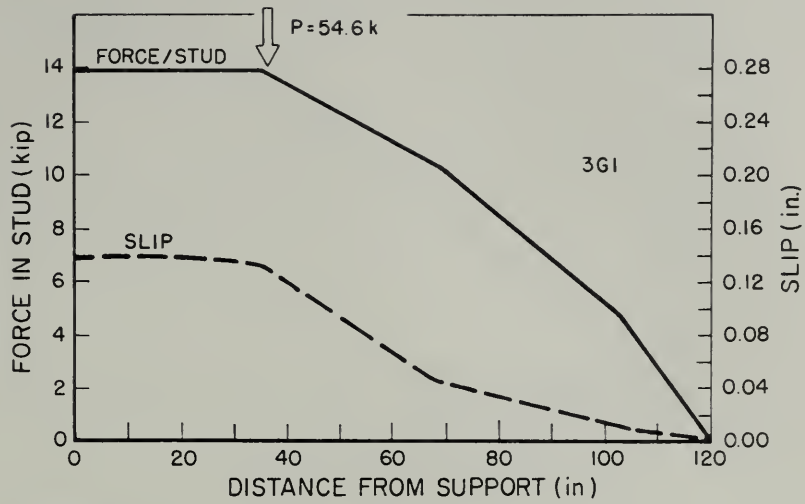
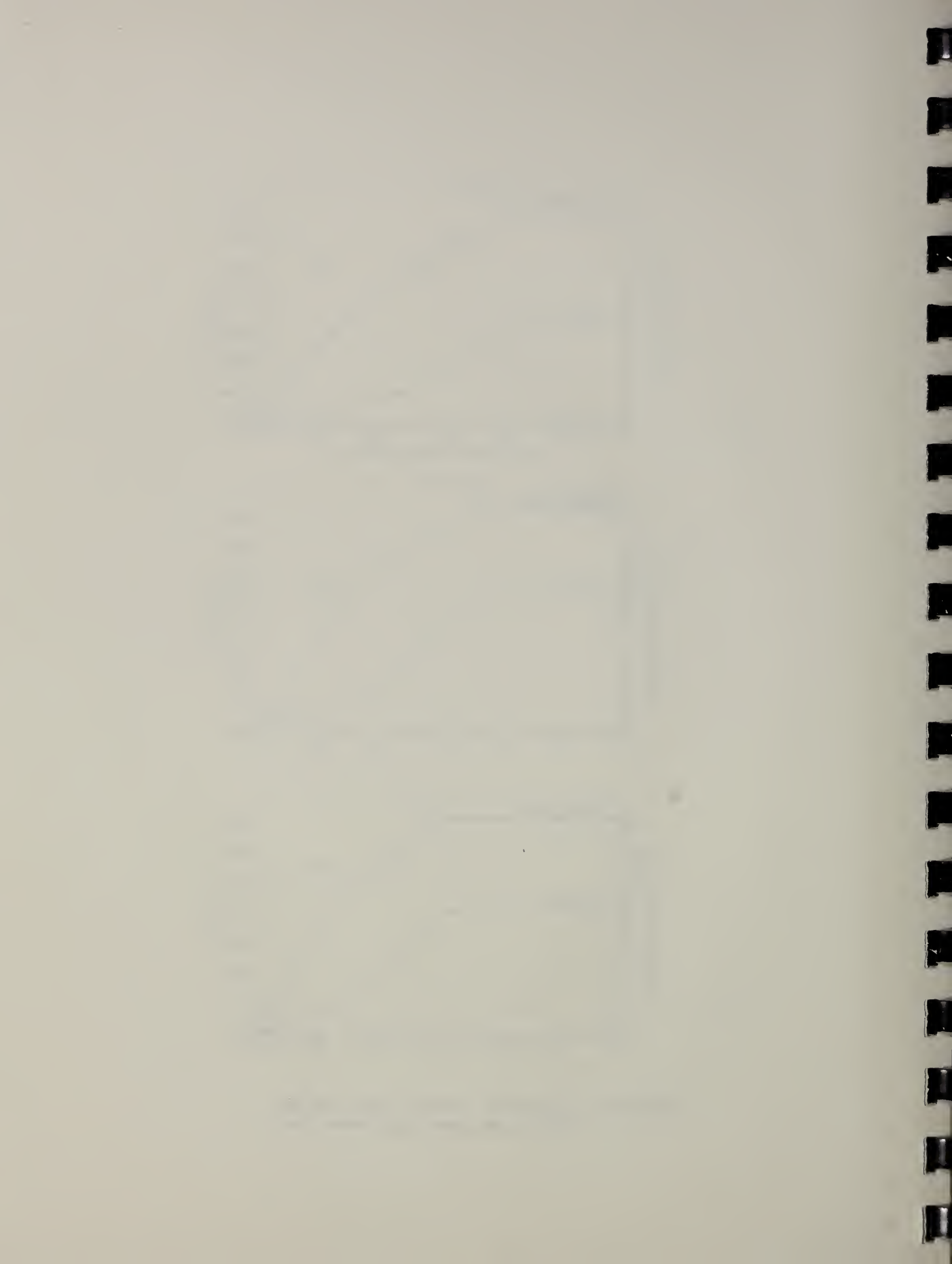


FIGURE 4.14 Theoretical Connector Force and Slip Distributions along the G-Series Beams



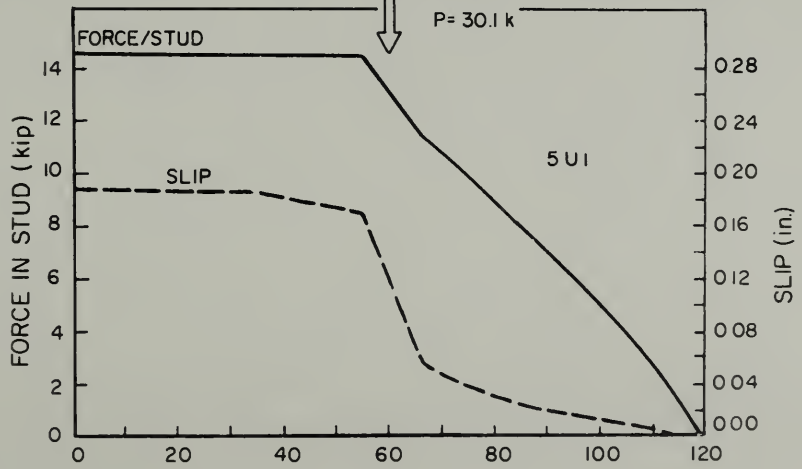
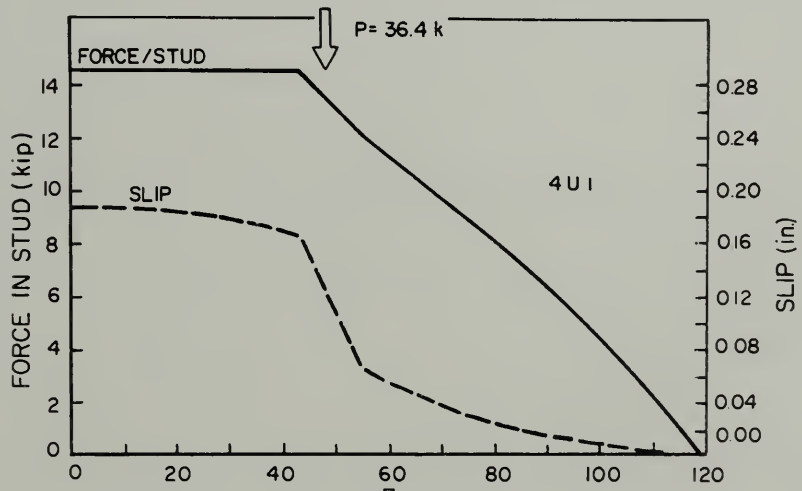
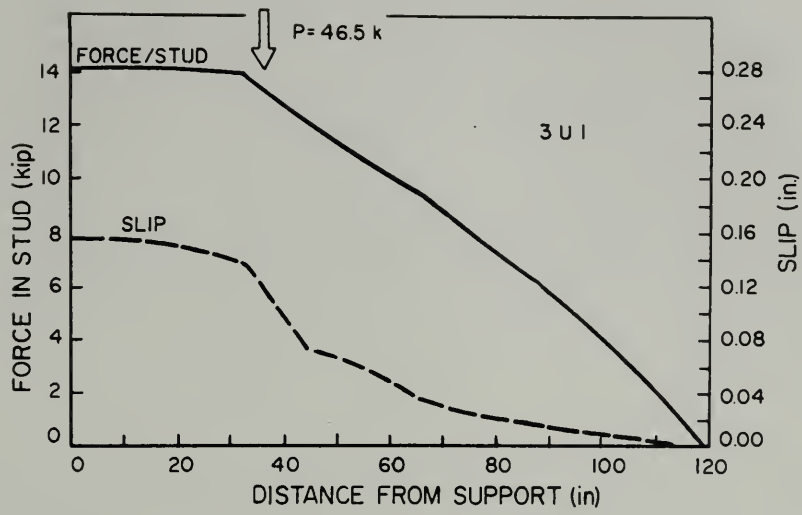


FIGURE 4.15 Theoretical Connector Force and Slip Distributions along the U-Series Beams

